From the Institute of Natural Science
at the Department of Landscape, Water and Biogeochemical Cycles
at the Justus-Liebig University Gießen

A new method for spatio-temporally explicit predictions of groundwater, surface water and habitat interactions in riparian ecosystems

Dissertation

for the degree Doctor of Natural Science (Dr. rer. nat.)

submitted by Nadine Maier, M. Sc.

Gießen, 2018

A dissertation submitted by M.Sc. Nadine Maier to the Institute of Natural Sciences at the Department of Landscape, Water and Biogeochemical Cycles of the Justus Liebig University Giessen for the degree of Doctor of Natural Sciences (Dr. rer. nat.)

Referees from the Justus-Liebig University Gießen:

Prof. Dr. Lutz Breuer (1st Supervisor)

Prof. Dr. Dr. habil. Dr. h. c. Annette Otte (2nd Supervisor)

Prof. Dr. Jürg Luterbacher

Prof. Dr. Jan Siemens

Submitted: 17th July 2018

Abstract

Floodplains are dynamic and complex systems. Their hydrological regime allows for the creation of specific conditions for flood meadows with a wide habitat heterogeneity and specialized floodplain plant species. At the same time, floodplains are the most-endangered ecosystems worldwide, as they are characterized by extremely high land loss. Therefore, they are one of the main focuses of national and international nature conservation and restoration efforts. The aim of such restoration measures is not only to restore the retention function, but also the habitat function for typical, highly specialized, and endangered species. However, compared to the importance of ecosystem services provided by floodplains and their role in biodiversity, there is little research on how scientifically-based information can be integrated in the planning and decision-making of restoration projects in order to make them more efficient and effective. Plant distribution is strongly related to hydrologic conditions on a high temporal and spatial resolution. For example, flood sensitive species prefer elevated microsites and will die during large inundation periods. To elucidate the relevance of a detailed knowledge of the hydrological regime, a parsimonious surface water-groundwater model was developed using the Catchment Modeling Framework (CMF). Further, this process-based hydrological model was linked with a species distribution model in order to predict rare and endangered species. The nature reserve Kühkopf-Knoblochsaue (34.5 km^2) serves as the study area. This reserve is of particular importance for rare and endangered flora and fauna. As a first step, the model was developed, adjusted, and tested for the past 16 years. Next, the surface water-groundwater interaction model was linked with a species distribution model to predict the occurrence of rare and endangered species. A comparison study showed that the incorporation of temporally and spatially high-resolution data from a hydrological model, as developed here, results in superior model qualities. In addition, the relevance of a broad set of hydrological predictors to simulate whole plant communities with diverse specific eco-hydrological requirements was shown. Applications of different climate models to the surface water-groundwater interaction model showed large spatial and quantitative changes in the inundation characteristics in the near and far future. A linkage of these hydrological regime projections with the species distribution model pointed out the possibilities for habitat projections and the advantages for conservation measures.

Table of contents

List of tables

List of figures

1. Extended Summary

1.1. Introduction

1.1.1. Environmental relevance of riparian ecosystems

Floodplains are among the most-endangered ecosystems worldwide (Opperman et al., 2010). In Germany, the floodplains of the largest rivers have lost on average two-thirds of their original extent (Brunotte et al., 2009). A consequence of the continuous decline in floodplain area is the loss of biodiversity. Even the remaining active floodplain areas, retaining more or less their typical flooding dynamics, are developed areas or are used for agriculture and have consequently lost at least part of their habitat function (Follner et al., 2010).

Restoration of species-rich flood meadows is an important contribution to maintain the biodiversity of plants and fauna on flood meadows. Preconditions for successful restoration management are suitable site conditions, such as soil nutrients, the availability of seed sources, and moisture regime (Bakker and Berendse, 1999). As floodplains are frequently inundated and nutrient-rich sediments are deposited, river floodplain soils are among the most fertile soils (Zorn et al., 2005). In order to overcome the issue of limited seed material dispersal in floodplains, the best solution up to date is to transfer seed-containing plant material with or without topsoil removal (Donath et al., 2007; Harnisch et al., 2014; Hölzel and Otte, 2003). While the availability of seed source and soil nutrients can be easily influenced and assessed, evaluation of the hydrological conditions is more difficult, though not less important. Consequently, restoration projects are often challenged by the complex hydrological conditions of the target areas (Malanson, 1993). The hydrological conditions are of particular significance for plants, as they are rather sensitive to the soil moisture conditions, e.g., flood sensitive species occupy elevated microsites, whereas flood tolerant species occur in depressions (Jung et al., 2008; Ludewig et al., 2014; Vervuren et al., 2003). In light of this, it is especially important to incorporate hydrological conditions in the planning of flood meadow restoration projects (Gattringer et al., 2017, 2018). Ideal tools for enhancing conservation decisions are species distribution models (Guisan et al., 2013). So far, only a few studies have used hydrological information to simulate the distribution of riparian vegetation or the occurrence of plant species (Leyer, 2005; Mosner et al., 2011, 2015). There are two main reasons for neglecting hydrological conditions within species distribution modeling on floodplains. On one hand, the lack of available data with a sufficient temporal

and spatial resolution and on the other hand, the difficulties in obtaining and portraying conditions in sufficient resolution.

Floodplains are comprised by different components, including surface water, groundwater, and precipitation, interacting on a high temporal and spatial resolution. The driving factor of the eco-hydrological functions on the floodplain are the connectivity and interaction of shallow groundwater with the surface water (Hayashi and Rosenberry, 2002; Krause et al., 2007a). These interactions are mainly defined by the physical soil properties and the presence and location of embankments, which influence the hydrological regime and the in- and outflow of river water on the floodplain. The regular inundations of a floodplain are defined by characteristics such as the height of the water level, flood duration, and recurrence intervals (van Eck et al., 2004; Hayashi and Rosenberry, 2002; Krause et al., 2007a; Maltby and Barker, 2009; Woodcock et al., 2005).

1.1.2. Modeling of riparian ecosystems

Due to the importance of the connectivity between surface water and groundwater for the eco-hydrological functions, floodplains should be simulated with fully-integrated models that have explicit representation of water table gradients and groundwater flow (Acremann and Miller, 2007) and consider surface water-groundwater interactions (Furman, 2008; Refsgaard et al., 1998; Sophocleous, 2002). As floodplains act as collecting point for river water, hillslope-derived water, and groundwater, the groundwater level is usually very high in floodplains (Burt et al., 2002). The groundwater level is influenced by the surface water in two ways: laterally across the channel banks and vertically across the floodplain surface. A high temporal resolution of such models is equally essential, as the interaction often shows a high temporal variability (Jung et al., 2004; Krause et al., 2007a).

Compared to the significance of floodplain ecosystems, only a few studies have focused on modeling floodplains with models maintaining the simultaneous simulation of both components - the surface water and the groundwater. There are three main reasons for the lack of application of such models: (1) strong interactions between surface water and groundwater are difficult to model (Branfireun and Roulet, 1998; Price and Waddington, 2000); (2) these models require a high-level modeling expertise (Ameli and Creed, 2017; Golden et al., 2014); and (3) these models require high computational power (Ameli and Creed, 2017). An additional difficulty is the parameterization of such large groundwater models, as the effort for this process is immense (Acremann and Miller, 2007).

However, if these problems could be successfully overcome, then those powerful hydrological models can be combined with habitat models. Applications of such complex habitat models have the potential to improve the outcome of conservation efforts, as they are an efficient tool for predicting possible habitats for species (Guisan et al., 2013). In Germany, biodiversity conservation and restoration focuses on the active floodplain. A lot of effort is given to the protection and reintroduction of rare and endangered floodplain species, but the decisions as to whether a specific site is suitable and promising for restoration is currently often based on soft data and subjective appreciation. This is commonly accomplished by searching for potential restoration sites and convincing landowners and farmers to restore their intensively-used meadows. Including detailed hydrological information and habitat models in such decision processes bear a great potential to make these decisions more efficient and effective. The correlation of hydrological conditions with the requirements of plant species can help locate promising regions for restoration, where conditions are satisfactory, and thus the probability of species settling is high. Consequently, likely unsuitable regions can be excluded from the beginning, and the focus can be on more promising regions. There are further advantages: by incorporating predicted hydrological conditions for the future into habitat models, even the probability of a plant occurring under climate or land use change can be assessed.

1.2. General objectives of the study

This dissertation aims to expedite the scientifically-based decision-making to enhance the success rate of restoration measure on flood meadows. The study can serve to support the conservation and restoration of rare and endangered floodplain species. Within this study, a method is developed for spatio-temporally explicit predictions of groundwater, surface water, and habitat interactions in riparian ecosystems. In addition, the obtained knowledge and the modeling strategy developed here can generally be transferred to other ecological disciplines, for example, to simulate the effect of restoration measures on stream ecology or the spatio-temporal development of intermittent streams.

Due to the interdependence between plant species distribution and hydrological conditions, as well as the lack of the corresponding hydrological data and the lack of such

information in the scientific species distribution modeling context, the following main objectives were designed for this dissertation:

1) Set up a simplified physical-deterministic model to simulate the surface water-groundwater interaction and the inundation of floodplains.

This is accomplished by establishing a parsimonious model that provides key processes to accurately represent the water pathways with the aim to reduce the computational run time and to investigate the model's parameter uncertainty (Chapter 2). As a test case, the model is applied to the floodplain "Kühkopf-Knoblochsaue," Hesse, Germany.

2) Investigate the model uncertainty and its suitability to project future hydrological conditions under climate change, particularly with regard to the occurrence and duration of flooding events of floodplains.

A modeling framework is set up, integrating projections of two climate models, three emission scenarios, a rainfall–runoff model, and the coupled surface water–groundwater model from the first objective (Chapter 3).

3) Implement spatio-temporal explicit simulations of groundwater and surface water indicators of the floodplain in a habitat model to improve the prediction of potential habitats with a specific focus on rare and endangered floodplain species.

For this purpose, the dynamic hydrological information is converted into static variables and integrated in a habitat model, which in turn predicts the probability of occurrence for 23 flood meadow plant species (Chapter 4).

To achieve the objectives, the work was divided into three sections, which resulted in three publications. After a brief introduction to the study area (Chapter 1.3.1) and the presentation of the modeling concept (Chapter 1.3.2), the publications are summarized in chapters 1.4.2 to 1.4.4.

1.3. Material and methods

1.3.1. Overview over the study area

The research area (N: 49°52′ – 49°46′, E: 8°22′ – 8°29) is located in Hesse, Germany, approximately 30 km south of Frankfurt am Main (Figure 1.1 a, b). The study area covers approximately 43 km² and includes the nature reserves "Kühkopf-Knoblochsaue" (24 km²), "Bruderlöcher" (0.17 km²), "Großes Michelried bei Erfelden" (0.23 km²), and a part of the "Riedwiesen von Wächterstadt" reserve (0.76 km²). The remaining area is unprotected area (Figure 1.1, c). The nature reserve is of particular importance for rare and endangered flora and fauna and is protected by the European Habitats Directive (Council Directive 92/43/EEC).

An embankment construction divides the Holocene floodplain into three compartments:

- The functional floodplain: land between the river and the summer embankment, regularly flooded during high flow of the Rhine.
- The hybrid floodplain: land between the summer and the winter embankment. This area is only flooded by extremely high water levels of the Rhine (> 4m above mean water level) or in the event of breaking embankments. Inundation can occur also due to ascending groundwater.
- The fossil floodplain: the part of the floodplain on the landward side of the winter embankment. Inundation can occur due to ascending groundwater (Hölzel and Otte, 2009).

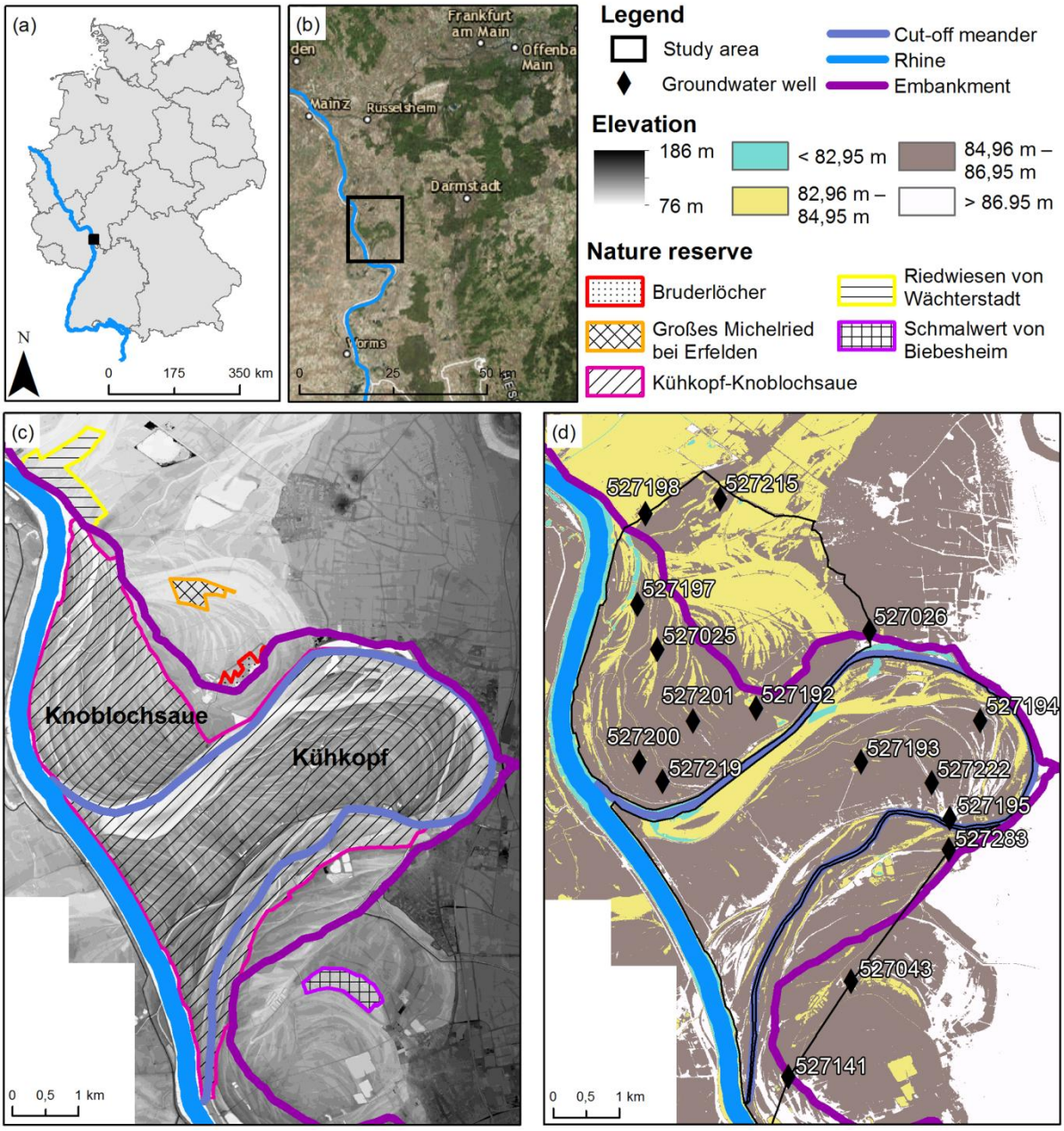

Figure 1.1: Maps of the study area: (a) location of the study area within Germany, (b) major cities around the study area (Esri, 2018), (c) digital elevation (Hessian Administration for Soil Management and Geographical Information, HVBG, Wiesbaden, Germany) of the study area with the location of the nature reserve, and (d) elevation variation of the study area with the location of the groundwater wells. The black border depicts the boundary of the hydrological (sub-)models.

Land use

The study area experienced a large decrease (up to 90%) of flood meadows in the 1980s. Disastrous floods in 1983 destroyed large parts of the summer embankments in the study area. Due to high remediation costs, about 300 ha of agricultural land (equally distributed between meadows and forest) were made available for restoration measures instead (Dister et al., 1992; Hölzel, 2006). In the 1990s, another 100 ha in the Knoblochsaue were converted to grassland (Hölzel, 2006). The flood meadows harbor numerous typical, rare and endangered species. Typical and endangered species like *Arabis nemorensis*, *Cnidium dubium*, *Iris sibirica*, and *Viola pumila*, reach their western limit here. In this regard, the nature reserve is of particular importance (Donath et al., 2009; Hölzel et al., 2002).

Equally important for the nature reserve are the hardwood and softwood forests, which comprise up to 1160 ha of the nature reserve. The area covered by forest in the Kühkopf has doubled since the 1800s to 800 ha. The area covered by forest in the Knoblochsaue remains nearly unchanged from the 1800s to present (350 – 360 ha) (Gonnermann, 2002; Reif et al., 2016).

Soils

The nature reserve is located in the area of the gently-sloped meandering stretch with low flow velocities. This causes mainly fine sediments of the silt and clay compositions to be transported and deposited. The deposited layers of clay vary in their thickness, ranging from 30 up to 200 cm (Baumgärtel, 2004; Reif et al., 2016; Wiedner, 1990). Mainly representative in the active floodplain are the carbon-containing sandy-gravelly sediments (alluvial pararendzina) and carbon-containing silty-loamy sediments (alluvial gley, vega). In the fossil floodplain of the Knoblochsaue, carbon-containing clayey floodplain sediments dominate (pelosol) (Rosenberger, 2007; Wiedner, 1990).

The combination of relatively warm and dry conditions in the summertime with the fine-grained alluvial soils leads to a variable soil water balance, a very rapid decrease in plant-available water, and development of desiccation cracks (Burmeier et al., 2010).

Meteorological conditions

Meteorological information is available from the weather station in Darmstadt (N: 49°52.85', E: 8°40.67'). The annual precipitation is about 730 mm (winter: 166 mm, spring: 170 mm, summer: 225 mm, autumn: 169 mm), and the mean annual temperature is 10.5 °C (winter: 2.3 °C, spring: 10.4 °C, summer: 18.8 °C, autumn: 10.5 °C) between 2000 and 2016. (Figure 1.2).

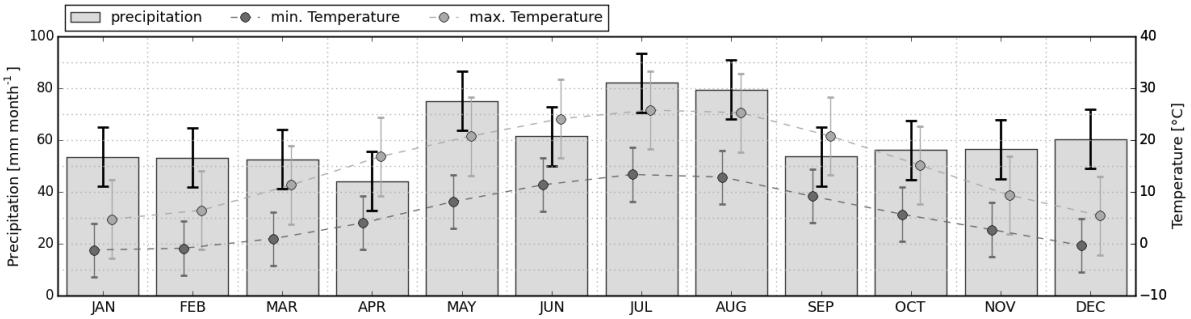

Figure 1.2: Mean ± SD monthly rainfall and mean ± SD monthly minimum/maximum temperature recorded at Darmstadt weather station between 2000 and 2016.

Hydrological conditions

The Nierstein-Oppenheim gauging station (N: 49°51.89', E: 8°21.14') is located northwards, approximately 4 km downstream from the study site. The mean water level between the years 2000 and 2015 was 82.95 m. The critical level of 4 m above mean water level, which floods the hybrid floodplain, was exceeded about 55% of the days in this period. The lowest measured water level was recorded at 81 m (28/09/2003), and the highest was 87.10 m (06/04/2013).

Hydrogeological conditions

About 28 groundwater wells are located around the study site, of which 16 are relevant and used for the hydrological models of the study area (Figure 1.1, d). The water levels are observed in weekly time steps by the Hessian State Office for Conservation, Environment and Geology (HLNUG). The groundwater wells are located between 89 and 3757 m away from the cut-off meander and between 573 and 5375 m away from the Rhine River. In general, the mean annual fluctuation of the water level at the wells decreases with increasing distance from the Rhine River. The only exceptions are the groundwater wells behind the embankment, showing a lower annual fluctuation, despite a short distance to the Rhine.

Installation to improve data availability

In the interest of modeling water levels on high temporal resolution and due to the lack of such observation data, several Odyssey capacitance probes (Odyssey by Dataflow Systems Pty Ltd, Christchurch, New Zealand, http://www.odysseydatarecording.com) were installed at different locations on the study site. The water level was monitored in hourly time steps with a measurement accuracy of 0.8 mm (Dataflow Systems Limited, 2018). The recording started on July 1st, 2015 at four sites, spread over the study area. Another observation point was added two weeks later on July 15th, 2015. Due to high water levels flooding the sensors and/or technical issues with the sensors, there are several gaps in the records. After August 24th, 2016 only three capacity probes were in use.

1.3.2. Surface water-groundwater interaction model

Physically based, spatially distributed models attempt to represent the physical processes of the real world and are thus a valuable tool to assess the three-dimensional nature of floodplains (Bernard-Jannin et al., 2016). The main advantage of such physically based models is their ability to simulate the interaction between the surface and the subsurface domain. There are two possible methods for simulating this interaction: coupled models (also referred as loosely coupled models) containing two or more individual models that are coupled by the exchange of the model results, and integrated models (also referred as fully coupled models) that solve the surface and subsurface water flow equation simultaneously (Barthel and Banzhaf, 2016; Condon and Maxwell, 2013). Existing models differ in the spatial resolution and the governing equations, strategies, and technical solution for coupling (Maxwell et al., 2014).

The Catchment Modeling Framework (CMF, Kraft et al., 2011) represents a very suitable tool box for simulating the water fluxes on a floodplain with a model tailored towards the research question at hand. Its major advantage is the flexible modular framework, offering a wide range of possible hydrological model setups. A further advantage is the extendibility of CMF. Individual processes can be adapted to the available observation data, and subroutines can be replaced or added. CMF is based on the concept of finite volume method (Qu and Duffy, 2007), allowing for the use of an irregular grid for the discretizing of lateral spatial continuous water storage.

1.3.2.1. Model set up

The study area was divided into two parts ("Knoblochsaue" and "Kühkopf"), parameterized, and simulated independently. Each submodel was further discretized into irregular polygons according to elevation and land use. The allocation was performed in a way that variation in elevation is kept to a minimum. Larger differences in height within one polygon are caused by special conditions, for example, embankment, ponds, or local depressions. The submodel area of the Knoblochsaue has a height variation between 81.35 m and 90.36 m a.s.l. in total. The height variation within one polygon is between 0.88 m and 6.92 m (*mean height difference within one polygon*: 3.19 ± 1.12 m, *mean size of polygons*: 5.4 ± 7.7 ha, *N:* 272 polygons). The height variation of the Kühkopf area is almost twice that of the Knoblochsaue with 16.05 m, ranging from 81.10 m to 97.15 m a.s.l.. The height variation within one polygon is between 0.93 m and 7.27 m (*mean height difference within one polygon*: 3.72 ± 1.13 m, *mean size of polygons*: 7.43 ± 6.68 ha, *N:* 263 polygons). As fully distributed and coupled subsurface-surface water models generally require a high computing time, even increasing with spatial resolution (Clark et al., 2015), attempts were made to find a balance between the complexity and accuracy to maintain an acceptable computational time.

Both submodels are based on the same modeling concept and vary only in their spatial representation, i.e., the arrangement and quantity of grid cells. Thus, the following description refers to both sub-models, if not explicitly stated otherwise.

The models include the key processes to represent the water pathways accurately (Figure 1.3). For simplicity, the model was set up as single layer groundwater flow model, i.e., there is no vertical discretization. The saturated flow is calculated with a Darcian approach. The presence of surface water, throughfall, and infiltration capacity determine the infiltration rate. Precipitation is split into two parts: precipitation reaching the surface of the polygon directly, and intercepted rainfall. The latter either evaporates or reaches as canopy throughfall the surface water of the polygon, calculated with the interception model from Rutter and Morton (1977). Infiltration in the soil is calculated according to the Richard's equation. The potential evapotranspiration rate is calculated with the FAO version of the Penman-Monteith equation (Allen et al., 1998). The actual evapotranspiration rate is limited by drought stress, and is calculated from the groundwater level, the canopy wetness, and height of the surface water.

The adjacent Rhine River is directly connected to the groundwater of the floodplain and is mainly responsible for the groundwater level changes and the riverside inundation on the active floodplain. Observed water levels are implemented as a Dirichlet boundary condition through Open Water Storages. For the Kühkopf submodel, the extrapolated water level of the cut-off meander of the Rhine was used as a surrounding Dirichlet boundary condition. At the landsite area (Knoblochsaue: northeast, Kühkopf: southeast), the data from the groundwater wells are implemented likewise as Dirichlet boundary condition.

Realistic estimations of initial groundwater levels were obtained via external drift kriging (Goovaerts, 1997) with the available groundwater data.

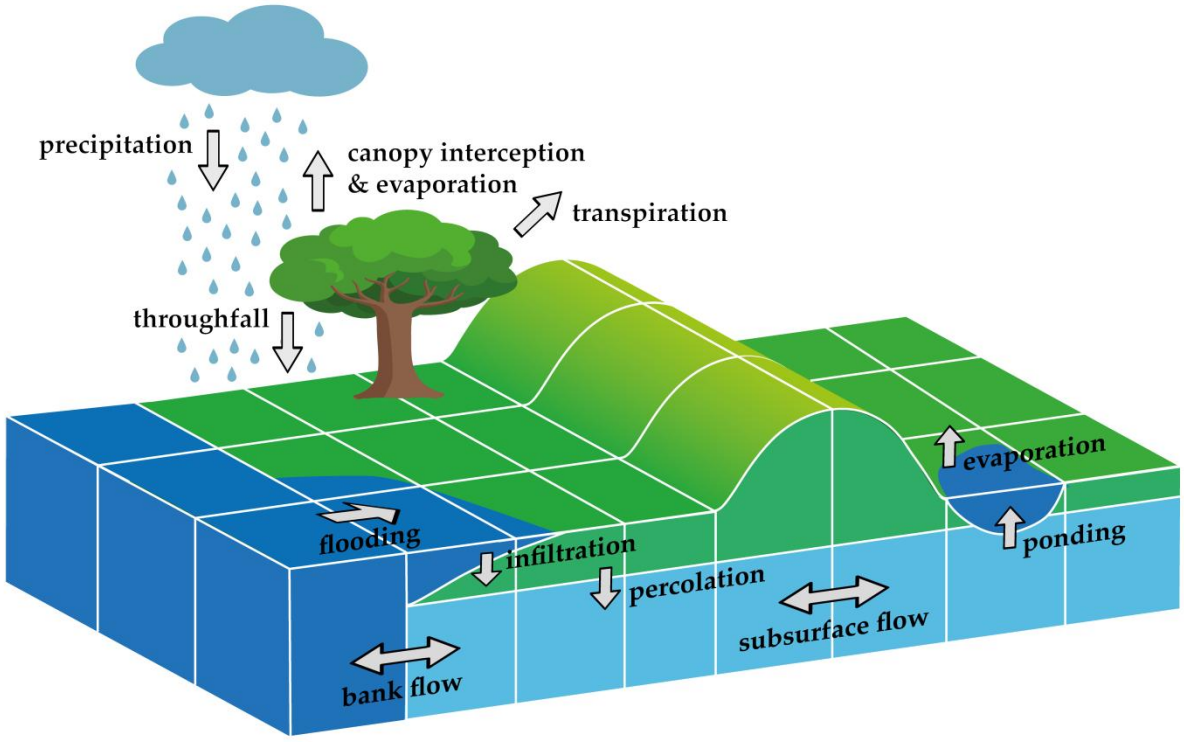

Figure 1.3: Three-dimensional sketch of the study area Kühkopf-Knoblochsaue with typical structures (darker blue: Rhine River and surface water, lighter blue: groundwater, green: flood meadow with embankment and depressions) and the relevant water flux processes simulated by CMF.

1.3.2.2. Surface water flow

CMF is principally capable of simulating surface water flow as a kinematic or diffusive wave. For flat areas, like the study site, the diffusive wave represents a feasible approximation for the surface water flow (Singh, 1996). However, this approximation requires long computing times, especially during large flooding events. To overcome these long computing times, the St. Venant surface flow is replaced by a newly developed simplified function, introduced as the "flood-wave scheme." This function calculates the distribution of the surface water at steady-state for each day, based on the water level of the Rhine River. The concept is straight forward: each day, the water level height of the Rhine River is compared to its neighboring polygons. If the water level of the Rhine River is higher than the surface of the polygons, the surface water level of polygons are set to the same level as the water level of the Rhine River. The surface water potential of all other cells is recursively adjusted if they can be flooded by an already flooded cell (Figure 2.1).

1.3.2.3. Model uncertainty

The model setup was designed as a parsimonious model solution. The reduction to key processes, the single-layer groundwater model, and particularly the simplification of surface water flow equation resulted in a significantly reduced computational run time. This model setup allowed for the investigation of the parameter uncertainty of the model following a GLUE-like method (Beven and Binley, 1992).

For both submodels, the same soil parameters were calibrated: saturated conductivity (m d^{-1}), porosity (m^3 m^{-3}), residual water content (m^3 m^{-3} pores m^{-3} soil), and soil thickness (m). As the parametric equations describe the processes of the real-world aggregated in space and time, the parameters are considered as effective, without a direct physical representation.

With the Statistical Parameter Optimization Tool for Python (SPOTPY) by Houska et al. (2015), 5000 parameter sets were generated, using a Latin hypercube sampling approach (McKay et al., 1979). The root-mean-square error (RMSE) was used as an objective function, rating the performance of the parameter set in its ability to simulate the observations.

1.4. Results and discussion

1.4.1. Correlation of Rhine water level with groundwater level

The records of the groundwater levels show a high correlation with the water level of the Rhine. The floods in May and June of 2016 are especially well reflected in the groundwater level in the wells 527026, 527200, and 527283. The groundwater levels in well 527200 show clear fluctuations in the summer of 2017, which follow the course of the water level of the Rhine. However, since from summer 2016 to spring 2017 no correlation between the fluctuations in the Rhine water level and the groundwater level is recorded, this strong reaction of the groundwater level to the water level fluctuations of the Rhine should be treated rather critically. A measurement error should therefore be considered here.

The time differences between the occurrence of flood peak in the Rhine water level and that of the groundwater level (as clearly distinguishable individual events) are estimated to be 48.2 h on average for the groundwater well 527026, and 88.6 h for the groundwater well 527200. Subplots (e) and (f) depict negative values, caused by the location of the Nierstein-Oppenheim gauging station (about 4 km downstream the study area). Therefore, there is also a temporal gap between the Rhine water level in the vicinity of the study area and at the gauging station. The negative values likely show a very short reaction time of the groundwater to an increase of the Rhine water level.

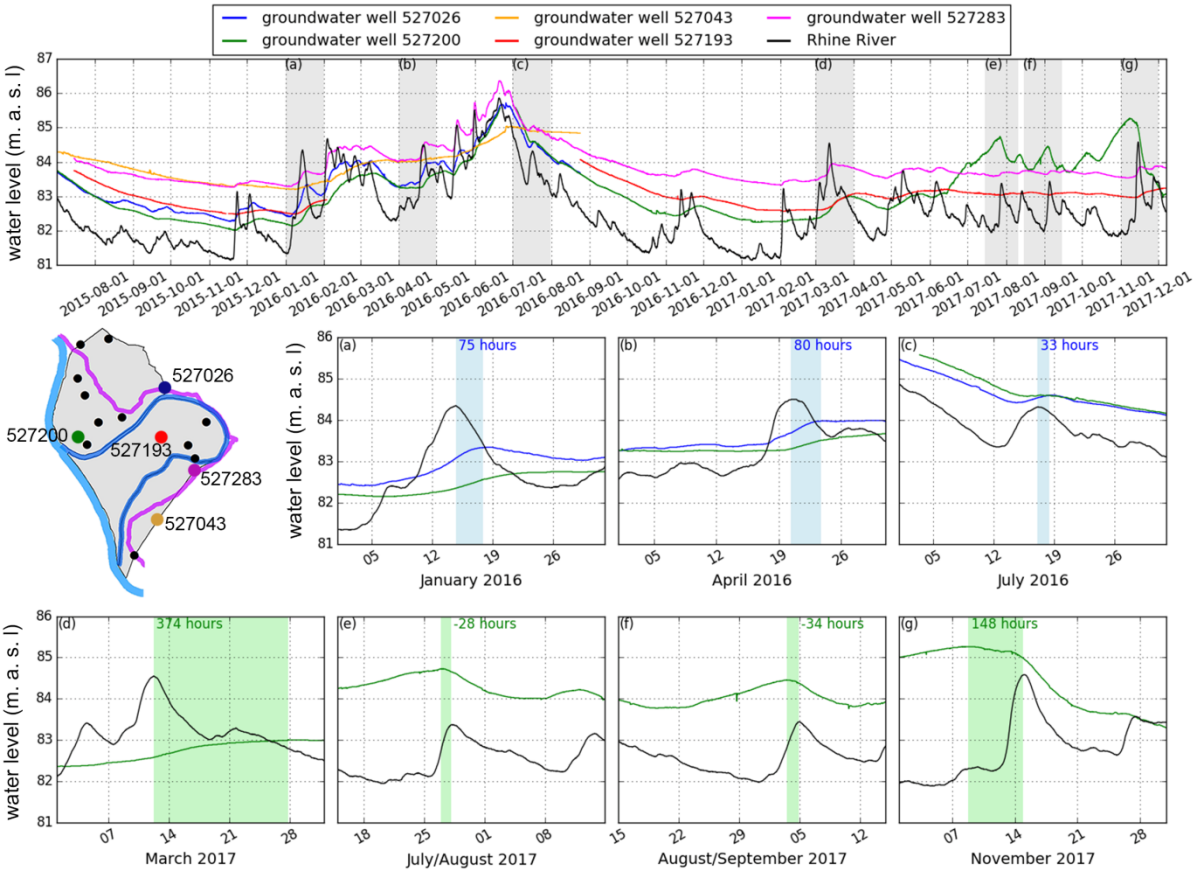

Figure 1.4: Time series of the hourly measured groundwater levels for five different groundwater wells between July 2015 and December 2017 and the time series of the Rhine for the Nierstein-Oppenheim gauging station (top). Subplots a-c (middle) depict details of the time series for well 527026; subplots d-g (bottom) depict details of the time series for well 527200. The time gap between the peaks of the water levels is given in the top of the subplot. The map in the middle left shows the locations of the different depicted wells. Grey: study area, blue: Rhine and cut-off meander, violet: embankment, black: groundwater wells.

1.4.2. Model calibration and validation

The results of the model calibration and validation are described in detail in Chapter 2 and are published in the paper:

> *Maier, N.; Breuer, L.; Kraft, P. (2017). Prediction and uncertainty analysis of a parsimonious floodplain surface water-groundwater interaction model, Water Resources Research, 53, 7678–7695, doi: 10.1002/2017WR020749.*

Additionally, the publication shows a performance test of the simplified surface water flow equation described in Chapter 2.

The weekly groundwater levels of six (Knoblochsaue) and four (Kühkopf) groundwater wells were used to calibrate and validate the submodels. The calibration period comprised 2.5 years (01/08/2002 – 30/06/2004), including a large fraction of the hydrological variability, while the validation period comprised 9.5 years (07/01/2004 – 31/12/2013). The cutoff criterion to judge a model run as a behavioral run, i.e., an acceptable simulation, was set to 0.26 m for the Knoblochsaue and 0.38 m for the Kühkopf for the mean RMSE over all groundwater wells considered for the calibration of the respective submodel. The mean RMSE of both submodels decreases by 0.2 m in the validation period compared to the calibration period (Knoblochsaue: $RMSE_{calibration}$ = 0.25 m; $RMSE_{validation}$ = 0.23 m. Kühkopf: $RMSE_{calibration}$ = 0.38 m; $RMSE_{validation}$ = 0.36 m). The range of individual RMSEs varies up to 0.41 m (Knoblochsaue) and 0.67 m (Kühkopf) for the calibration period. While the upper boundary of individual RMSEs decreases for validation period for the Knoblochsaue (0.35 m), it increases for the Kühkopf (0.79 m).

Overall, the performance of the Knoblochsaue submodel showed a much smaller RMSE than for the Kühkopf submodel, i.e., the Knoblochsaue submodel is performing much better. This is clearly noticeable in the uncertainty ranges, which are much larger in the Kühkopf submodel than in the Knoblochsaue submodel (exemplarily shown for two groundwater wells in Figure 1.5). The inferior performance of the Kühkopf model is likely caused by the terrain structure, the simplified representation of it, and the corresponding flow paths. To improve the model, the topographical structure should primarily be delineated in a more detailed way. However, this would mean that the model's required computational time would increase significantly due to the higher number of polygons and processes (Clark et al., 2015).

For both submodels, the ranges of parameters for residual wetness were equal (0.10 – 0.30 m^3 m^{-3} pores m^{-3} soil). The range of the soil thickness (Kühkopf: 3.60 – 9.76 m; Knoblochsaue: 5.10 m – 8.00 m) and the porosity (Kühkopf: 0.10 – 0.33 m^3 m^{-3}; Knoblochsaue: 0.30 – 0.34 m^3 m^{-3}) were larger in the Kühkopf submodel than in the Knoblochsaue submodel. Saturated conductivity resulted in lower values in the Kühkopf submodel (160 – 1779 m d^{-1}) than in the Knoblochsaue submodel (2193 – 4986 m d^{-1}).

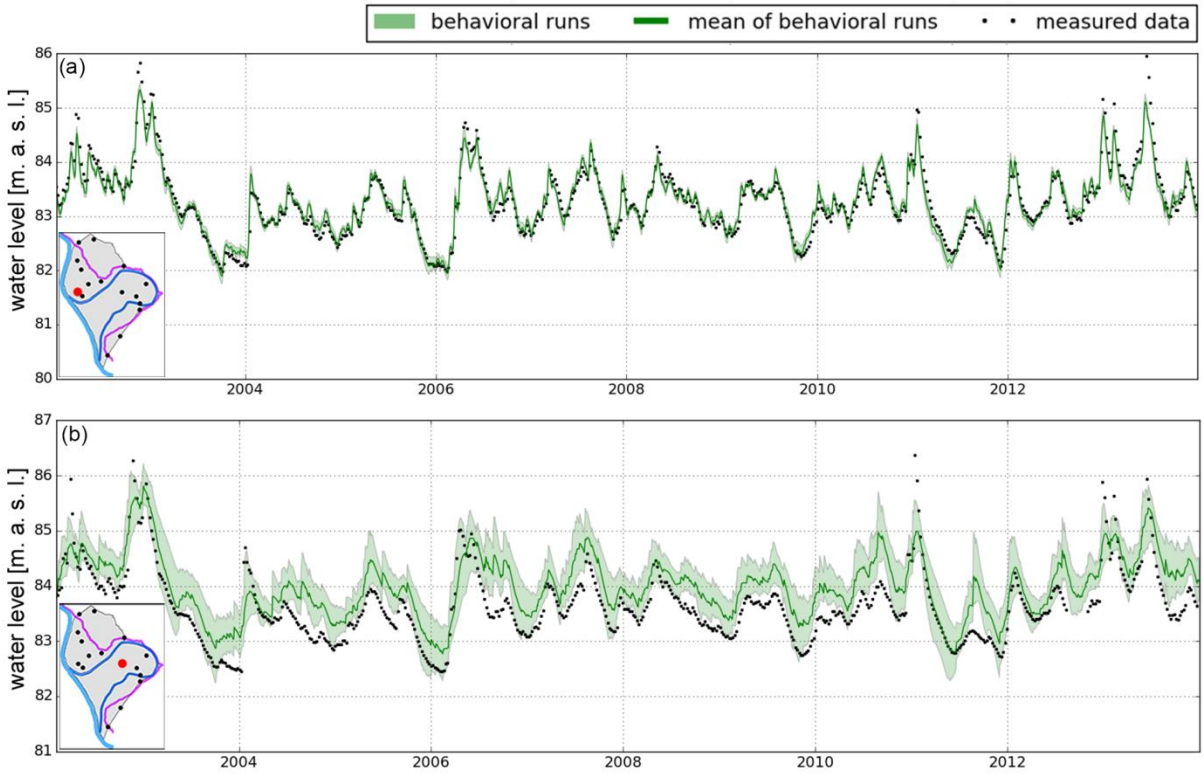

Figure 1.5: Time series of the simulated water levels by the CMF model, compared to the measured data by the HLNUG for each of the groundwater wells in the Knoblochsaue (top) and the Kühkopf (bottom). The map (bottom left) shows the location of the relevant groundwater well (red) and the remaining groundwater wells (black) in the study area. Grey: study area, blue: Rhine and cut-off meander, violet: embankment, black: groundwater wells.

To test whether the weekly available groundwater data are sufficient for model calibration, the model performance was also evaluated using the measured daily groundwater levels. An example of two groundwater wells is shown in Figure 1.6. In the Knoblochsaue reserve (Figure 1.6, top), simulations follow the daily water level measurements of the odyssey capacitance probe very well (RMSE = 0.20 m). In contrast, the simulations in the Kühkopf

(Figure 1.6, bottom) show much larger fluctuations than observed by the odyssey capacitance probe (RMSE = 0.56 m).

To summarize, the simulations of the groundwater levels of the Knoblochsaue show a low RMSE, based on both weekly and daily water levels. The simulations of the Kühkopf are less precise, and the simulations do not follow the real water levels measured on daily time steps. Therefore, the Knoblochsaue submodel is recommended for further applications.

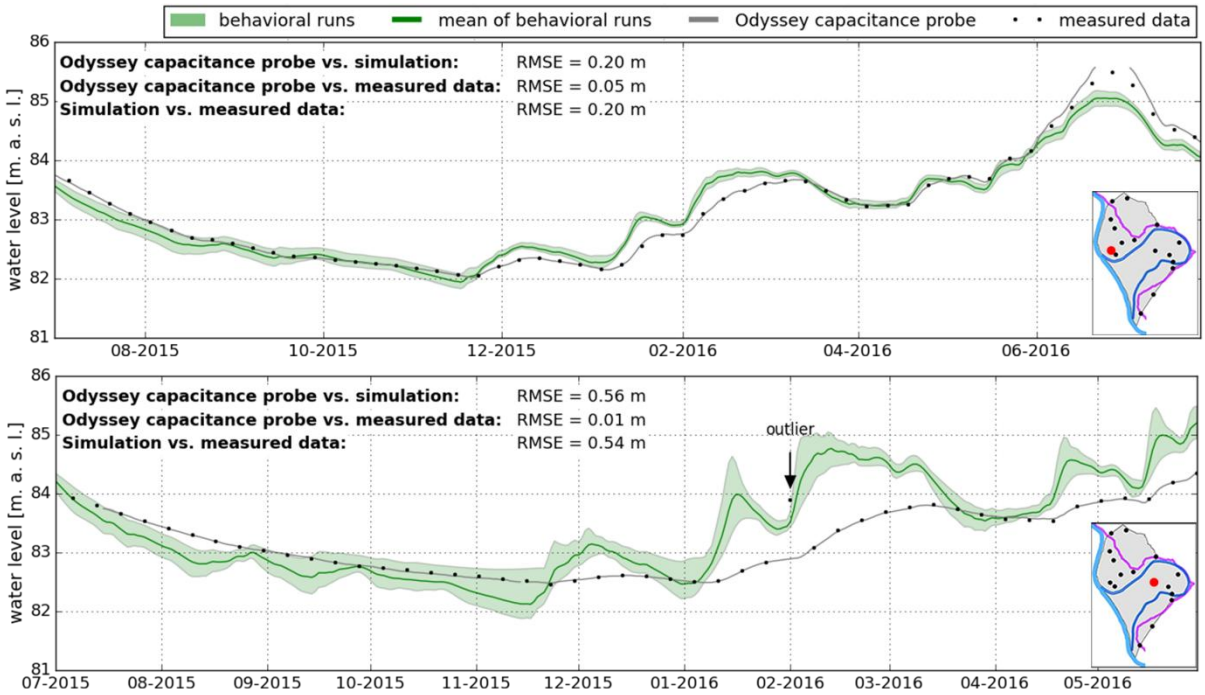

Figure 1.6: Simulation of the CMF model, compared to the measured water level by the capacity loggers and the measured data by the HLNUG, exemplarily shown for groundwater wells in the Knoblochsaue (top, 1.7.2015 – 27.7.2016) and the Kühkopf (bottom, 1.7.2015 – 30.5.2016). Performance as RMSE is shown for all possible comparisons. Measured data by the HLNUG include one outlier measurement, which is not included in the estimation of the RMSE. The map (bottom right) shows the location of the relevant groundwater well (red) and the remaining groundwater wells (black) in the study area. Grey: study area, blue: Rhine and cut-off meander, violet: embankment, black: groundwater wells.

1.4.3. Projecting floodplain inundation under climate change

The results of this chapter are described in detail in Chapter 3 and published in the paper:

> *Maier, N.; Breuer, L.; Chamorro, A.; Kraft, P.; Houska, T. (2018). Multi-Source Uncertainty Analysis in Simulating Floodplain Inundation under Climate Change. Water, 10, 809, doi: 10.3390/w10060809.*

Based on the previously described study's results, the impact of climate change on the inundation characteristics was evaluated for the Knoblochsaue, because this submodel performed much better than the Kühkopf submodel. Therefore, a modeling framework of bias-corrected climate model data was set up to project future discharge of the Rhine River via a rainfall-runoff model, and the groundwater and surface water level via the CMF model. Therewith, the contribution of multiple uncertainty sources within the modeling framework was assessed.

The submodel of the Knoblochsaue reserve was slightly modified for this analysis, due to the limited availability of data for the future. The original model was forced by three input sources: (1) climate data, i.e. rainfall, temperature, relative humidity, and wind speed; (2) the water level of the Rhine; and (3) the water level data of three groundwater wells on the upslope (landside) boundary.

Climate data were selected from two general circulation models (GCMs) from the Coupled Model Intercomparison Project Phase 5 (Taylor et al., 2012a), namely: HadGEM2-ES (later abbreviated as HadGEM) from the Met Office Hadley Centre and MPI-ESM-LR (later abbreviated as MPI-ESM) from the Max Planck Institute for Meteorology. Three representative concentration pathways (RCP) were considered: RCP 2.6 (low concentration), RCP 4.5 (medium concentration), and RCP 8.5 (high concentration). All climate data were bias corrected with the quantile mapping method (Maraun et al., 2010; Themeßl et al., 2011).

The data for the second input source, the water level of the Rhine River, were generated using a rainfall-runoff model. For this data generation, the HBV model (Bergström, 1995; Lindström et al., 1997) was used as a conceptual semi-distributed hydrological model to simulate the discharge of the Rhine. After calibration and validation, the model was forced with the projected and bias corrected climate data. To assess the uncertainty, the parameter and the predictive uncertainty were considered. The parameter uncertainty was assessed by the GLUE methodology (Beven and Binley, 1992). From 100,000 simulations with parameter

sets that were generated following a Latin hypercube procedure, the best 10% were kept as behavioral runs. With these selected parameter sets, future discharges were projected, and the associated uncertainty was estimated. Synthetic time series (5^{th}, 50^{th}, and 95^{th} percentiles) were generated from all behavioral runs and transformed to daily water levels by an existing rating curve. Predictive uncertainty, representing the aggregated effects of data and model structural errors of the best model run, was estimated by means of a statistical model error, for which the Box–Cox transformation was used (Box and Cox, 1982). The estimated parameters for the transformation equation for the past were then applied to discharge simulations under climate change. The three different synthetic time series were generated via the same process. Finally, these synthetic time series were used as input data for the CMF model.

As no groundwater data are available for the future, the upslope boundary condition was replaced with a no-flow boundary. A subsequent recalibration of the model resulted in a similar performance and optimal parameter sets.

Due to the numerical stability and computation effort, only one soil parameter set for the CMF model, based on numerical stability and performance, was used for the future projections. Thus the parameter uncertainty of the CMF model is not considered. With two GCMs, three RCPs, five water level projections for the Rhine, and one soil parameter set for the CMF model, 30 different spatio-temporal simulations of the water level and inundation of the floodplain were generated as future projections. Two periods were defined for the projections: near future (2021–2050) and distant future (2071–2100). At the end, two indicators were used to characterize the inundation characteristics: the mean annual inundation days and the mean inundation period. Inundation was defined as surface water level higher than 5 cm.

Comparisons of the different projections of annual inundation days resulted in the following ourcomes: (a) under the HadGEM, the spatial extension and the magnitude of annual inundation days were larger (Figure 1.7, top); (b) under the MPI-ESM model, similar annual inundation days for all RCPs and both time periods were projected, whereas under the HadGEM model the projections varies more between RCPs (Figure 1.7, middle, light grey); (c) the simulations considering the different uncertainties of the projected Rhine water level (parameter and predictive uncertainty) showed the same pattern as the RCPs; and

(d) considering the predictive uncertainty, the spatial extension and magnitude was slightly higher than when the parameter uncertainty is considered (Figure 1.7, bottom, darker grey)

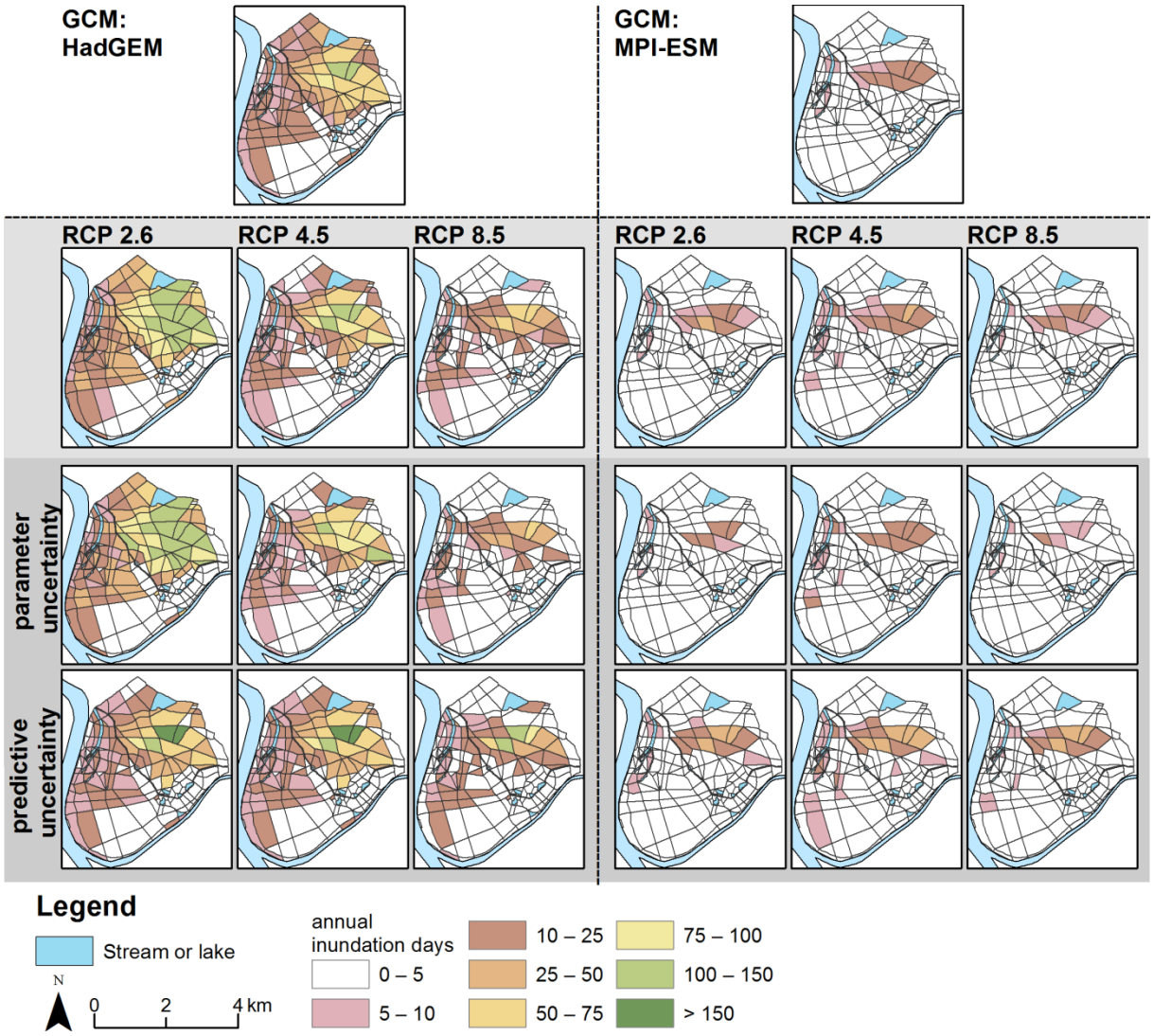

Figure 1.7: Annual inundation days for the near future (2021–2050), divided between the GCMs (top), the GCM-RCP combinations (middle, light grey), and the combination of GCM, RCP, and uncertainty of the HBV model (bottom, darker grey).

The comparison of the projected annual inundation days of the near and distant future to simulated annual inundation days of the past (2002–2015) showed similar patterns: (a) under the MPI-ESM model, similar changes (decrease of annual inundation days) were projected for all RCPs and both time periods; (b) compared to the HadGEM model, the spatial extension of areas affected by changes under the MPI-ESM model was smaller;

(c) the magnitude of changes was much larger under the HadGEM model than under the MPI-ESM model; and (d) the variation in the RCPs was much larger under the HadGEM model than under the MPI-ESM model in terms of absolute values (Figure 3.4 and Figure 3.5).

In summary, the differences in the spatial extend and magnitude of mean annual inundation days and mean inundation periods were larger between the GCMs than between the RCPs (with some exceptions), and between the different used input data (i.e., different predicted water levels of the Rhine. Therefore, further studies on the impact of climate change on inundation characteristics should focus more on the uncertainties caused by the climate models.

1.4.4. Species distribution modeling in floodplain habitats

The results of this chapter, with a more detailed focus on the habitat model, are described in Chapter 4 and are submitted to the journal *Ecohydrology* under the title:

> *Gattringer*, J.P., Maier*, N.; Breuer, L.; Otte, A.; Donath, T.W., Kraft, P.; Harvolk-Schöning, S. (2018). Modeling of rare flood meadow species distribution by a combined habitat-surface water-groundwater model. *shared first-authorship*

Numerous flood meadow species have adapted to the specific hydrological regimes of floodplains. To predict spatially explicit suitable locations for species, species distribution models (SDMs) are a good choice. They are based on statistical correlations between observations and the environmental conditions at the observation point (Elith and Leathwick, 2009; Guisan and Thuiller, 2005; Peterson et al., 2011). In the context of flood meadow species, such environmental variables would involve information on inundation length and depth, as well as recurrence intervals of floods and soil moisture conditions.

Hydrological information implemented in the SDM as environmental variables (also called hydrological predictors) is derived from the developed CMF model. The simulated long-term time series of the water level of both submodels were transformed to static hydrological predictors by downscaling (inverse distance weighting) the water level of the polygons from the CMF model to a high spatial resolution raster (5 x 5 m). From over 80 different a priori conceived hydrological predictors, the 15 most important ones were selected by an iterative

process and based on species-specific flooding experiments (Gattringer et al., 2017, 2018). Hydrological predictors include, for example, information on groundwater level range, standard deviation, or average and longest durations below/above certain groundwater level thresholds. Additionally, one meteorological (longest period of wet days) and three morphological predictors (height above mean sea level, distance to the Rhine or the cut-off meander and distance to any water surface) were added as environmental variables.

In order to test the significance of the high temporal and spatial resolution hydrological predictors obtained from the CMF model (sgm: surface water-groundwater model), two other datasets of hydrological predictors were generated. The first set of data used for comparison was based only on weekly measured groundwater levels at the 16 different sites in the floodplain (gww: groundwater wells). The second set of data was based only on the water level of the adjacent Rhine River (riv: river). Additionally, the model performance without any hydrological information (nhy: non-hydrological), i.e., with only meteorological and morphological predictors, was tested.

The results focus mainly on floodplain meadow species (*Arabis nemorensis*, *Galium boreale*, *Peucedanum officinale*, *Sanguisorba officinali*, *Silaum silaus*, *Thalictrum flavum*, and *Veronica maritima*) after Burkart (2001) and on rare and engendered species (*Arabis nemorensis*, *Bromus racemosus*, *Galium boreale*, *Iris spuria*, *Peucedanum officinale*, *Serratula tinctoria*, and *Veronica maritima*), as they are specialized species and species valuable to consider for restoration projects. For both groups, the SDM with hydrological predictors derived from the CMF model is superior to the other setups, i.e., setups considering hydrological predictors from groundwater level or river water level and those not considering any hydrological predictors (Figure 4.3). Testing several combinations and quantities of predictors led to the conclusion that six to ten specific predictors are needed to satisfactorily simulate habitats and occurrences for rare and endangered species. The most frequently used hydrological predictors included parameters indicating inundation length and dry or wet conditions. These results reflect the complexity of the habitat requirements of flood meadow species being able to cope with both flooding and drought periods (Burkart, 2001). Even though not all the 15 hydrological predictors are essential for simulating all species, it became clear that removing selected predictors for model simplification resulted in a model failure for several species. Thus, it can be concluded that a large set of hydrological predictors is required to be

able to simulate whole plant communities with their diverse specific eco-hydrological requirements.

The superior results of the habitat model including hydrological predictors from the CMF model became visible when the time series were analyzed in more detail. The hydrological model is a respectable representation of the natural conditions in a high spatial and temporal resolution, including components such as climatic conditions, soil properties, surface water distribution, surface water-groundwater interaction, and groundwater level. Thus, the model is able to reflect the soil moisture content, altering the water storage capacity of the soil and thus driving the flood extent, flood duration, and inundation height of water in the floodplain. Inundation caused by high water levels of the Rhine can be attenuated if the soil is capable of draining a large volume of water, but at the same time, large floods can occur when the soil is already saturated. The CMF model is capable of representing such conditions. For the two days shown in Figure 1.8, predictors based on the CMF model would result in different values, whereas predictors based on the water level of the Rhine would result in the same value, because the water level of the Rhine is the same on both days.

Overall, creating a habitat model with predictors, derived from perfectly spatially distributed hydrological measurements would be ideal. However, this is nearly impossible due to high costs. A few sporadic or poorly distributed measurements lead to less dependable results, as those involve some failures in the representation. For example, the rapid reaction of groundwater to changes in the water level of the river cannot be represented. Thus, generating hydrological predictors from a hydrological model with an appropriate representation of the natural conditions in a high spatial and temporal resolution including various components (climatic conditions, soil properties, surface water distribution, surface water-groundwater interaction, and groundwater) seems to be a good compromise between cost and the objective to protect rare species.

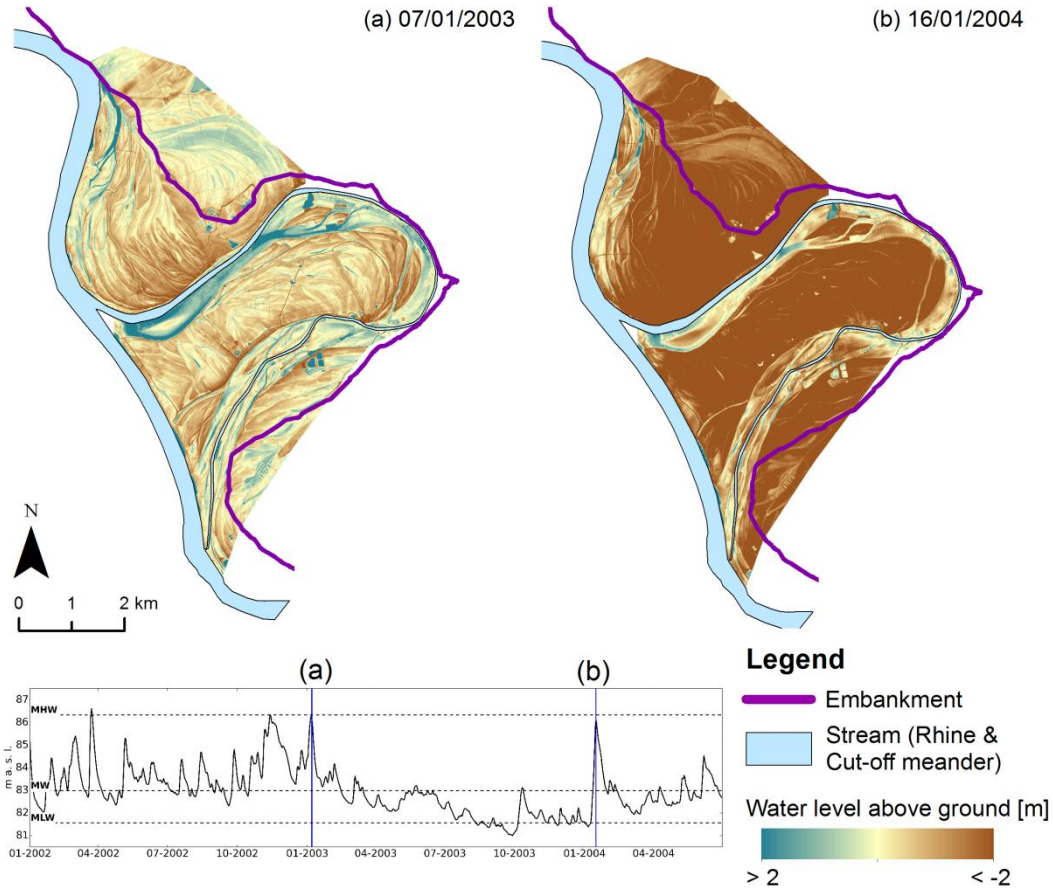

Figure 1.8: Representations of the groundwater and surface water level in the study site at two different days (07/01/2003 and 16/01/2004). The water level of the Rhine is depicted in the bottom of the figure (MHW: mean high water, MW: mean water, MLW: mean low water). The blue lines indicate the water level of the days depicted in the top of the figure. The water level of the Rhine was 86.15 m on both days.

1.5. Conclusion

This work showed new methods for determining spatio-temporally explicit predictions of groundwater, surface water and habitat interactions in riparian ecosystems. First, a hydrological model was developed, and then the model was linked with a species distribution model. The model was developed for the floodplain of the Rhine River that covers the Kühkopf-Knoblochsaue nature reserve. This region is very beneficial for the modeling approach, as abundant data particular for groundwater levels and species distribution are available.

The physically based, deterministic surface water-groundwater model build with the Catchment Modeling Framework is able to represent the main processes, which dominate the groundwater dynamic and surface water distribution. The established simplified surface water equation reduces the computation time of the model significantly, and it thereby allowed for facilitation of comprehensive model parameter uncertainty analyses. Additionally, long term projections of future conditions were possible. It was shown that in long-term simulation (a) the climate models introduced large uncertainties in the projections, and (b) depending on the climate model, the difference between the RCPs was much smaller than between the climate models. This indicates that we cannot yet quantify any potential benefit in greenhouse gas mitigation with regard to the investigated inundation characteristics.

From the simulated long-term hydrological dynamics of the floodplain, hydrological predictors were derived as inputs for the species distribution model. From over 80 different conceived predictors, 15 hydrological predictors were identified as the most important by an iterative process and based on species-specific flooding experiments (Gattringer et al., 2017, 2018). Furthermore, the SDM was extended with one meteorological and three morphological predictors. Comparisons with two other datasets of hydrological predictors showed that the quality of the SDM was significantly higher when using hydrological predictors gathered from the CMF model. Hydrological predictors based only on weekly measured groundwater levels at 16 different sites in the floodplain and based only on the water level of the adjacent Rhine River led to significantly worse, but still decent SDM results. The worst results were obtained by the SDM when no hydrological predictors were incorporated. These results emphasize the importance of taking hydrological conditions into account when modeling the distribution of species in a floodplain, as stated by other authors

(Kopeć et al., 2013; e.g., Leyer, 2005). Removing less frequently used predictors resulted in a model failure for several species, i.e., the prediction for those species is unsatisfactory. Thus, it can be concluded that a set of hydrological predictors, including predictors indicating drought and wet conditions, is required to be able to simulate whole plant communities with their diverse and specific eco-hydrological requirements.

Overall, the results underline the advantage of spatio-temporally explicit modeling of the hydrological regime on the floodplain in order to achieve valuable predictions of potential habitats, especially for rare and endangered floodplain species. Such scientific findings and approaches can make a major contribution to practical nature conservation.

1.6. Outlook

Useful for conservation measures is the prediction of potentially restorable areas or areas that offer suitable conditions for rare and endangered species in the future. The knowledge of such sites offers the opportunity to focus the restoration measures more precisely with a higher degree of sustainability and endurance for the future. In this respect, however, both climate and landscape changes must be taken into account. Therefore, implementations of predicted hydrological conditions in the established modeling framework were carried out in a first pilot study in order to project the species distribution under climate change. In the following the preliminary results are presented and discussed. Furthermore, possible land use changes and the possibility of implementation in the modeling framework are outlined.

1.6.1. Species distribution under climate change

The model framework of surface water-groundwater-species distribution proposed in this thesis can be used to project areas with high occurrence potential of species under climate change. As one example, the occurrence for rare and endangered species from the Red List (*Arabis nemorensis, Bromus racemosus agg., Inula salicina, Lysimachia vulgaris, Peucedanum officinale, Veronica maritima, Rhinanthus alectorolophus* and *Serratula tinctoria*) in the study area were projected for the years 2050 and 2100 under climate change conditions.

Due to large computational time and power, the modeling framework considered only one uncertainty source, namely the climate models. Those were identifies as the largest uncertainty source in previous climate change impact studies on this study area (Chapter 3)

and as well by other studies (Dobler et al., 2012; e.g., Kay et al., 2009; Prudhomme and Davies, 2009).

Future predictions were given by 15 regional climate models (RCMs) from the Coordinated Regional Downscaling Experiment EURO-CORDEX-11 (resolution: 0.11 degree), namely: (1) CNRM-CERFACS-CNRM-CM5-ALADIN53, (2) CNRM-CERFACS-CNRM-CM5-CCLM4-8-17, (3) CNRM-CERFACS-CNRM-CM5-RCA4, (4) ICHEC-EC-EARTH-CCLM4-8-17, (5) ICHEC-EC-EARTH-RACMO22E, (6) ICHEC-EC-EARTH-RCA4, (7) MOHC-HadGEM2-ES-CCLM4-8-17, (8) MOHC-HadGEM2-ES-RACMO22E, (9) MOHC-HadGEM2-ES-RCA4, (10) MPI-M-MPI-ESM-LR-CCLM4-8-17, (11) MPI-M-MPI-ESM-LR-RCA4, (12) MPI-M-MPI-ESM-LR-REMO2009, (13) NCC-NorESM1-M-HIRHAM5, (14) IPSL-IPSL-CM5A-MR-RCA4 and (15) IPSL-IPSL-CM5A-MR-WRF331F. For all RCMs, two representative concentration pathways (RCPs) were applied, namely RCP 4.5 and RCP 8.5.

As final results, the occurrence probabilities of the species were predicted by the SDM. In order to decrease the uncertainty of future predictions, the focus should be only on areas with a high degree of agreement between the projections under the different climate models. Therefore, a cutoff value of 10% or 20% deviation between the predictions was defined, so that areas with high uncertainty between the climate models were excluded. Additionally, areas that can be generally restored without the need to clear a forest, for example, are important for restoration measures. Therefore the mean occurrence probability of each species was intersected with the actual land use. Finally, these restrictions resulted in projections of occurrence probability for meadows with a small difference between the projections under different climate models.

The first results indicated for some species (*Arabis nemorensis, Peucedanum officinale, Serratula tinctoria*) a large agreement in the projected occurrence probability, considering both a 10% and a 20% difference in the occurrence probability between the RCMs. This is greatly reflected in a high percentage of restorable area (Figure 1.9, top). For other species (*Inula salicina, Lysimachia vulgari, Veronica maritima, Rhinanthus alectorolophus*), a larger area is suitable for restoration when assuming a difference between the projections of the RCMs of 20% as satisfactory, instead of a difference of 10%. The area with occurrence potential significantly decreases for all species if only areas with an occurrence potential above 25% or 50% are considered (Figure 1.9, middle and bottom). There is little difference in the restorable area between RCPs, except in one case. For *Bromus racemosus agg.*, under the

RCP 4.5 a rather small restorable area is projected, and under RCP 8.5, it is much larger (Figure 1.10).

As mentioned, the climate models are only one uncertainty source when projecting future conditions. To consider the full range of possible climate change impacts, more uncertainty sources should be considered. It is recommended to (1) include a different method for the bias corrections of the climate data (e.g., Lafon et al., 2013; Teng et al., 2015), (2) utilize different rainfall-runoff models to assess the model structure uncertainties (e.g., Breuer et al., 2009), (3) use different parameter sets for the CMF model (e.g., Saha et al., 2017), and last but not least, (4) use different species distribution modeling techniques in order to consider the uncertainties of the species distribution model (Breiner et al., 2018; e.g., Pearson et al., 2006).

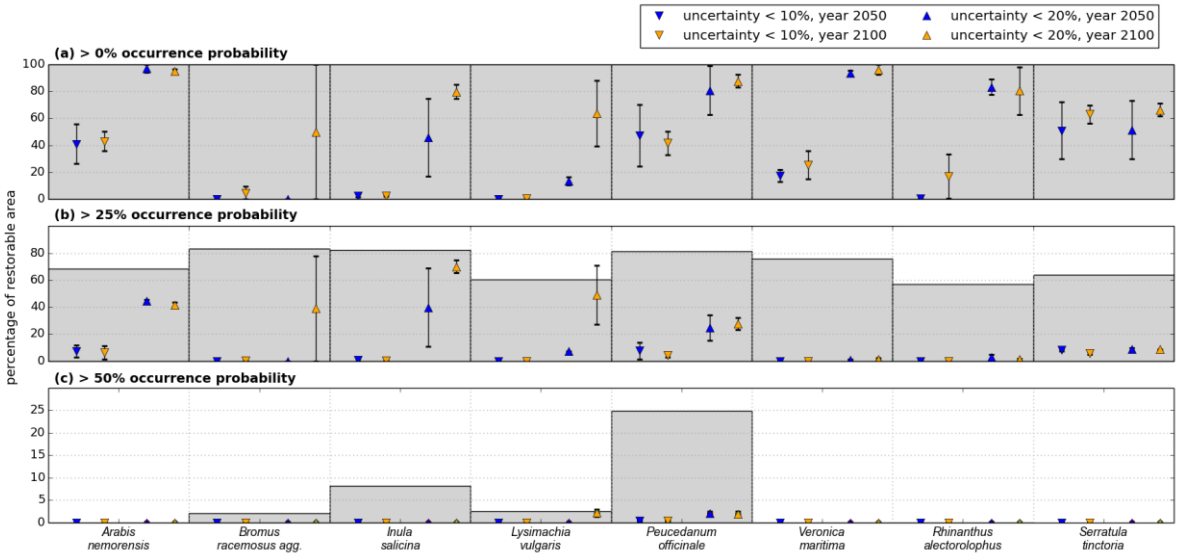

Figure 1.9: Percentage of restorable area with a difference of less than 10% (marker: downwards triangle) or less than 20% (marker: upwards triangle) between the projections under the different RCMs for eight species. The grey area/bar in the background depicts the predictions for the year 2016. The blue and orange colors depict the predictions of the year 2050 and 2100, respectively. The markers depict the mean of the projections under RCP 4.5 and RCP 8.5 with the corresponding errors. Restorable area is represented as different levels of occurrence probability (top: > 0% occurrence probability occurrence probability, middle: > 25% occurrence probability, bottom: > 50% occurrence probability).

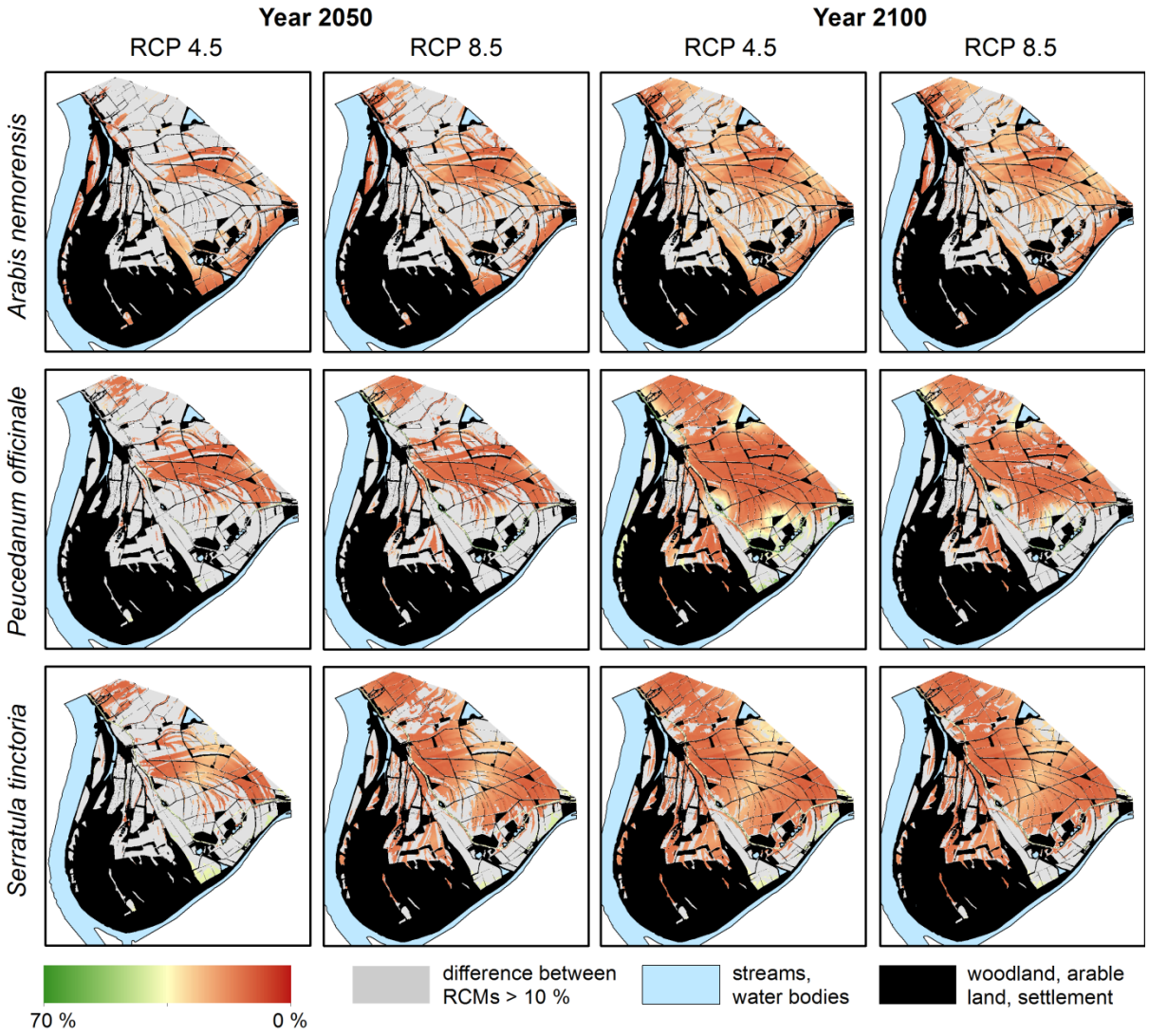

Figure 1.10: Occurrence probability (in percentage) for the species *Arabis nemorensis* (top), *Peucedanum officinale* (middle), and *Serratula tinctoria* (bottom) for the years 2050 and 2100 for both RCP 4.5 and RCP 8.5. Areas with a difference of more than 10% between the 15 RCMs are colored in grey. Streams and water bodies are depicted in blue. Areas that cannot be used for restoration, based on current land use, are marked in black.

1.6.2. Species distribution under land use changes

One could argue that in the future not only the climate will change, but also land use and management. Land use changes can be caused, for example, by humans or natural catastrophe. Naturally, there is an interaction between land use changes and climate change (Oliver and Morecroft, 2014). Usually the effect of the combinations of land use and climate change is much larger than the single effects on the impact on biodiversity (Oliver and Morecroft, 2014). Land use changes can cause an effect on the climate by altering the carbon balance in atmospheric and terrestrial pools (Bonan, 2008; Cramer et al., 2001). In addition, different land covers can cause changes in the climate, such as the changes in surface fluxes of radiation, heat, moisture, and momentum (Betts, 2005). On the other hand, climate changes can cause land cover and land use changes, for example, by altering the climatic conditions for vegetation types (Cramer et al., 2001).

Different scenarios can be imagined on how land use or morphological characteristics could be changed in the study area and therefore can cause changes in the habitat availability and suitability for plant species. As an example of land use changes, the decrease of agricultural land in the active floodplain or the decrease of grassland due to transformations into riparian forest could be considered here (Xu et al., 2017). At the same time, relocation of embankment, floodplain reconstruction, or river regulation are possible changes of the morphological structures (Moss and Monstadt, 2008; Schneider, 2010).

As climate changes and land use changes interact with each other, it is important to consider both in future projections. Both changes can influence water availability and thus cause changes in biodiversity and habitat availability. The CMF model offers the possibility of implementing such land use changes and can therefore project future water availability conditions. The complete model framework is thus capable of improving the accuracy of future predictions for species habitats. This, in turn, is vital for wetland management, especially where species conservation and other ecosystem service provision relies on detailed, high-resolution, hydrological conditions (Acreman et al., 2009).

Overall, it has been shown, that there are many opportunities to enhance conservation measures with scientific knowledge and modeling strategies. Therefore, the research in this field should be advanced further to open more possibilities for the promotion of restoration measures.

2. Prediction and uncertainty analysis of a parsimonious floodplain surface water – ground-water interaction model

This chapter is published in the journal *Water Resources Research* 53, pages 7678-7695, 2017. doi: 10.1002/2017WR020749

Nadine Maier[1], Lutz Breuer[1] and Philipp Kraft[1]

[1] Chair of Landscape, Water and Biogeochemical Cycles, University of Gießen, Germany.

Abstract

Floodplains provide a variety of hydrological and ecological functions and are therefore of great importance. The flooding frequency, as well as the height and duration of inundations are particularly relevant for ecosystem states and are dependent on the exchange between surface water and groundwater. In this study, we developed a fully distributed model approach to simulate distributed groundwater levels in a floodplain in Hesse, Germany (14.8 km^2). To overcome the problem of large computation times we simplified the surface water equation. Thus, the water surface of flooding is at the same level everywhere and the dynamic effect of the flooding is ignored. In this way, it was possible to run the model 5,000 times and investigate its parameter uncertainty using Latin hypercube sampling. Behavioral model runs were selected based on a threshold criterion of a mean root mean square error that was smaller than 0.26 m. All the simulated groundwater wells show an individual RMSE between 0.17 and 0.41 m for the calibration period. Regarding the parameterization, the model shows rather large variance in parameters that are capable of generating good simulations: a range of saturated conductivity of 2,793 m/day, porosity of 0.4 m^3/m^3, residual wetness of soil of 0.2 m^3/m^3/soil and range of soil thickness of 2.9 m.

2.1. Introduction

Floodplains, with their high water storage capacity, biological productivity and diversity, are among the most endangered ecosystems worldwide (Funk et al., 2013; Tockner and Stanford, 2002). Flood meadows are declining as a result of reduced hydrological dynamics (Tockner and Stanford, 2002) and land use changes (Wesche et al., 2012). The riparian zone of a floodplain often consists of fluvially derived sediments from ancient and current stream systems and represents a buffer zone between aquatic and terrestrial environments (Gregory et al., 1991; Woessner, 2000). Floodplains offer a wide range of hydrological and ecological functions. The basic functions of floodplains include the promotion of natural regulation and retention during hydrological extremes (Krause and Bronstert, 2007; Sophocleous, 2002), as well as the exchange of organic matter, nutrients and pollution between the river and the terrestrial ecosystem (Kiedrzyńska et al., 2015; Tockner et al., 1999). The driving factor for the eco-hydrological functions is the interaction of the surface water of the connected river, the surface water in the floodplain and the shallow groundwater (Hayashi and Rosenberry, 2002; Krause et al., 2007a). In addition to the exchange of surface water and groundwater, the timing, frequency and extent of inundation periods are important for floodplain ecosystems (Bernard-Jannin et al., 2016), as their habitats are sensitive to flooding (Russo et al., 2012).

The exchange between surface water and groundwater reflects a complex spatial and temporal pattern. A model of complete surface-subsurface flow should include and couple both components (Furman, 2008). Physically based, spatially-distributed models seem to be valuable tools for assessing the three-dimensional nature of the system, as they are capable of taking environmental characteristics into account (Bernard-Jannin et al., 2016). Several models of this problem domain exist, but differ in the governing equations, strategies and technical solution for coupling and the spatial resolution (Maxwell et al., 2014). Most models use the Richards' equation for subsurface flow and the Saint-Venant equation (kinematic, diffusive or dynamic wave) for surface flow (Furman, 2008).

Recently, Barthel and Banzhaf (2016) published a review of groundwater-surface water interaction with a focus on regionally integrated models. They identified four frequently used, fully coupled models (ParFlow, HydroGeoSphere, InHm, OpenGeosys). An intercomparison of seven different coupled subsurface-subsurface models (CATHY, HydroGeoSpehere, OGS, PIHM, ParFlow, PAWS, tRIBS-VEGGIE) for different benchmark problems was performed by Maxwell et al. (2014) for simulation times in the range of

minutes. They concluded that for simple test cases, the model agreement is good, but the disagreement increases with the complexity of the test cases. Although there are several models in the literature that are capable of simulating groundwater – surface water interactions, their application to case studies, different times and special scales is rare and they are more or less applied to experiments and small catchments (Barthel and Banzhaf, 2016; Ebel et al., 2007; Jones et al., 2008; Loague et al., 2005). Most models involve important simplifications. Full three-dimensional numerical solutions of saturated-unsaturated zone processes and surface and groundwater flow combination are not usable for large catchments because of their long computational run time (Bernard-Jannin et al., 2016; Krause and Bronstert, 2007). Bernard-Jannin et al. (2016) summarized, that these models can be only applied at the reach scale for short periods. The performance of such models is usually evaluated using data on river discharge and not groundwater heads. Distributed hydrological response data, such as piezometric data, are often not available, despite the importance for model calibration and evaluation, which is a barrier for meaningful comparison as stated by Sebben et al. (2013).

The interactions between the, usually very shallow groundwater and surface water, which is typically closely connected to rivers, is important for the eco-hydrological functions of floodplains (Butturini et al., 2002; Hancock et al., 2005). Surface water can enter the floodplain laterally across the channel banks or vertically across the floodplain surface through Darcy flow. Consequently, the groundwater level of the floodplain increases in response to increased stream stage (Hester et al., 2016).

Floodplains, as part of catchments, usually have a very flat area and their water balance is affected by groundwater processes and interactions with surface water. Both factors make watershed delineations of floodplains, based on only surface watersheds, difficult and questionable. The groundwater catchment boundaries of floodplains do not correspond to the spatial extent of the delineated surface watershed (Krause and Bronstert, 2005).

Pressure head gradients, hydraulic permeability of the hyporheic zone and riverbed geometry are controlling factors for the characteristics, intensity and direction of groundwater-surface water interactions (Krause and Bronstert, 2007; Sophocleous, 2002). This interaction is often characterized by high temporal and spatial variability (Krause et al., 2007a). Krause and Bronstert (2005) applied the IWAN model to the Havel River basin, in north east Germany and identified a 998 km^2 portion of the floodplain in which the water

balance is mainly affected by the surface water dynamic of the adjacent river. In further studies, they quantified the exchange fluxes across the groundwater and surface water and the groundwater recharge. They concluded that the groundwater–surface water interactions have a greater influence on the groundwater recharge dynamics in the floodplain than on the vertical groundwater recharge (percolation, root water uptake) (Krause et al., 2007a, 2007b). However, Pirastru and Niedda (2013) conducted a study in a floodplain aquifer in northwest Sardinia in Italy, and found that simultaneous processes of lateral groundwater flow and vertical recharge are responsible for the water table fluctuations, but the relative contribution of the flows varies with soil moisture content and groundwater depth.

Wu and Zeng (2013) described three main sources for uncertainties related to groundwater modeling: conceptual uncertainty, parameter uncertainty and input uncertainty. They conclude that the main focus in groundwater modeling is parameter uncertainty, which arise mainly from spatial and temporal variability and the scaling effect of parameters (Wu and Zeng, 2013). Two typical input variables in groundwater models are hydraulic conductivity and recharge. The different spatial scales of variation for these parameters are small compared to the size of the modeled region (Li et al., 2003). Additionally, a main limitation of groundwater models is the number of observations available to characterize subsurface variability. Other authors focus on other uncertainties: Rojas et al. (2010) summarized from different studies that the uncertainties in groundwater models mainly arise from the definition of alternative conceptual models. This uncertainty cannot be compensated by parametric uncertainty. Conceptual uncertainties are mainly due to inadequate representation of physical processes, an incomplete understanding of the geological situation or an inability of the model to explain all observations of the state variables (Singh et al., 2010). Following the concept of equifinality, many combinations of model structures and parameter sets are capable of simulating systems in an acceptable way. The best simulations, based on likelihood measurements, are combined into a set of behavioral runs that give a good prediction of the system.

Compared to the importance of the ecosystem services provided by flood plains, only a few studies have focused on the simulation of groundwater level at the same time as simulating flooded areas. Current analyses of the parameter uncertainty of this type of coupled model are common in catchment hydrology but have been scarcely performed for coupled groundwater – surface water models, as the computational time of such models is typically

large and the performance of a great number of simulation runs is thus restricted. Following Pappenberger and Beven's (2006) typology of uncertainty handling in hydrology, groundwater models are commonly of a deterministic type, whereby modelers prefer to use physically based measured parameters and respective equations. Sanchez-Vila and Fernàndez-Garcia (2016) and Cirpka and Valocchi (2016) delineated the associated uncertainty of conceptual model choices as the primary objective of the stochastic analysis. As one reason for the low impact of stochastic hydrology on practice, Cirpka and Valocchi (2016) named the lack of usable tools for stochastic analysis and is consequently recommend for the generation of realistic realizations of subsurface properties as easy-to-use tools.

Fully distributed and coupled groundwater-surface water models tend to require a large computational power and time. With increasing spatial resolution, the computational time increases simultaneously. The resulting challenge is to find a balance between model complexity and accuracy to represent the observed processes (Clark et al., 2015). It should be considered whether it makes sense to increase the complexity when only limited spatial information is available and how restrictive the increased computational time is when increasing the complexity of the model. In this study, we present a simplified physical-deterministic model of a floodplain to simulate the groundwater situation and the flooding events and to ultimately achieve spatially distributed information on inundation height, flooding frequency and duration. Our major aim is to establish a parsimonious model that provides key processes to accurately represent the water pathways. With the minimization of the processes, we seek to limit the challenge of overparameterization (James and Burges, 1982). Our overall objective was to find a parsimonious model solution to reduce the computational run time to investigate the model's parameter uncertainty using Latin Hypercube sampling-based uncertainty analyses. We represent the physical properties on a lower level and accept parameters in the calibration even if they are outside of the normally accepted range. Ignoring "physical" ranges of parameters is, in the face of structural uncertainty, a technique that has been relatively successful in rainfall-runoff models and is encouraged by Pappenberger and Beven (2006).

2.2. Methodology

2.2.1. The Catchment Model Framework (CMF)

The hydrological model framework CMF (Catchment Model Framework) developed by Kraft et al. (2011), is a toolbox to construct a wide range of different model structures following the finite volume approach. Water fluxes in landscapes are represented in CMF as a network of storages and boundary conditions. Flux-governing equations are placed between the storage units to create the individual model. Models created with CMF differ in the number and connectivity of water storages and the type of equations for calculating the flux between the storage units and boundary conditions. Conceptual catchment models consist of a few storage areas connected by simplified equations such as the linear storage equation or tipping bucket approaches. Spatially differentiated models are created using numerous spatially explicit defined storages, such as soil- and groundwater layers with small area, connected by Darcian equations. Using the finite volume approach for discretizing continuous water storage, inspired by Qu and Duffy (2007), the use of an irregular grid for the lateral spatial discretization is possible. In contrast to Qu and Duffy, we used an irregular polygon grid, not a triangular one. A full description of the model toolbox can be found in Kraft, 2011, 2012. The application of the finite volume method to the partial differential equation results in a system of ordinary differential equations (ODEs) with one equation per water storage. CMF includes several ODE solvers, ranging from a primitive explicit solver without error control to implicit multistep methods with error prediction. For large, stiff systems resulting from spatially explicit discretizations, the CVODE solver from the SUNDIALS package by Hindmarsh et al. (2005) provides the best solution. The CVODE solver uses a Backward Differentiation Formula (BDF) with orders varying between 1 and 5, chosen for the stability of the solution. The application of BDF creates a non-linear equation system that must be solved with an appropriate numerical method to solve the resulting non-linear equation system. CVODE provides a choice of variants of the Newton method. We followed Qu and Duffy (2007) using a simplified Newton method suitable for large systems, the so-called Krylov-Newton iteration in the default setting of the CVODE solver, as explained in the CVODE manual (Hindmarsh and Sandu, 2016).

2.2.2. Using CMF for a spatial explicit groundwater model

For this study, CMF was used to set up a single layer groundwater flow model. The study area is discretized into irregular polygons according to elevation and land use. Saturated lateral flow is calculated with a Darcian approach. The local water balance of the subsurface storage of a single cell is given as

$$\frac{dV_i}{dt} = I_i(t) - ET_{act}(t, h_i)) - \sum_{j=1}^{N_i} A_{i,j}(V_i, V_j) K_{i,j} \frac{h_i - h_j}{d_{i,j}}$$

where i indicates the current cell, V is the water volume stored in the subsurface in m³, $I(t)$ is the infiltration rate at time t in m³/day, h is the groundwater head as a function of the stored volume V, $ET_{act}(t,h)$ is the actual evapotranspiration from the cell in m³/day, N_i is the number of cells sharing a boundary with i, j indicates a cell adjacent to i, $A_{i,j}(V_i,V_j)$ is the saturated area between the cells, calculated from the water levels and the boundary length in m², $K_{i,j}$ is the lateral saturated conductivity between the cells i and j in m/day, and $d_{i,j}$ is the distance between the cells i and j in m.

The infiltration rate depends on the presence of surface water, throughfall and infiltration capacity. If surface water is present, the infiltration rate equals the infiltration capacity until the subsurface storage is saturated. Without surface water, the infiltration equals the throughfall from the canopy, calculated with the interception model from Rutter and Morton (1977). The potential evapotranspiration rate is calculated with the FAO version of the Penman-Monteith equation (Allen et al., 1998). The actual evapotranspiration is limited by drought stress, calculated from the groundwater level and the canopy wetness. Evaporation from the canopy is calculated with the Penman-Monteith equation without stomatal resistance, replacing evapotranspiration through the leaves. Infiltration is calculated with a Darcian approach, where the gradient is calculated between the ponded water level, respectively air potential of the surface, and the groundwater level. Saturated conductivity is used for the conductance term. On a dry surface, when the throughfall intensity is below the infiltration capacity, the throughfall is directly routed to the matrix. The study area is scarcely covered by snow, so snow accumulation and melt were not considered in the model. The lower boundary is handled as a no-flow boundary condition, whereas lateral boundary conditions are implemented as a Dirichlet boundary with a time-varying groundwater head.

2.2.3. Surface water flow equation

Equations for surface water flow are mostly derived from Saint-Venant equations or one of its approximations (kinematic, diffusive or dynamic wave on one or two dimension) (Furman, 2008; Vasiliev, 1987). CMF is capable of simulating surface water flow as a kinematic wave or diffusive wave. Kinematic waves give a good approximation in watersheds with steep slopes, whereas diffusive waves are better in cases of flat slopes (Singh, 1996) such as floodplains. However, surface flow described by a diffusive wave results in large computational model run times, especially during larger flooding events. To enable parameter uncertainty estimates, we replaced the St. Venant surface flow with a simpler "flood-wave scheme". Instead of calculating the transient states of flooding, the scheme calculates the distribution of surface water at steady state.

The main concept of the wave is a comparison of surface water heads: at every time step the water level of the river is compared to the adjacent floodplain cells and the surface water head is adjusted, if the height of the cell is below the water level of the adjacent river. The surface water potential of all other cells is recursively adjusted if they have can be flooded by the adjacent river. The effect on computation time and the surface water potential compared to the diffusive wave is shown in the results section. A graphical explanation is given in Figure 2.1.

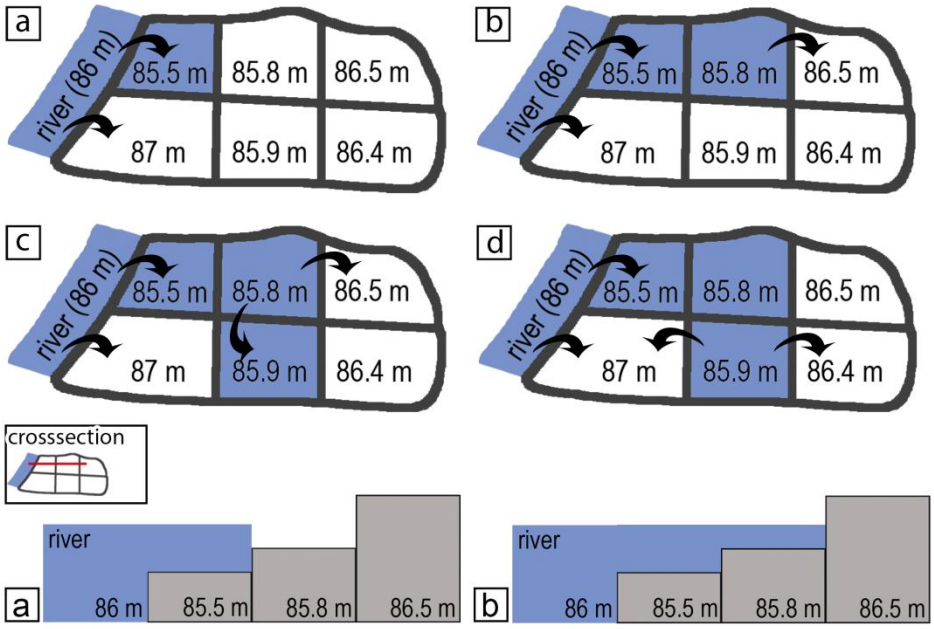

Figure 2.1: Sequence of CMF model time steps A-D, showing the flooding process by the flood-wave scheme developed for this model setup. Height refers to meters above sea level. The sequence of A-D is performed for each time step anew and vice versa for falling water levels. Additionally the cross section of the developed CMF model shows the flooding process via the flood-wave scheme for time step A and B.

2.2.4. Uncertainty estimation method

To estimation of the uncertainty, we followed the first steps of the GLUE method (Beven and Binley, 1992). The method is based on the dilemma of "equifinality", which states that many possible parameter sets can result in the same model outcome (Beven, 1993). GLUE is a widely used Bayesian technique to investigate model performance and parameter uncertainty. Instead of one optimal parameter set, GLUE results in several acceptable model runs with different parameter sets. If the objective function of a model run and its corresponding parameter set is below a predefined threshold the model run is named the "behavioral run". By contrast, non-behavioral model runs do not provide good fits of the available observables (Beven, 2001). For this study, only the separation of the model runs into behavioral runs and non-.behavioral runs based on a predefined objective function was applied. The further steps of the GLUE method were neglected.

To calibrate, analyze and optimize the parameters, the open source python package SPOTPY (Houska et al., 2015) was used. This package contains a number of algorithms and objective functions to calibrate and validate models. SPOTPY allows samples from different parameter distributions and at the same time is perfectly combinable with CMF. To obtain evenly distributed parameters, parameter selection with SPOTPY was performed using Latin hypercube sampling, a stratified random sampling method (McKay et al., 1979). We used the root mean square error (RMSE) as the objective functions. Additionally, the mean absolute error (MAE) was calculated and is given in the following. The MAE represents the average of the absolute values of differences between simulated and observed groundwater heads. The RMSE accounts for the square root of the average of the squared differences, and thus is an appropriate measure to evaluate the spread of the error. An important criterion for the evaluation of the model is the ratio of the objective function to the total difference in water levels of the groundwater, also called the normalized root-mean-square error (NRMSE) (Ely and Kahle, 2004).

2.2.5. Case study

2.2.5.1. Study site and data

The flood-meadow "Knoblochsaue" is located on the right bank of the Rhine, approximately 30 km south of Frankfurt am Main in Hesse, Germany (49°49'N, 8°26'E) (Figure 2.2). The flood-meadow is part of the nature reserve Kühkopf-Knoblochsaue, the largest of its type in Hesse. The nature reserve is of particular importance for rare and endangered flora and fauna and protected by the European Habitats Directive (Council Directive 92/43/EEC). The study area has a size of approximately 14.9 km^2, whereas 6.4 km^2 are inactive. Although the active floodplain is frequently flooded, dikes against inundations protect the inactive floodplain.

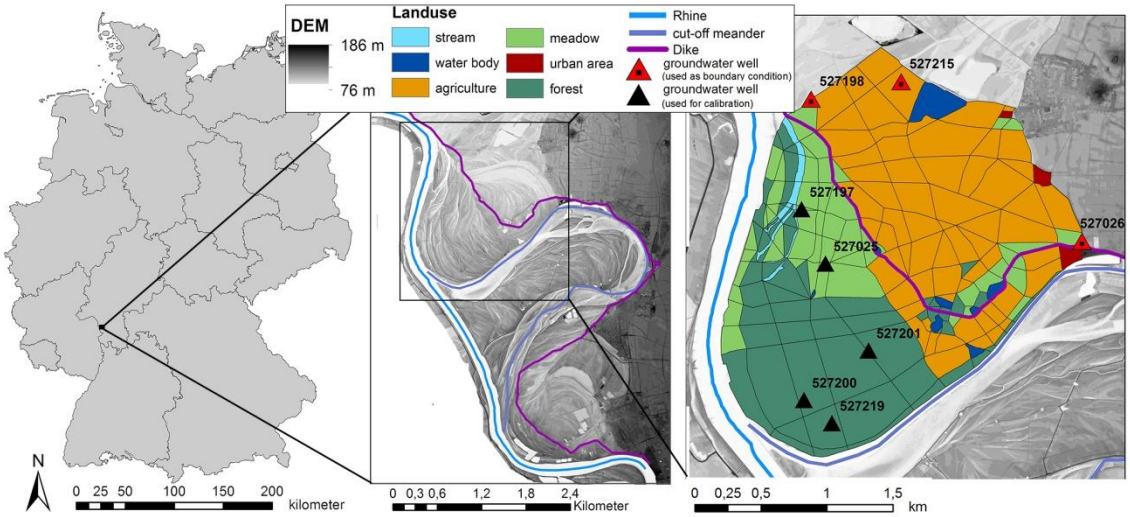

Figure 2.2: Geographic location (left), digital elevation of the larger nature reserve (middle) and setup of the CMF model with its irregular grid and land use for the study site (right).

Strong seasonal changes between water excess and drought are prevalent in this region. In spring, the area is usually flooded for several weeks from the Rhine (active floodplain) or ponding water occurs on the inactive floodplain. By contrast, the region is dominated by water deficiency in the summertime, with little rainfall and a small amount of available field capacity of clayey soil (clay content >60%). This effect leads to a very rapid decrease in plant available water and development of desiccation cracks (Burmeier et al., 2010).

2.2.5.2. Climatic conditions

The climate data provided by the Deutschen Wetterdienst (DWD) in daily time steps included minimum and maximum temperature, mean relative humidity and mean wind speed. The annual mean temperature between 2002 and 2013 was approximately 10°C and the mean relative humidity was 78%. Rainfall data from the Raunheim station (50°0'N, 8°25'E), which is located approximately 10 km north of the study region were used as daily input data (DWD). The annual precipitation from 2002 to 2013 was 570 mm, with 2002 being the wettest year with 692 mm and 2003 being the driest year with only 382 mm (Figure 2.3).

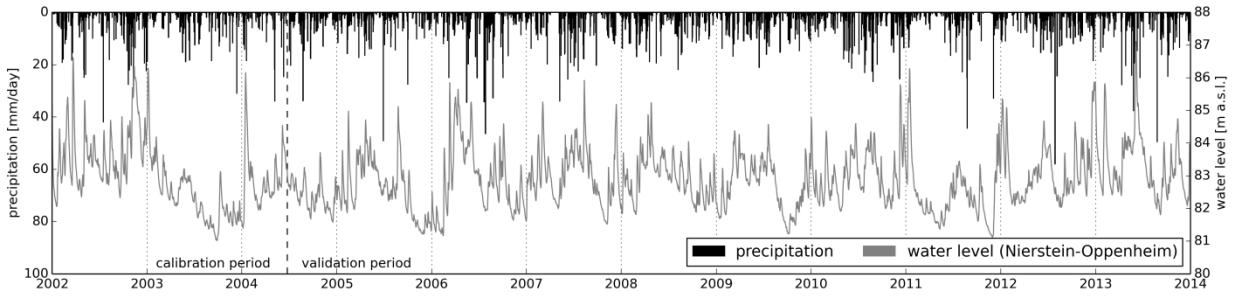

Figure 2.3: Daily precipitation (black bars) and water level of the Rhine (gray) at the gauging station Nierstein-Oppenheim for 2002 to 2013. The dashed line divides the time series in the calibration and validation periods.

2.2.5.3. Hydrology

Daily water level measurements for the Rhine gauging station Nierstein-Oppenheim (49°51'N, 8°21'E), approximately 3.5 km downstream, are available (Figure 2.3) (Federal Waterways and Shipping Authority (WSV) provided by the Federal Institute of Hydrology (BfG)). During the observation period (2002-2013), the highest water level was reached in April 2003 (87.10 m a.s.l) and in March 2003 (86.62 m a.s.l). The water level in autumn and winter 2002 was higher than in any other year, although all years had at least one flood event in winter.

Weekly measurements of a total of nine groundwater wells are available for the study site (Hessian State Office for conservation, Environment and Geology (HLNUG)). Three groundwater wells are located in the active floodplain and six in the inactive floodplain, with 360 m to 1,010 m distance to the Rhine or the cut-off meander of the Rhine. The groundwater level time series of the groundwater wells in the floodplain correlate, with a short time lag, with the water level time series of the Rhine. The flood signal smooths out with increasing distance to the river.

2.2.5.4. Prior modelling efforts

In 2011 a private company (Björnsen Beratende Ingenieure GmbH) was hired by the Federal Institute of Hydrology (Bundesanstalt für Gewässerkunde (BfG) to build a classical MODFLOW-based groundwater model of the region, including high-resolution hydrogeological base data. Unfortunately, the results were never published, and the report is only available on request from the Federal Institut of Hydrology or the private company (Lippert et al., 2012). The model was parameterized in a bottom up approach, gathering

information on conductivity and porosity from pump tests and maps and fine tuning of parameters (mainly hydraulic conductivity, storage coefficient, leakage factor of the water bodies) by manual calibration. Due to the complex hydrogeological settings in the alluvial flood plain, where highly conductive sand and gravel layers are intermixed with clayey aquitards, the mean error (ME) between predicted and measured piezometer heads was approximately -0.5 – 0.5 m, which is above the mean standard deviation of the groundwater level at the available piezometers. The groundwater model was calculated in monthly time steps, so that the calculated monthly average groundwater level was not necessarily comparable to the observed values. The simulated groundwater levels of monitoring points near the Rhine are lower than the observed levels, and thus the flooding parameters have a higher risk of underestimation. Results of this classical MODFLOW model are used to compare the performance of this model with our model, as far as possible.

2.2.6. Model setup

A Darcian model of the water flow in the nature reserve "Knoblochsaue" was established in CMF to simultaneously simulate the surface water and groundwater flow and subsequently assess the impact of inundation on groundwater level. The model divides the study area laterally into 272 irregular polygonal cells with sizes between 336 and 480,000 m^2.The variation in cell size is based on similar land use and elevation, so that the standard deviation of the elevation in one cell, based on a 1 m digital elevation model, is in average 0.5 m with a maximum at 2.3 m. Further elevations of the cells in which groundwater wells are located were set to the elevation of the respective groundwater well. For simplicity, the cells are not discretized vertically. The Rhine level data are used as a Dirichlet boundary condition on the riverside of the study area, affecting both the groundwater model and the flood wave scheme. The data from three groundwater wells were used as Dirichlet boundary conditions facing the upslope area. The data from the other six groundwater wells were used to calibration of the model. Initial conditions, i.e. the water level of each cell of the model at the first day of simulation, were calculated by external drift kriging (Goovaerts, 1997). To predict the groundwater level at any point, this method uses the known water level of the groundwater wells, the topographic elevation of the groundwater well and the topographic height of the point of estimation.

2.2.7. Calibration and validation of the model

The available time series of driving data is split into a calibration period of 2.5 years (1.7.2002 – 30.6.2004) and a validation period of 9.5 years (7.1.2004 - 31.12.2013). The standard deviation (SD) of the groundwater level during calibration is 0.72 m, and 0.54 m during validation. The calibration period was selected to cover a large fraction of the hydrological variability to achieve optimal parameter identification, as suggested by Gupta and Sorooshian (1985), and can be divided in to three hydrological characteristics, which are further described in Table 2.1. The first 2.5 years of available data are less variable and were omitted from the analyses.

Table 2.1: Differentiation of calibrated period by hydrological characteristics

Date period	Water level of the Rhine	Groundwater level
07.01.2002 – 14.10.2002	82.1 – 86.6 m	1.50±0.33 m SD
01.02.2003 – 01.10.2003	84.2 – 81.0 m	2.14±0.52 m SD
01.01.2004 – 01.03.2004	81.5 – 86.0 m	1.35± 0.48 m SD
Total calibration period:		
07.01.2002 – 30.6. 2004	81.0 – 86.6 m	3.22± 0.72 m SD

Four different soil parameters were calibrated: saturated hydraulic conductivity, porosity and residual wetness of the soil and the thickness of soil layer. The parameter ranges are given in Table 2.2. As the soil thickness also represents the lower boundary of the model, the minimum limit of the soil thickness was to the maximum distance of the groundwater level to the surface at any time during the observation period. High values for saturated conductivity were assumed, as pump experiments failed to alter the groundwater level, indicating very rapid lateral flow conditions. The parameters are considered constant over space, as we consider effective parameters and attempt to build a parsimonious model.

Table 2.2: Calibrated parameters for model and parameter ranges

Parameter	Saturated conductivity	Porosity	Residual wetness (residual water content)	Soil thickness
Unit	[m/day]	[m^3/m^3]	[m^3/m^3 / porosity]	[m]
A priori range	100 – 5,000	0.20 – 0.70	0.1 – 0.3	3.0 – 8.0
Range for all model runs	2,000 – 5,000	0.30 – 0.60	0.1 – 0.3	4.5 – 8.0
Range for behavioral model runs	2,193 – 4,986	0.30 – 0.34	0.1 – 0.3	5.1 – 8.0

The calibration and validation of the model is based on comparisons of the simulated values with observed values of groundwater heads in the groundwater wells on a weekly basis. Therefore a spatially and temporally variable criterion is used for calibration and validation of the model. River discharge is not used for model evaluation, as it is a driving force.

We generated 5,000 parameter sets with SPOPTY, using a Latin hypercube sampling approach and performed the simulations parallel to the 128 cores of the high performance computing cluster at Justus Liebig University. For the objective function RMSE, i.e. the mean RMSE of all calibration points, a "behavioral" threshold criterion of ≤ 0.26 m (1/3 SD of the groundwater wells during calibration period) was defined.

2.3. Results

2.3.1. Testing the simplified surface flow approximation

We tested the simplified flood-wave scheme, on a subset of the total floodplain (35 cells, 1.9 km^2) for 80 days in hourly and daily time steps (Figure 2.4). In comparison, applying the diffusive wave equation for the same surface water flow, the computational time of the model was approximately three times slower. With increasing flood intensity, the computational time of the simulation increased, especially for the model with the diffusive wave equation; thus, the difference in computational time between the two models increased further. During the simulation period, three flooding events with increasing intensity occur.

Figure 2.4 A shows the potential of the surface water of the lowest cell adjacent to the Rhine. During the first flood event, the timelag between the peak, using the flood-wave and the diffusive wave equation, is 8 hours (depth of flood 0.5 m). For the second flood event, the time lag is 1 hour (depth of flood 1.2 m) and for the third flood event (depth of flood 2.2 m) the time lag is 28 hours. The simulation was performed with the same setup in daily timesteps (Figure 2.4 B). The difference in surface water potential then decreases and the time lag between the flooding peaks for various surface water flow equations is for two of the three flood events in one day. Obviously is further the overestimation in flooding height by the flood-wave approximation, because flood propogation is ignored as the surface water distribution is calculated at the steady state. Because of the lack of observational data from frequently flooded regions, the surface water flow approximation cannot be evaluated in their performance. We conclude that the revised and simplified flood-wave shows a negligibly small discrepancy with the commonly used diffusive wave approximation, especially in daily time steps . The major advantage of the simplification is the substantially improved model run time. Against this background of the shorter simulation times, the discrepancy between the approximations is acceptable, particularly for daily time steps.

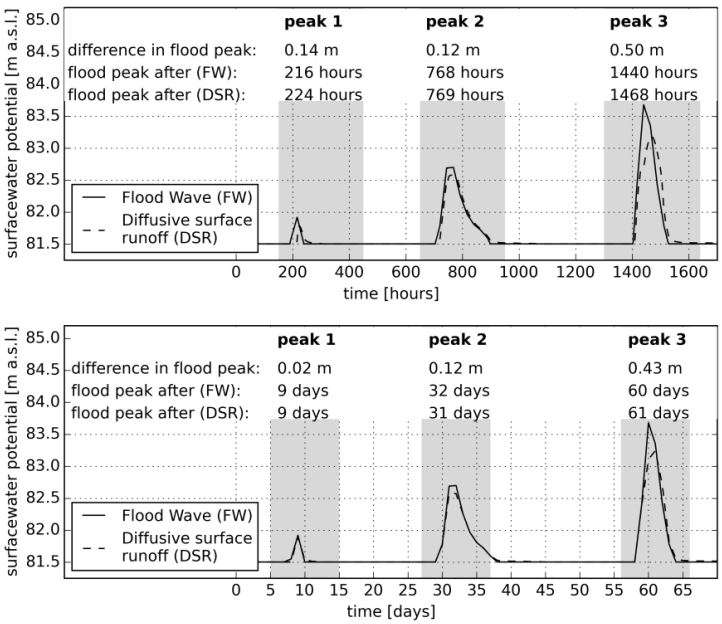

Figure 2.4: Comparison of surface water potential for a test model using either the diffusive surface water flow equation or the flood wave surface water flow equation. Supplementary information provides (a) the difference in surface water potential between the diffusive surface water and the flood wave equation (in m) and (b) the day with the highest surface water potential.

2.3.2. Model performance

For each of the four parameters a reasonable physical a priori range of values was specified. In a priory test runs, the parameter ranges were further adapted to the ranges given in Table 2.2. The interaction scatter plots (Figure 2.5) show a clear boundary for the porosity parameter at 0.35 (Figure 2.5 B) for good predictions. The best predictions are achieved with porosity values < 0.35 and high saturated conductivity (ksat) (> 3500 m/day) (Figure 2.5 E) or soil thickness between 5.5 and 7.0 m (Figure 2.5 H) or residual wetness of soil between 0.17 and 0.3 (Figure 2.5 F).

Of the 5,000 simulation runs with various parameter sets, 756 did not converge and were rejected due to their numerical properties. From the remaining 4,244 realizations, 155 produced behavioral runs below the cutoff criterion (mean RMSE ≤ 0.26 m). For these 155 behavioral runs, additional simulations for the validation period were performed. Figure 2.6 shows the capability of the CMF model to predict the groundwater level of the six groundwater wells in the floodplain. The highest RMSE for any of the six groundwater observation wells during the calibration period is 0.41 m (well 527192) (Table 2.3). The groundwater level of well 527197 showed the largest range during the calibration period, (absolute range; 4.5 m, max. range between two observations: 2.9 m). The peak RMSE of this groundwater well is likely caused by proximity to an old meander that is usually flooded by the Rhine.

The calculated RMSE varies for the various previously defined phases within the calibration period (Table 2.1, Figure 2.6). During the first period (fluctuating water level) the RMSE of the different groundwater wells is between 0.15 and 0.31 m. The RMSE of the second period (continuously decreasing water level) is the lowest between 0.05 and 0.17 m and the RMSE values during the third period (rapid increase of water level) range widely from 0.06 to 0.64 m.

From 155 parameter sets of the behavioral runs, 119 were able to simulate the validation period (Figure 2.7); the others led to numerical errors (convergence failure). The minimum RMSE and MAE are somewhat smaller during the longer validation period (RMSE: 0.16 – 0.23 m, MAE: 0.11 – 0.15 m) than the calibration period (RMSE: 0.18 – 0.28 m, MAE: 0.12 – 0.19 m).

The RMSE of the behavioral runs is between 0.16 m and 0.41 m for the different sites. The range of observed heads is between 3.04 and 4.55 m. This result indicates that the RMSE relative to the range in observed heads (NRMSE) is approximately 4.6 to 10.4%. The MAE is between 0.12 and 0.34 m and thus the MAE relative to the range in observed heads (NMAE) is approximately 3.3 to 8.5%. A relationship of less than 10% is defined as acceptable (Drost and Lum, 1999), which is given for all behavioral simulations of the model. A summary of the ranges of the objective functions is given in Table 2.3.

Table 2.3: Summary of the objective functions for the calibration and validation period. Depicted are the mean, minimum and maximum root mean square error (RMSE) and the mean absolute error (MAE) for each groundwater well in the study area. Highest values are in bold.

Objective function	**Groundwater well**					
	527025	527192	527197	527200	527201	527219
Calibration period						
RMSE mean [m]	0.28	0.26	0.36	0.19	0.21	0.22
RMSE min [m]	0.22	0.23	**0.28**	0.18	0.19	0.20
RMSE max [m]	0.32	0.28	**0.41**	0.22	0.25	0.24
MAE mean [m]	0.22	0.19	0.28	0.14	0.16	0.16
MAE min [m]	0.16	0.17	**0.19**	0.12	0.14	0.14
MAE max [m]	0.26	0.21	**0.34**	0.17	0.20	0.19
Validation period						
RMSE mean [m]	0.32	0.36	0.33	0.20	0.24	0.28
RMSE min [m]	**0.23**	0.22	**0.23**	0.16	0.17	0.17
RMSE max [m]	0.42	**0.49**	0.45	0.29	0.41	0.37
MAE mean [m]	0.24	0.27	0.25	0.15	0.19	0.21
MAE min [m]	**0.16**	0.15	0.15	0.11	0.12	0.12
MAE max [m]	0.37	**0.42**	0.39	0.24	0.37	0.31

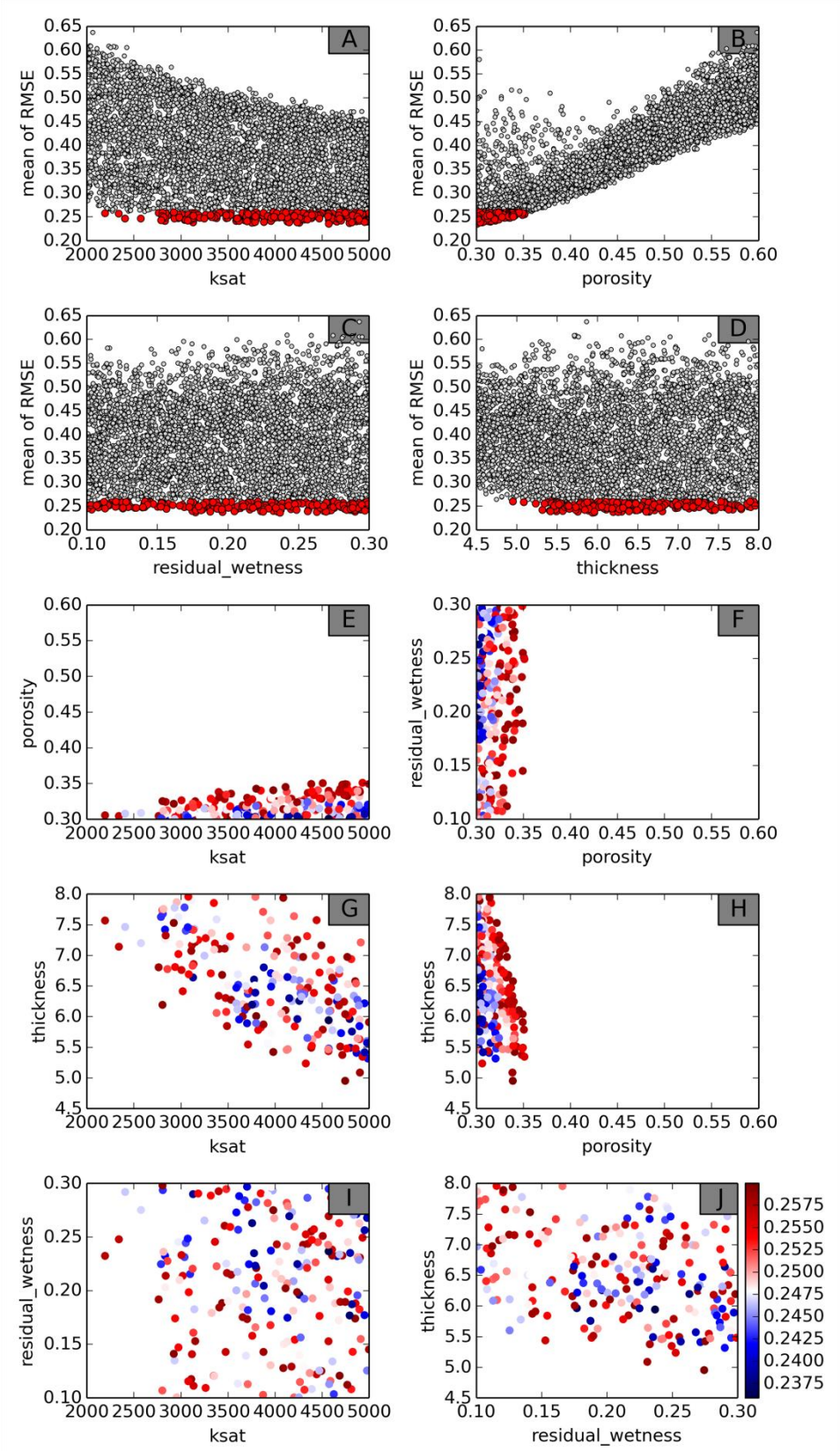

Figure 2.5: Scatter plot of the mean RMSE of each simulation against the parameters (A-D). Behavioral runs are marked in red. Parameter interactions for all model runs (E-J) are colored from blue to red for a mean RMSE ≤ 0.26 m.

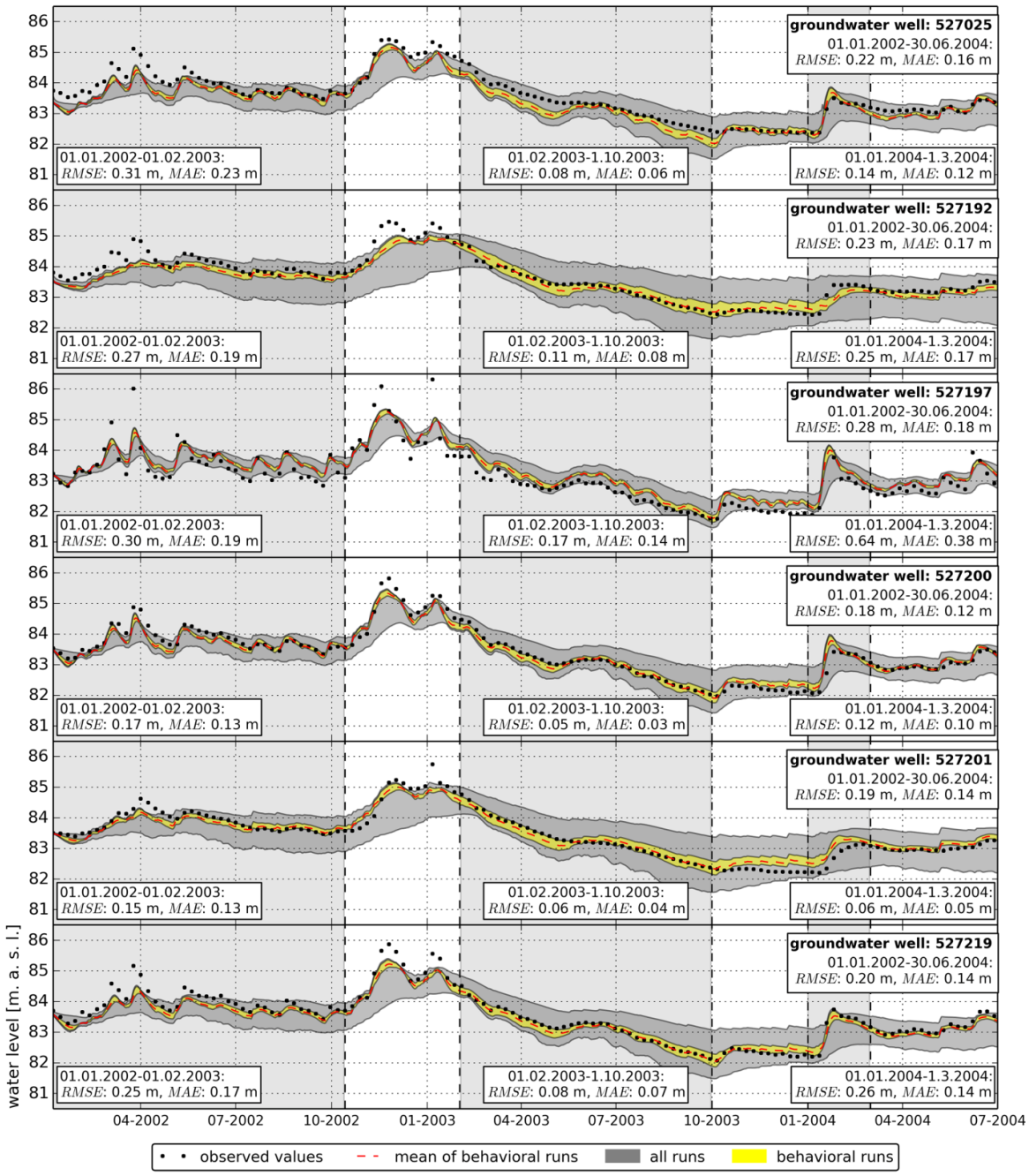

Figure 2.6: Comparison of simulations with observed groundwater levels. Performance measures depicted are the best obtained.

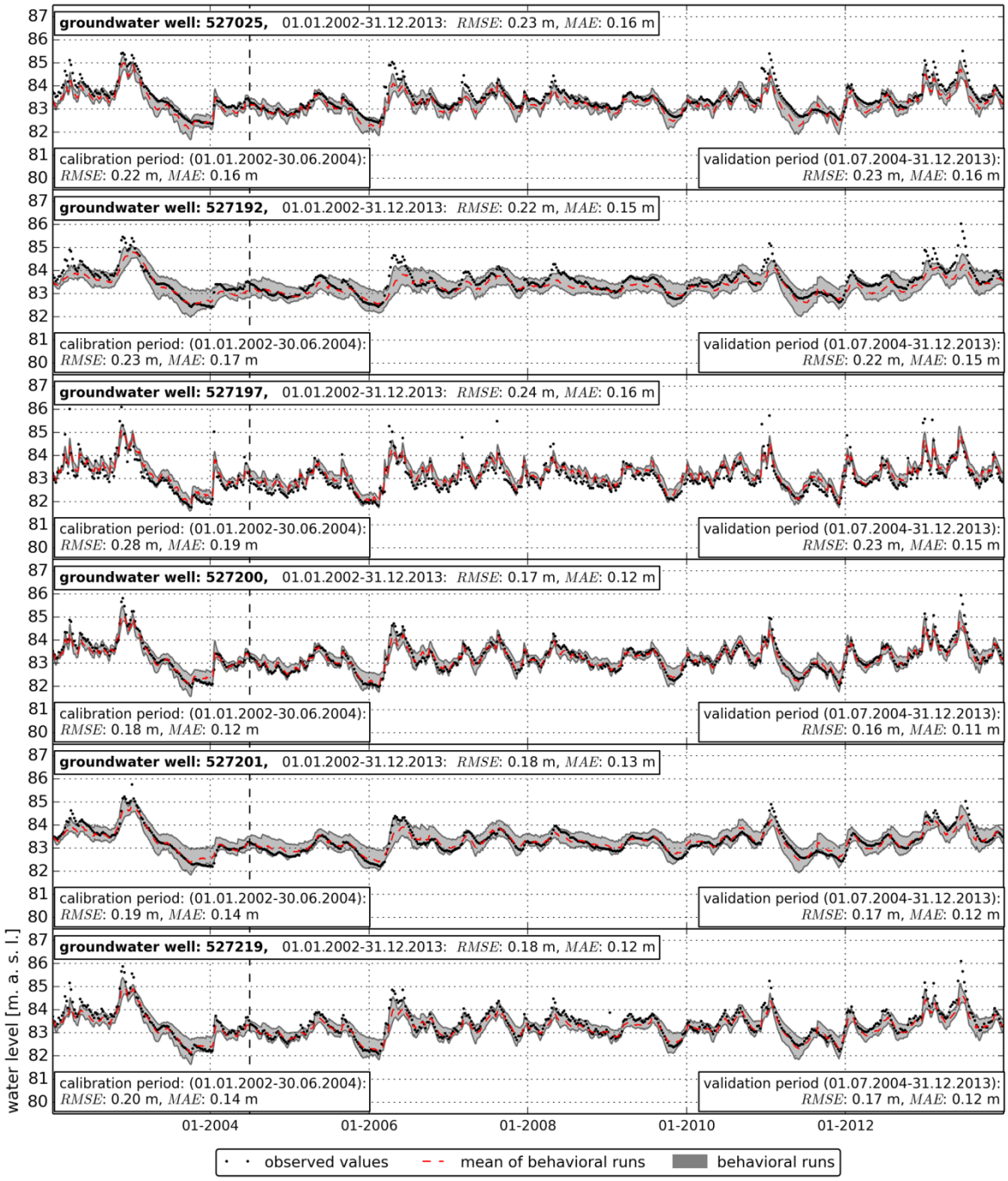

Figure 2.7: Comparison of simulations with observed groundwater wells for behavioral runs for total time series (calibration and validation period). Performance measures depicted are the best obtained.

The exchange between the surface water and groundwater for exemplary polygons of the models for the time period from 01.07.2002 to 01.07.2003 is shown in Figure 2.8. The gray area represents the uncertainty of the behavioral runs. The groundwater feeds into the surface water when the water table reaches the surface. Water fluxes between the polygons led to an inversion of water flux within a polygon from the surface water to the groundwater. The uncertainty of the water fluxes between the surface water and groundwater are larger for deeper areas. The infiltration volume over the entire study area of 14.9 km² is 21.98 x 10^6 m³ during the calibration period for the total catchment, where from 12.08 x 10^6 m³ in the active floodplain. The exfiltration volume is 2.98 x 10^6 m³ over the entire area and 2.49 x 10^6 m³ in the active floodplain. Exfiltration occurred during the calibration period on 57% of the days and infiltration on 91% of the days.

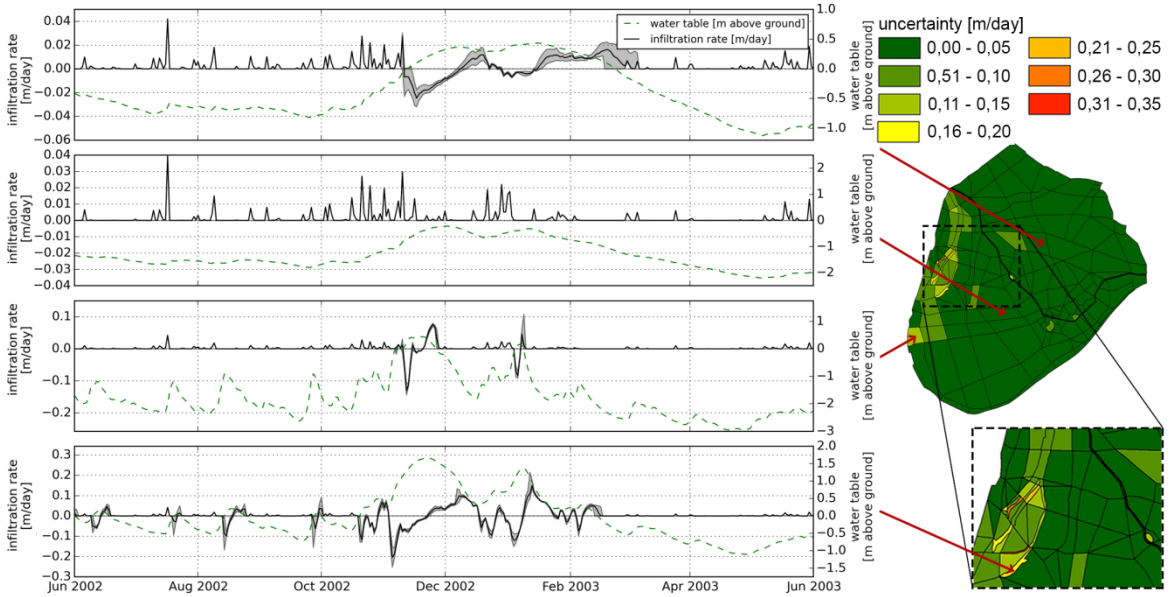

Figure 2.8: Results of the exchange between surface water and groundwater, shown for four polygons of the model for the time period between 01.07.2002 and 01.07.2003. The gray area represents the uncertainty given by the behavioral runs: the black line represents the mean water flux. Positive values indicate water fluxes for surface water to groundwater and negative values the inverse fluxes. The green line represents the water table of the polygon. The lowest time series represents total infiltration and exfiltration rate over entire study area and the active floodplain, as well as the water level of the adjacent river. The position of the presented polygons is marked in the map of the study area (right). The polygon colors in the map represent the maximum uncertainty (in m/day) at any time.

Temporally distributed results of the inundated area of the study area are shown in Figure 2.9. The uncertainty for the inundated area of the active floodplain (Figure 2.9, middle) is much smaller than the uncertainty of the inundated area of the inactive floodplain (Figure 2.9, bottom). On the right site of Figure 2.9 is the inundated area at different water levels of the river. The inactive floodplain has a larger uncertainty over a larger range of water levels than the active floodplain, for two reasons. First, the mean size of the polygons in the inactive floodplain is approximately 0.01 km² larger than in the active floodplain. The area of deeper polygons in the inactive floodplain is on average 2.5 times larger than the area of the higher polygons. Thus an inundation (of a few mm) of one or two addition cells can explain the uncertainty, as seen in Figure 2.9. Second the inundation in the inactive floodplain is controlled by water fluxes from the groundwater to the surface water, where as in the active floodplain inundation arises for surface water fluxes from the adjacent river. Following the inundation in the inactive floodplain mainly depends on the soil parameters.

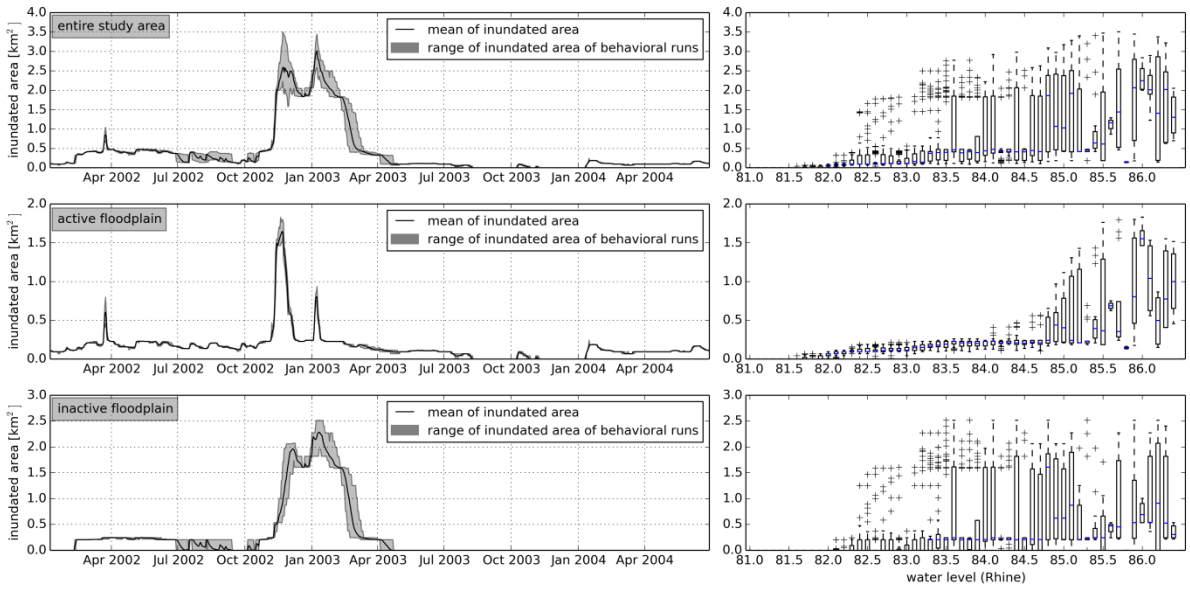

Figure 2.9: Time series of the inundated area (in km²) for the complete calibration period and boxplots of the inundated area at different water levels of the Rhine. At the top is the entire study area, in the middle only the active floodplain, and in the lower part the inactive floodplain.

Spatially distributed results of the model runs of inundation height, flooding time and duration are shown in Figure 2.10. Natural areas of streams and lakes are treated and implemented in the model similar to all other polygons. Thus, these polygons (purple and yellow border in Figure 2.10) show almost the whole year surface water levels above cell elevation and depict the largest values of the shown parameters. Approximately 28% of the cells (4.2 km²) between 2002 and 2013 are on average flooded for more than one day flooded. The maximum flooding height for those years is on average 0.45 m above ground (excluded polygons representing streams and lakes), and the longest flooding period has an average duration of 25 days. The surface water behind the dike (north-east part of the study area) is a result of the rising groundwater level.

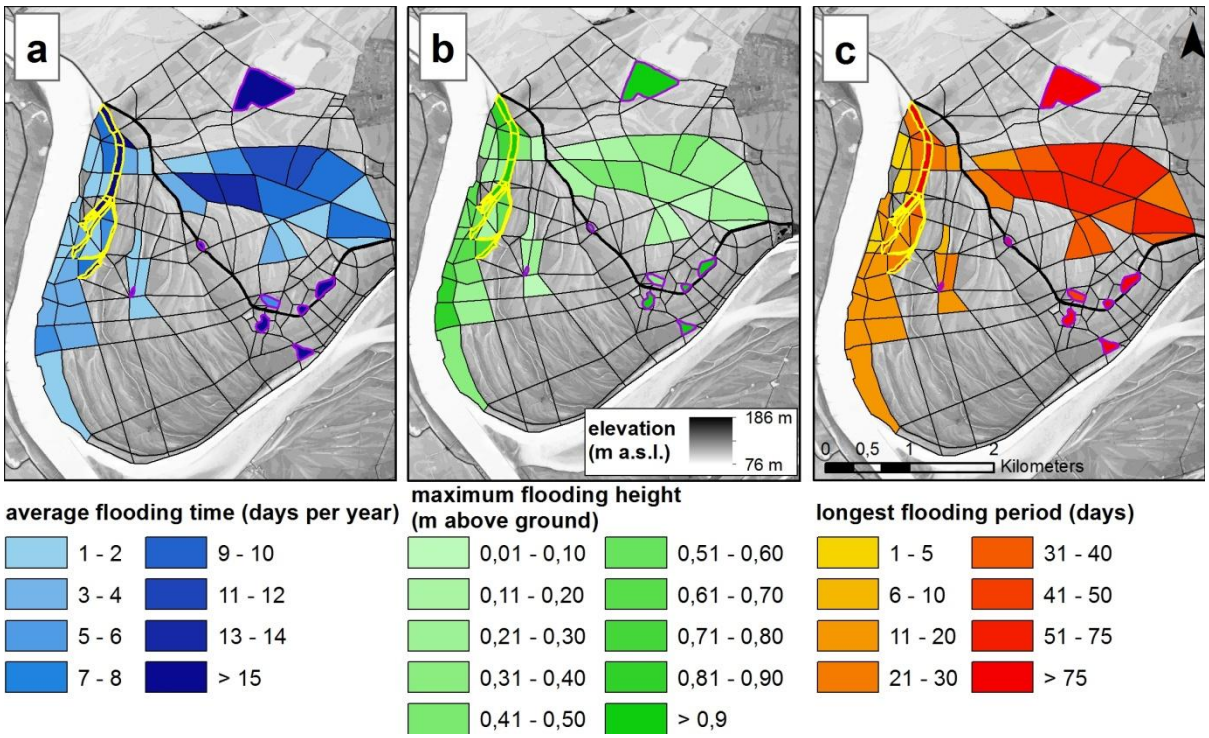

Figure 2.10: Comparison of average flooding time (a), maximum flooding height (b) and longest flooding period (c) for the polygons of the study area. Polygons with yellow borders are defined as streams. Polygons with purple borders are defined as lakes. Streams and lakes depict the largest values of each hydrological parameter.

2.4. Discussion

The model developed and used in this study meets all requirements given by Krause et al. (2007b) to simulate the water balance of inter-connected surface water-floodplain landscapes. Due to the shallow groundwater level and highly conductive soils, soil water and groundwater dynamics were modeled in an implicitly integrated way. The direct interaction between the groundwater and surface water are modeled explicitly. Variations in surface water infiltration and groundwater exfiltration are represented in space and time (Krause et al., 2007b). The modification of the surface water equation, from the diffusive wave to the newly developed flood-wave scheme, considerably decreased the computational run time, especially during flooding events. At the same time, the results are comparable for both model setups, in particular if the simulation is based on daily time steps, an adequate time step for models with total simulation times of several years. Bernand-Jannin et al. (2016) concluded that physically based coupled groundwater-surface water models can only be applied at reach scales and for short times. By contrast, we show that using acceptable model simplifications and reduced computational model run times, even complex, distributed groundwater–surface water models can simulate larger floodplains for several years. With these preconditions, we were able to run an uncertainty analysis with several thousand different model runs and resulting parameter sets. Additionally, we show that our model mainly depends on the porosity of the soil, whereas the other calibrated parameters (saturated hydraulic conductivity, residual wetness and soil thickness) have only a minor influence on the model outputs. Modeling complete time series, not just short flooding events, is necessary to use the resulting model as an input for habitat models and extrapolation in time. However, using measured groundwater heads at the upslope side of the model as a boundary condition is the main problem for calculating scenarios. The model has also been calibrated with a no-flow boundary condition on the upslope side of the model domain. The results for the active floodplain are nearly unchanged and the prediction for the piezometers used as driving data in the presented model, show an RMSE of up to 0.47 m. The results of this model are shown as supplemental material (Appendix 2-1).

We showed that our simplified model is able to produce good simulations of groundwater levels and the surface water–groundwater interaction with high temporal resolution. We achieved even better results than a further developed classical MODFLOW model with monthly time steps with a uniform spatial cell discretization of 20 m x 20 m.

Only a few studies have dealt with similar aspects, but with respect to catchment modeling. Jones et al. (2008) used the InHM model to simulate the response of a 75-km² catchment to two discrete rainfall events (420 and 900 hours duration). They showed moderate agreement in measured and simulated runoff and subsurface hydraulic head and concluded that fully coupled surface-subsurface models are applicable at the watershed scale and likely at a larger scale. Heppner et al. (2007) used InHM to simulate a continuous hydrologic response for a 0.1-km² catchment (R-5 catchment in Oklahoma, USA) and showed an overestimation of runoff for smaller contributions of runoff and an overestimation for relatively large contributions of runoff. Simulated subsurface outflows match the observed estimates only in the average of six simulation years, whereas the separated simulation years are over- or underestimated. Other authors applied coupled groundwater–surface water models for smaller catchments and/or a shorter time scale (Camporese et al., 2010; Ebel et al., 2008; Gauthier et al., 2009; Krause and Bronstert, 2007). However the objectives of those studies, the shown examples and other studies, are different; none focused on the model's parameter uncertainty or even described an extended calibration process. Ajami et al. (2015) assessed the impact of uncertainty on the initial conditions for a 208-km² catchment with the ParFlow.CLM model. They concluded that the subsurface initializations have a large impact on the magnitude and direction of surface water-groundwater exchanges. As the commonly used spin-up approach for initializing ParFlow.CLM models is computationally intensive for catchment and regional scales, they suggest a method to reduce this computational time, but leave out the test of this suggested method. In addition, studies using the groundwater head for evaluation are rare (Krause et al., 2007b), and consequently a comparison is difficult. Hattermann et al. (2004) evaluated groundwater heads over time and which showed even smaller values of MAE (0.026 m, 0.053 m) for two sub basins (1,993 km², 574 km²) with the SWIM model (Krysanova et al., 1998), a variant of the SWAT model (Arnold et al., 1993). Nevertheless, groundwater in SWIM is modeled at the sub-catchment scale following the topographic gradient and hence is not suitable for water flux calculations in flood plains. Krause et al. (2007a) determined an average BIAS below 0.13 m - similar to the results of our model - for floodplain parts in their study area, simulated with the IWAN model.

A major effect on inundation extent and flow prediction has the spatial resolution of a model (Hardy et al., 1999; Yu and Lane, 2006). At different spatial scales, different processes are dominant and different values for the model parameters are required. The estimated acceptable parameter sets of a model can consequently differ from the values measured in

situ at field scale. To make the model established here as simple as possible, we varied the grid size spatially, so that the elevation difference in one cell, based on a 1 m digital elevation model, was small (less than 1 m standard deviation). This adjustment resulted in the representation of important details (e.g., the dike) with cells of smaller size. Consequently, the obtained parameters of the best parameters sets are effective and not real.

2.5. Conclusion

By simplifying the surface water flow equation, our new groundwater-surface water model is able to simulate longer time periods within a reasonable computational time, facilitating extensive uncertainty analyses. The model can simulate floodplain inundation at high spatial and temporal resolution, providing excellent results. However, the model shows relatively large variance in parameters, particularly for saturated conductivity, that nevertheless result, in behavioral model runs. Further model improvements should focus on larger and rapid fluctuations in groundwater levels of wells close to the adjacent Rhine River.

In the future, we will further test our model for transferability in space (to other floodplains) and time (historical inundations and future projection). The model could ultimately be used for the assessment of ecosystem services such as flood prevention or habitat protection.

For the latter, different hydrological parameters, such as the number of flooding days or length of flooding periods can be used as inputs for other models, such as habitat models, to identify possible habitats for regeneration measures. To further specify possible habitats, spatial downscaling of the hydrological parameters is recommended.

Acknowledgments

The authors declare no conflicts of interest. This research was funded by the Deutsche Bundesstiftung Umwelt DBU (Project No.31612-33/0; www.dbu.de). The funder had no role in the study design, data collection and analysis, decision to publish, or preparation of the manuscript.The author thanks the two anonymous reviewers and Fulvio Boano for their insightful comments and suggestions that contributed to improving this paper.

The climate data are available from the Germany's national meteorological service (Deutscher Wetterdienst, DWD, http://www.dwd.de/cdc; ftp://ftp-cdc.dwd.de/pub/CDC). Daily water levels from the gauging station Nierstein are available from the Federal Waterways and Shipping Authority (Wasser- und Schifffahrtsverwaltung des Bundes, WSV) and provided by the Federal Institute of Hydrology (Bundesanstalt für Gewässerkunde (BfG)). Groundwater levels are provided by the Hessian State Office for conservation, Environment and Geology (Hessisches Landesamt für Naturschutz, Umwelt und Geologie, HLNUG).

Supporting information

Appendix 2-1

Additionally the model was set up with the same specifications as described in Chapter 2.2.6, only with the lack of no-flow boundary conditions on the upslope (compare Figure 2.2 – groundwater wells used as boundary conditions). Using the same threshold criterion for behavioral runs (RMSE ≤ 0.26 m) it leads to 59 behavioral runs. The results for the active floodplain are nearly unchanged: the lowest achieved RMSE is not more than 0.1 m higher. The prediction for the piezometers used as driving data in the presented model, show an RMSE of up to 0.47 m.

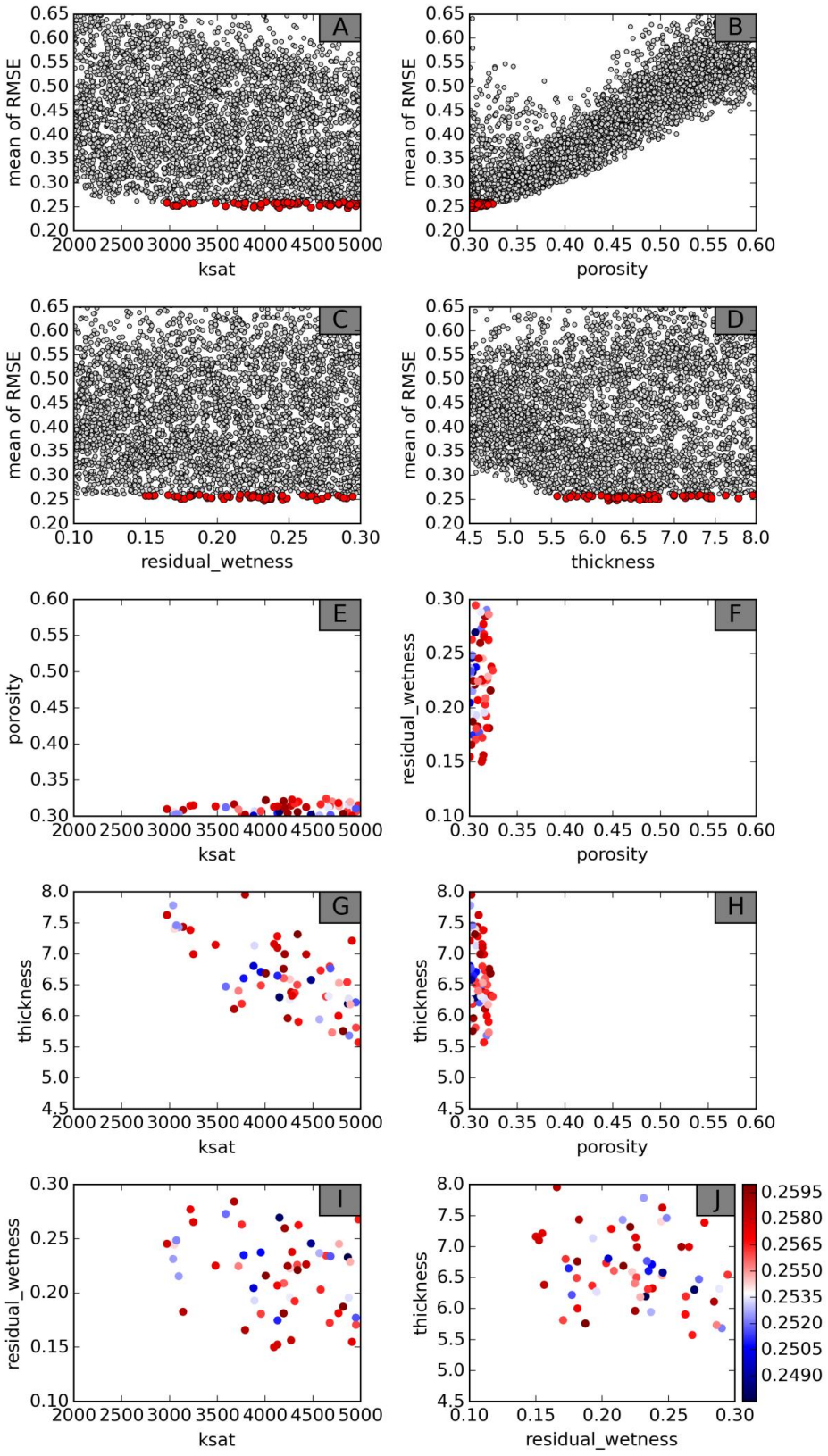

Scatter plot of the mean RMSE of each simulation against the parameter (A-D) Behavioral runs are marked in red. Parameter interactions for all model runs (E-J) are colored from blue to red for a mean RMSE ≤ 0.26 m.

3. Multi-Source Uncertainty Analysis in Simulating Floodplain Inundation under Climate Change

This chapter is published in the journal *Water* 10, article number 809, 2018. doi: 10.3390/w10060809

Nadine Maier[1], Lutz Breuer[1,2], Alejandro Chamorro[1], Philipp Kraft[1] and Tobias Houska[1]

1 Institute for Landscape Ecology and Resources Management (ILR), Research Centre for BioSystems, Land Use and Nutrition (iFZ), Justus Liebig University Giessen, Heinrich-Buff-Ring 26, 35392 Giessen, Germany; lutz.breuer@umwelt.uni-giessen.de (L.B.); alejandro.chamorro-chavez@umwelt.uni-giessen.de (A.C.); philipp.kraft@umwelt.uni-giessen.de (P.K.); tobias.houska@umwelt.uni-giessen.de (T.H.)

2 Centre for International Development and Environmental Research (ZEU), Justus Liebig University Giessen, Senckenbergstraße 3, 35390 Giessen, Germany

Abstract

Floodplains are highly complex and dynamic systems in terms of their hydrology. Thus, they harbor highly specialized floodplain plant species depending on different inundation characteristics. Climate change will most likely alter those characteristics. This study investigates the potential impact of climate change on the inundation characteristics of a floodplain of the Rhine River in Hesse, Germany. We report on the cascading uncertainty introduced through climate projections, climate model structure, and parameter uncertainty. The established modeling framework integrates projections of two general circulation models (GCMs), three emission scenarios, a rainfall–runoff model, and a coupled surface water–groundwater model. Our results indicate large spatial and quantitative uncertainties in the simulated inundation characteristics, which are mainly attributed to the GCMs. Overall, a shift in the inundation pattern, possible in both directions, and an increase in inundation extent are simulated. This can cause significant changes in the habitats of species adapted to these highly-endangered ecosystems.

3.1. Introduction

The ecohydrology of floodplains is highly influenced by regular floods, defined by characteristics such as the height of the water level, flood duration, and recurrence intervals (van Eck et al., 2004; Hayashi and Rosenberry, 2002; Krause et al., 2007a; Maltby and Barker, 2009; Woodcock et al., 2005). Consequently, a wide habitat heterogeneity exists and species which are highly-specialized on the present conditions can be found in these ecosystems (van Roosmalen et al., 2007; Taylor et al., 2012b). Apart from providing habitats for plants and breeding birds or fish, floodplains provide many other ecosystem services, including the regulation of floods, water supply, and nutrient retention (Tockner and Stanford, 2002). At the same time, floodplains are among the most-endangered ecosystems worldwide (Opperman et al., 2010). Flow regulation and damming, urban sprawl, and agricultural land use change have resulted in disconnected floodplains that can no longer sustain their original services.

Climate change is likely to have additional effects on floodplains and their functionality due to general changes in the hydrological cycle (Capon et al., 2013). More precisely, the seasonality and extremes of low and high flows will be altered (Demirel et al., 2013; Dokulil, 2014; Middelkoop et al., 2001). As flood characteristics are changed, a shift in habitat availability and species distribution is expected (Herron et al., 2002; Mortsch, 1998; Sorenson et al., 1998; Thompson et al., 2009).

Reconnecting floodplains to rivers is promoted as a key to restore floodplains' functionalities (Opperman et al., 2009, 2010). A common way to develop restoration plans or assess the effect of management options is through model projections. Floodplains should be simulated with fully-integrated models that consider surface water–groundwater interactions to capture all relevant ecohydrological processes (Alaghmand et al., 2016; Furman, 2008; Refsgaard et al., 1998). These models can enhance the understanding of the hydrological functions of floodplains and can provide insight into the potential impacts of climate change (House et al., 2016; Karim et al., 2016; Thompson et al., 2009).

Studies of climate change impact involve several cascading uncertainties related to the climate model itself, the emission scenario, hydrological model structure and parameters, spatial model input data, and initial conditions (Bredehoeft, 2005; Kay et al., 2009; Refsgaard et al., 2006; Teng et al., 2012; Wilby, 2005; Wilby et al., 2006). Studies have rarely considered

the propagation of the uncertainty from climate projections to rainfall–runoff models and flood inundation models (McMillan and Brasington, 2008; Pappenberger et al., 2005). One of the few existing modeling studies on climate change impacts on floodplains was carried out by Sorribas et al. (2016), who focused on the changes of discharge, inundation extent, and the uncertainty introduced by the general circulation model (GCM) in the Amazon. Thompson et al. (2009) used a coupled hydrological/hydraulic model (MIKE SHE/MIKE 11) to assess the impact of climate change on wet grassland in lowlands for different emission scenarios. Finally, Barron et al. (2012) investigated the impact on groundwater-dependent terrestrial vegetation using rainfall–runoff and groundwater models with data from 15 GCMs but did not consider any further sources of uncertainty.

This paper addresses this gap by studying the cascading effect of projected climate change impact on inundation frequency and duration on a floodplain of the Rhine River in Germany. We investigate the uncertainty through the modeling chain of a rainfall–runoff model (Hydrologiska Byråns Vattenbalansavdelning (HBV) and a coupled parsimonious surface water–groundwater model (catchment modeling framework (CMF)). For this, we use projections of two GCMs and three emission scenarios as driving forces for HBV to simulate the future discharge of the Rhine. The generated discharge time series by the rainfall–runoff model are then used to drive the surface water–groundwater model in order to project spatially-distributed flood characteristics in a specific floodplain of the Rhine and identify the uncertainties in the modeling procedure.

The guiding questions for our research are as follows: How are the changes in inundation characteristics related to the river discharge projections? How will the spatial distributions of inundation characteristics change on a small scale and through time? What are the main sources causing differences related to the projected inundation characteristics, and how is the uncertainty propagating throughout the modeling framework?

3.2. Materials and Methods

3.2.1. Study Site

The floodplain ''Knoblochsaue'' is located on the right bank of the Rhine, approximately 30 km southwest of Frankfurt in the Federal State of Hesse, Germany (49°49′ N, 88°6′ E). The floodplain is part of the nature reserve Kühkopf-Knoblochsaue, the largest of its type in Hesse (Figure 3.1). The nature reserve is of particular importance for rare and endangered flora and fauna and is protected by the European Habitats Directive (Council Directive 92/43/EEC). The study area is approximately 14.9 km². As the floodplain is frequently flooded, embankment protects a subarea of about 6.4 km² from inundations. This area is also referred to as the inactive floodplain.

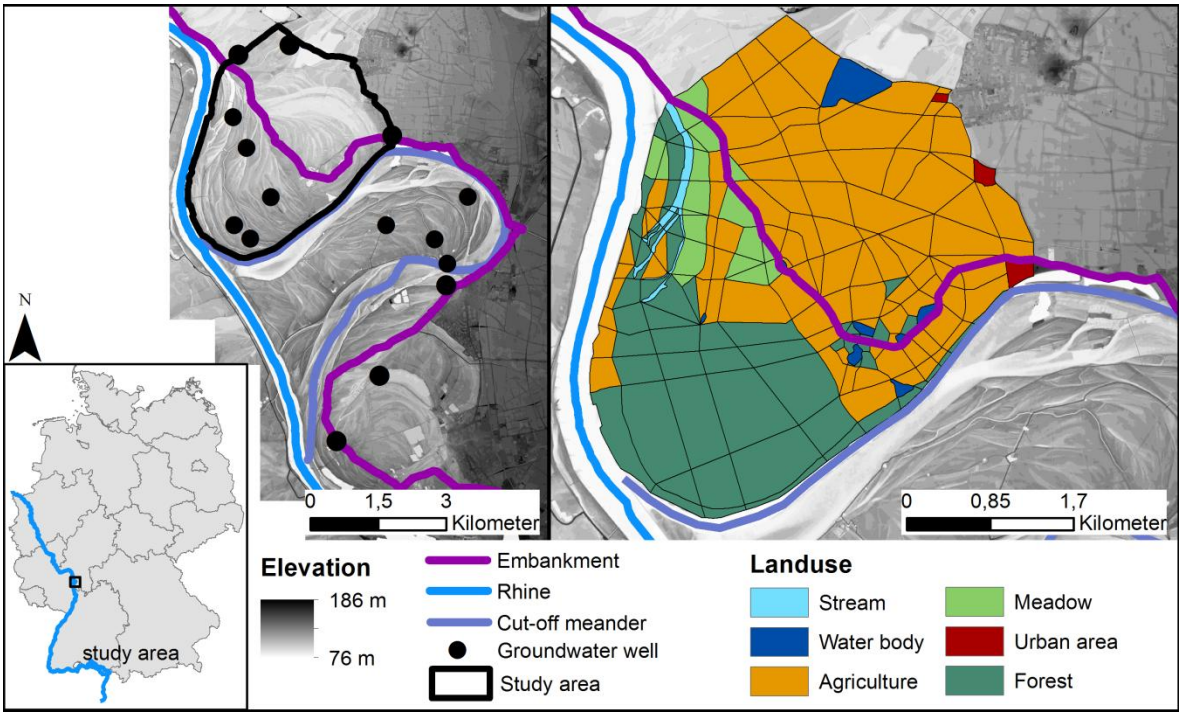

Figure 3.1: Geographic location of the study area (lower left), digital elevation of the larger nature reserve with the study area (middle), and the setup for the surface water–groundwater model in the catchment modeling framework (CMF) (right). The irregular polygons are based on similar elevation and land use.

Annual precipitation is about 618 mm and the mean daily temperature is about 10.7 °C (observed at the station Darmstadt (49°52′ N, 8°40′ E) by the German meteorological service) between the years 1981 and 2010. Daily water levels measurements for the Rhine are available for the gauging station Nierstein Oppenheim (49°51′ N, 8°21′ E; approximately

3.5 km downstream the study area). Average discharge between 2000 and 2014 was 1673 $m^3 s^{-1}$ (90% quantile: 2460 $m^3 s^{-1}$; 10% quantile: 1010 $m^3 s^{-1}$).

3.2.2. Surface Water–Groundwater Model

For this study, we modified a previously-developed parsimonious, physically-based surface water–groundwater model to simulate flood characteristics in the floodplain (Maier et al., 2017). The model is built with the catchment modeling framework (CMF), version v0.1315 (Kraft, 2011; Kraft et al., 2011) and includes the interaction between surface water and groundwater flow. CMF is a flexible modular framework suitable for different hydrological model structures (from detailed mechanistic to lumped large-scale linear storage-based models). The models differ in their number and connectivity of water storages as well as in the type of equation calculating the water fluxes between the components. In order to implement an irregular grid for the lateral spatial discretization, CMF is based on the concept of finite volumes for discretizing continuous water storages (Qu and Duffy, 2007).

The study area is divided into 272 irregular polygons with different sizes (336–480,000 m^2) based on similar elevation and land use (Figure 3.1 right). Land use was divided into six classes (stream, water body, agriculture, meadow, forest and urban area). The standard deviation of the elevation in one polygon was kept at a maximum of 2.3 m (mean: 0.5 m).

A vertical discretization is not considered to simplify the model. The model is forced by the daily water level of the stream and the groundwater level at the upslope edge of the study area, both set as a dynamic Dirichlet boundary condition. Precipitation and modeled evapotranspiration using the FAO guidelines (Allen et al., 1998) complement the system boundaries. More details about the study area and the model set up, including the surface water routines, can be found in Maier et al. (2017).

To reduce the amount of forcing data, we replaced the upslope boundary condition with a no-flow boundary. A subsequent recalibration of the model resulted in similar optimal parameter sets and an increase of the RMSE of less than 0.1 m in the active floodplain. We tested several CMF parameter sets from Maier et al. (2017) for numerical stability. Due to the numerical stability and computation effort, we selected only one parameter set. The parameter set defines the soil properties as follows: 2830 m d^{-1} for hydraulic conductivity, 0.3 $m^3 m^{-3}$ for porosity, 0.23 $m^3 m^{-3}$ for residual wetness, and 7.4 m for soil thickness.

3.2.3. Water Level Forcing

For CMF forcing, we need stream water level data. Measured data are used for current conditions, and we use projected data for our future climate scenarios. We applied the rainfall–runoff model (HBV) (Bergström, 1995; Lindström et al., 1997) in a modified version (Bárdossy and Singh, 2008) as a conceptual semi-distributed hydrological model to simulate the discharge of the Rhine River. It has been shown in recent comparison studies that HBV gives satisfactory results using various model performance criteria for the Rhine River (Huang et al., 2017; te Linde et al., 2008). Based on these studies and a previous study from Vetter et al. (2015), in which a minor part of the overall uncertainty was shown to be related to hydrological models, we only consider the HBV model to simulate discharge in the Rhine River and no further hydrological multi-model ensemble. We then transformed discharge projections from HBV to water levels by existing, calibrated, and validated rating curves.

The HBV model was set up for the Rhine catchment at the Mainz gauging station, which was separated into six sub-catchments. This subdivision was done in order to include different climatic conditions. For the semi-lumped model, only one parameter set for the entire catchment was considered.

We considered both the parameter and predictive model uncertainty of HBV. To capture the parameter uncertainty, the GLUE methodology (Beven and Binley, 1992) was applied. Accordingly, we ran the model 100,000 times following a Latin hypercube procedure using SPOTPY (Houska et al., 2015) with all the 12 input model parameters of HBV (Appendix 3-2). We used the Nash–Sutcliffe (NSE) coefficient (Nash and Sutcliffe, 1970) as the objective function in order to focus the model performance investigation on the high flows, which are of course the most important source for flooding. As behavioral runs, we chose the top 10% of all model runs, resulting in an acceptable threshold of NSE > 0.72. We projected the discharge with the parameter sets defined as acceptable for each climate scenarios. The years 2001 to 2009 were used as the calibration period and 2010 to 2013 as the validation period. Further, we used the 5^{th} and 95^{th} percentiles over each simulation and over each time step as the synthetic minimum and maximum water levels for the corresponding climate projection. The approach for the predictive uncertainty is based on heteroscedastic error modeling that represents the aggregated effects of data and model structural errors of the best model run found (McInerney et al., 2017). We applied the Box–Cox (Box and Cox, 1982) transformations with a fixed transformation value of $\lambda = 0.5$ to get a robust statistical model for the residuals

of discharge simulations. We ran the analysis with the best performing model run in a post-processing mode and checked our results for normality. However, we did not treat any potential autocorrelation effects in the residuals, which might result in an over-estimation of the predictive uncertainty (McInerney et al., 2017). The defined parameters for the transformation equation are then applied to the simulations under the climate change scenarios. Again, we used the 5th and the 95th percentiles of the predictive uncertainty as discharge projections. Additionally, we performed simulations with the best-performing HBV model.

3.2.4. Climate Forcing

We selected two general circulation models (GCMs) from the Coupled Model Intercomparison Project Phase 5 (CMIP5) (Taylor et al., 2012a): HadGEM2-ES from the Met Office Hadley Centre and MPI-ESM-LR from the Max Planck Institute for Meteorology. In recent studies, McSweeney et al. (2015) concluded that both GCMs perform satisfactorily for Europe, and Brands et al. (2013) showed that both models outperform the remaining models by reproducing the present climate conditions in Europe and Africa. Other than that, the two GCMs show differences in the annual mean temperature and annual mean precipitation in the contributing catchment area of the Rhine. The model HadGEM shows a larger annual mean temperature change and a larger decrease in the annual mean precipitation especially in summer and autumn when compared to MPI-ESM-LR (Keuler et al., 2016; Zubler et al., 2016). Both models consider three representative concentration pathways (RCP), i.e., the RCP 2.6 (low concentration), RCP 4.5 (medium concentration), and RCP 8.5 (high concentration).

Subsequently, we obtained six different climate projections from the combination of the GCMs and RCPs. The quantile mapping method (Maraun et al., 2010; Themeßl et al., 2011) was used to downscale the daily precipitation and temperature time series projections. We used quantile mapping for bias correction for two reasons. First, the uncertainty related to the GCMs is larger than the uncertainty associated with the downscaling and bias-correction method (Kay et al., 2009; Prudhomme and Davies, 2009; Quintana Seguí et al., 2010). Second, the quantile mapping method is reviewed by several authors in the context of hydrological impacts studies as a preferable method (Themeßl et al. 2011; Gudmundsson et al. 2012; Teutschbein & Seibert 2012; Chen et al. 2013).

This overall set-up results in 30 simulations of the CMF model for future projections through the combination of five projected water level time series derived from the HBV model (best-performing simulation, 5th and 95th percentiles of parameter and predictive uncertainty), the two GCMs (HadGEM and MPI-ESM), and the three RCPs (RCP 2.6, RCP 4.5, RCP 8.5). A summarizing figure of the methodology and the consecutive steps used is given in Figure 3.2.

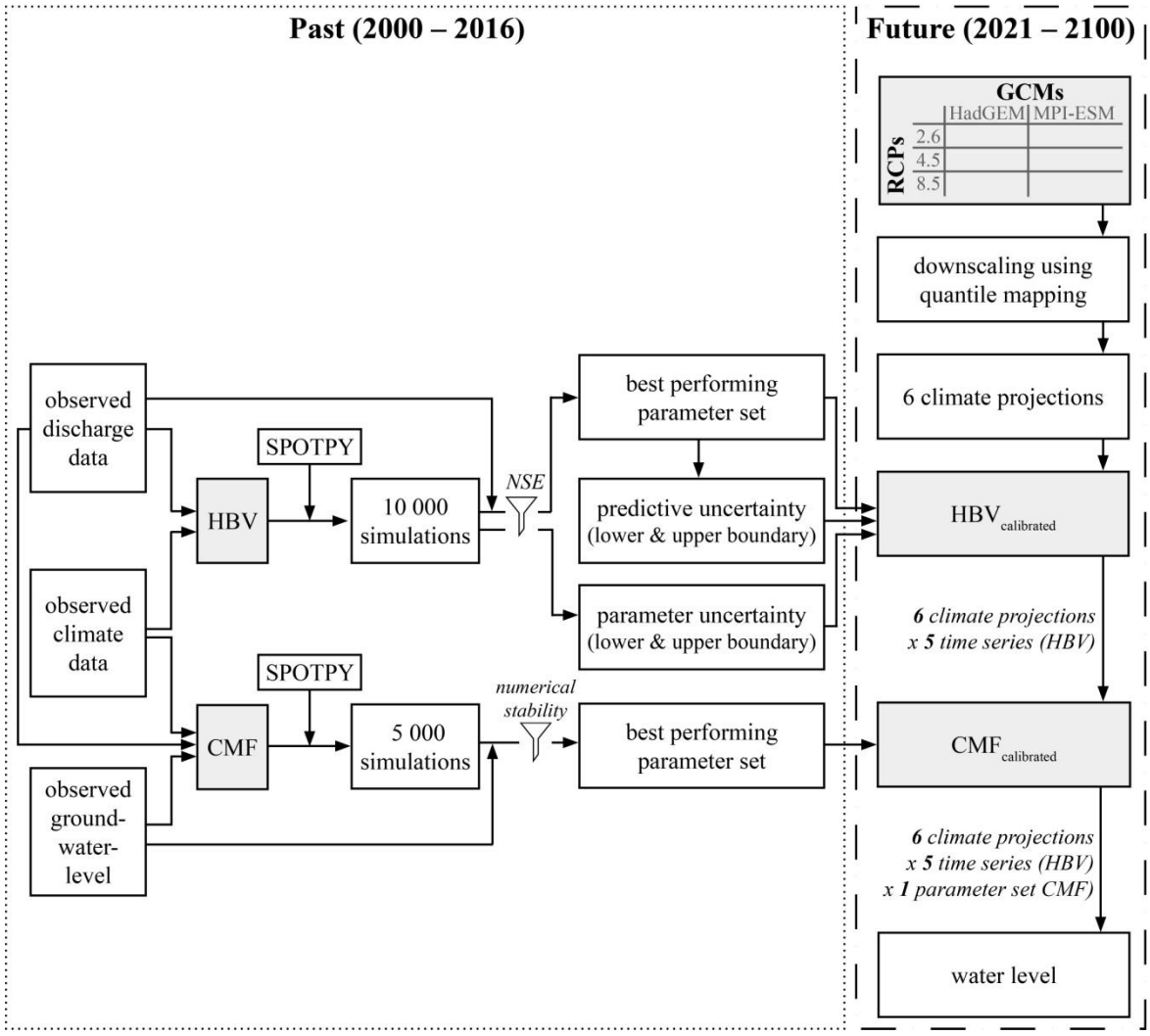

Figure 3.2: Flowchart showing the steps within the model framework. The steps within the dotted box represent steps forced by historical data and steps within the dashed box represent future projections. Models are depicted by grey boxes.

The reference height of a polygon is given by its average height over the entire polygon; i.e., each polygon is represented by one defined surface height. We define inundation as a water level of 0.05 m above the surface. For the following description of inundation in the study area, we used two inundation characteristics: the number of inundation days per year and the mean duration of an inundation period. Those metrics are useful when considering further consequences for example for flood meadow species composition, as those are influences by the inter-annual variation of flooding and droughts and the duration of flooding (David, 1996; Mathar et al., 2015).

3.3. Results

3.3.1. Projection of the Rhine River Water Level

The NSE for daily discharge during the calibration (2001–2009) and validation period (2010–2013) of the HBV model is 0.79 and 0.82, respectively (Appendix 3-2). Slightly worse results of the HBV-model can be found if only the high flows are considered (NSE: 0.54 for 70^{th} percentile based on observed discharge). In the next step, we forced the calibrated model with bias corrected precipitation and temperature data from the two GCMs (HadGEM2-ES and MPI-ESM-LR) and the three RCPs (RCP 2.6, RCP 4.5 and RCP 8.5) to project future runoff. From these, we derived projected water levels (Figure 3.3).

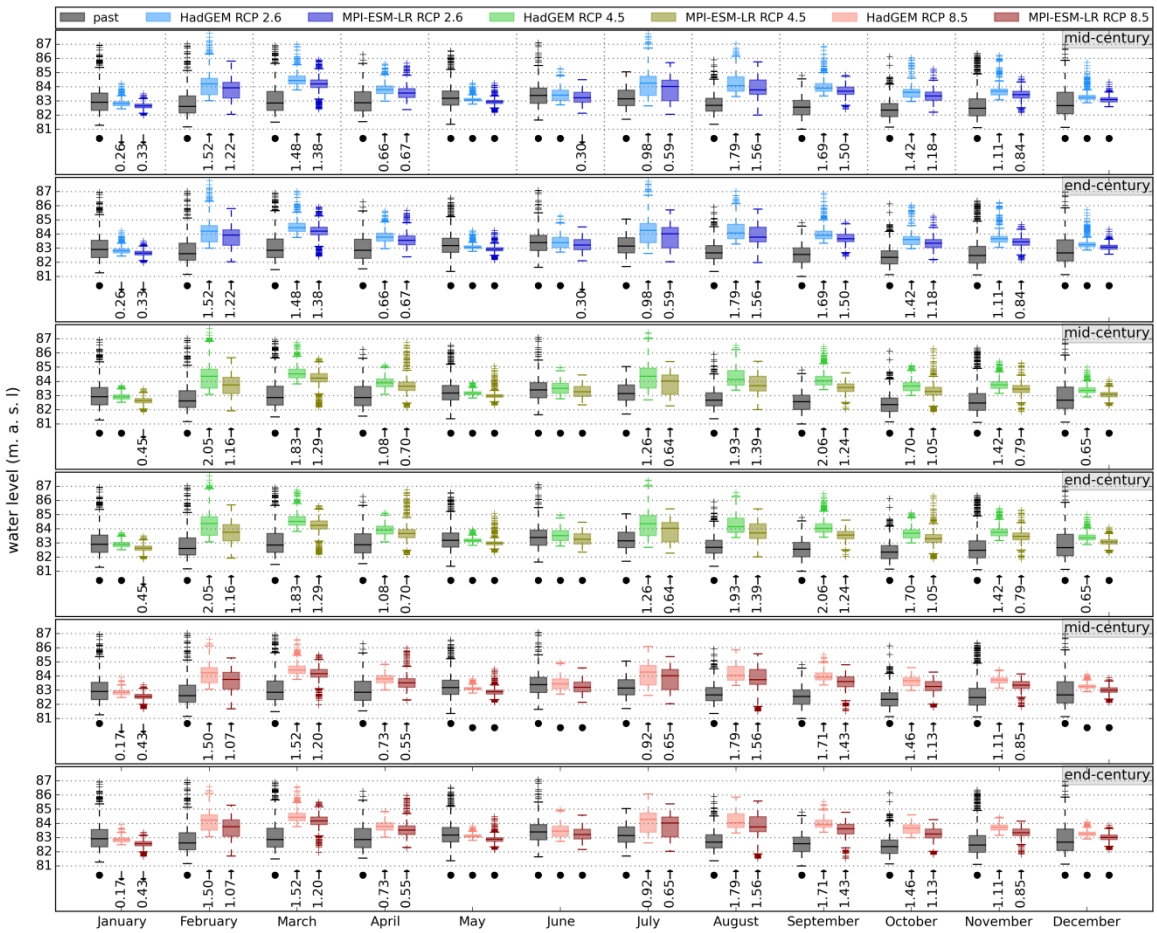

Figure 3.3: Monthly boxplots of HBV-simulated water levels of the Rhine using the best-performing model parameter sets for representative concentration pathway (RCP) 2.6 (bluish, top), RCP 4.5 (greenish, middle), RCP 8.5 (reddish, bottom) and for two different periods (top: mid-century 2021–2050, bottom: end-century 2071–2100). Black boxplots represent observations for the period 1990–2015. The linear trend of the water level change is given below each boxplot for the time from 1990 to 2015 (under black boxplots), from 2021 to 2050 (upper figure of each RCP group, under colored boxplots), and from 2071 to 2100 (lower figure of each RCP group, under colored boxplots). Points indicate no trend; upward arrows indicate an increasing trend and downward arrows a decreasing trend at the significance level of $p < 0.05$ based on the Mann–Kendall Test. For significant trends, the absolute change for the time period is given in meters.

Figure 3.3 shows the simulated past and future water levels of the Rhine per month. Additionally, the trends and absolute changes in mean water level are given below each box plot. Until 2050, all months except January, May, June, and December show an increase between 0.55 m and 2.06 m in the mean water level for almost all GCMs–RCPs combinations. In January, there is a small decrease in the water level (up to 0.45 m). The end-century period primarily shows the same pattern. However, some future projections turn from an increasing or no trend to no trend or a decreasing trend until the end of the end-century period. It should be noted that the total range of water levels decreases in almost all future projections compared to the past. An over 50% decrease in the water level range for single months compared to the past can be seen in January, May, June, October, November, and December. Comparing the two climate scenarios, it is striking that the mean water levels of the MPI-ESM model are always below those of the HadGEM model. At the same time, there is no clear pattern in either increasing or decreasing water level changes from the low concentration pathway (RCP 2.6) to the high concentration pathway (RCP 8.5).

The ranges of the uncertainty bands for the two uncertainty methods addressed here, i.e., HBV parameter and predictive uncertainty, are almost the same for the GCMs and RCPs during both the mid- and the end-century (Table 3.1; an exemplary time sequence is given in Appendix 3-4). We observed that the uncertainty band of the predictive uncertainty is about 50% larger than that of the parameter uncertainty. The mean range of parameter uncertainty between the 5th and 95th percentiles was 0.85 m for the past and between 0.35 m and 0.56 m for the future period. In contrast, the mean range for the predictive uncertainty increases from 1.16 m in the past period to 1.18 and to 1.35 m for the future periods.

Table 3.1: Mean uncertainty (i.e., range of the daily water levels, averaged over the time period) of the Rhine water level of the parameter and predictive uncertainty. GCM: general circulation model. RCP: Representative Concentration Pathways

Time Period	**Past**	**Mid-Century**						**End-Century**					
GCM model		HadGEM			MPI-ESM			HadGEM			MPI-ESM		
RCP		2.6	4.5	8.5	2.6	4.5	8.5	2.6	4.5	8.5	2.6	4.5	8.5
Parameter uncertainty	0.85	0.46	0.50	0.46	0.47	0.48	0.56	0.37	0.36	0.37	0.41	0.35	0.39
Predictive uncertainty	1.16	1.32	1.34	1.35	1.18	1.32	1.35	1.24	1.25	1.27	1.21	1.22	1.26

3.3.2. Projection of Spatial Inundation

The projected water levels of HBV are used to run the surface water–groundwater model CMF to simulate spatially distributed water levels of the floodplain on daily time steps. We used two different indicators to characterize inundation: the number of inundation days per year (Figure 3.4) and the mean duration of inundation period (Figure 3.5).

For the mid-century and the MPI-ESM model, a decrease of four to ten inundation days per year compared to the past period is estimated considering all three RCPs. This is observed for almost the same sites (polygons) in all three RCPs. Results for the HadGEM model are different. Some sites are estimated to have less inundation days on average, while the majority of polygons with changes depict an increase. Furthermore, the number of sites with projected changes of inundation days is higher for the HadGEM model than for the MPI-ESM model. Comparing the mid- to end-century projection, the number of polygons with a changing amount of inundation days at the end-century is less than in the mid-century for both GCMs. The magnitude of changes of inundation days towards the end-century is almost the same for the MPI-ESM model and the RCP 4.5 of the HadGEM model. Under the HadGEM, some sites change from an increase to decrease of inundation days during the mid-century to the end-century, respectively. For the mid-century, the spatial extension of changes in inundation days under HadGEM are decreasing with increasing RCPs, whereas for the end-century, the the spatial extension increases with increasing RCP. For MPI-ESM, the spatial distribution of polygons with changes in inundation days is nearly the same across all RCPs, and even the magnitude of the changes is similar. Overall, the differences between the RCPs are smaller compared to the differences between the GCMs.

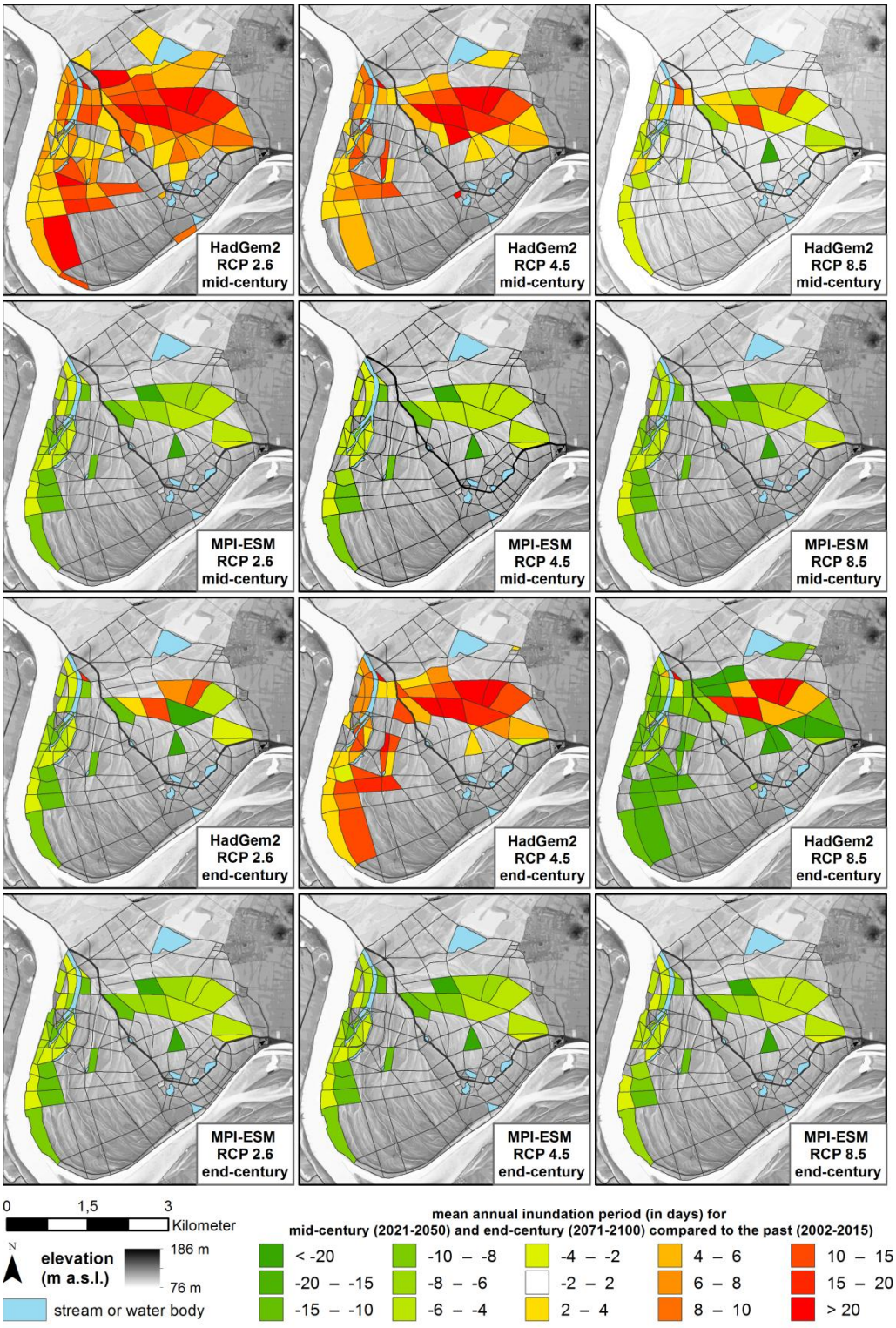

Figure 3.4: Spatial distribution of average inundation days (per year) for the mid-century (2021–2050) and end-century (2071–2100) compared to the past (2002–2015). Results are shown for the different combinations of GCMs and RCPs as the difference of inundation days for the future period minus those from the past. Results shown for the CMF model are forced by simulated water levels of the Rhine River, using the best-performing HBV parameter set for the calibration period.

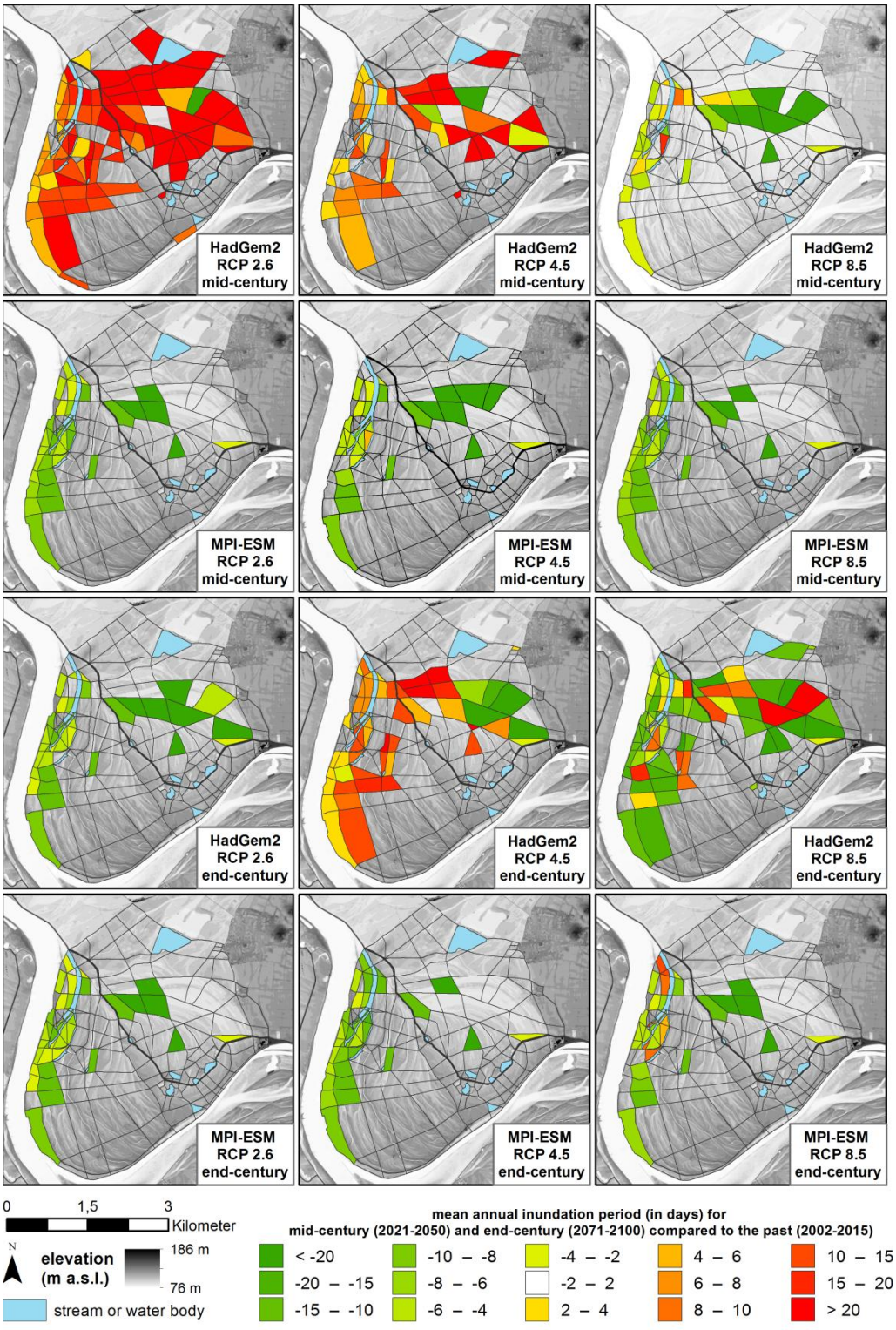

Figure 3.5: Spatial distribution of average inundation duration (days per year) for the mid-century (2021–2050) and end-century (2071–2100) compared to the past (2002–2015). Results are shown for the combinations of GCMs and RCPs as the difference of average inundation duration for the future period minus those from the past. Results shown for the CMF model are forced by simulated water levels of the Rhine River, using the best-performing HBV parameter set for the calibration period.

On the whole, the projections for the duration of the mean annual inundation period (in days) (Figure 3.5) show the same pattern as for the annual number of inundation days (Figure 3.4). The spatial extensions of changes in the MPI-ESM model are almost the same for all RCPs within both time periods. Under the HadGEM GCM, a broader variance in the sites affected by the changes can be seen for the three RCPs. The number of sites with projected changes and the intensity of changes are higher for HadGEM than for MPI-ESM. However, some sites demonstrate a contrasting change (increase/decrease) between the RCPs under HadGEM, whereas under MPI-ESM the tendency of all sites to change is almost the same between the RCPs.

3.3.3. Uncertainty of Projections

This section shows the projected annual inundation days and their differences in projections, considering various sources of differences within the projections, i.e., differences caused by the GCMs, the RCPs and the parameter and predictive uncertainty of HBV.

Figure 3.6 represents the difference of the annual inundation days clustered by the sources causing the differences (GCMs, RCPs, and HBV). The difference is calculated as the variation between the two components (for GCM: HadGEM and MPI-ESM, for RCP: RCP 2.8 and RCP 8.5, and for HBV: predictive and parameter uncertainty). For each source, we estimated the mean annual inundation days by averaging the mean annual inundation days of each possible combination with the other components of sources. The absolute difference between the two components of the source is then stated as quantitative uncertainty (for the corresponding source).

The magnitude of the differences is higher overall when results are clustered based on the considered GCMs or input-driving data for the groundwater–surface water model from the HBV model compared to the differences introduced by the RCPs. On the other hand, the spatial extension of differences is greater for the GCMs and RCPs than for the differences caused by HBV for the mid-century, and it is a bit larger for the GCM and HBV than for the RCP for the end-century. All in all, the spatial extension of differences is much larger for the mid-century than for the end-century for the GCM and RCP. For the HBV source, the spatial extension is nearly the same for the mid- and end-century. The mean difference for the mid-century is 12.6, 3.8, and 20.0 days for the GCM, RCP, and HBV source, respectively (end-century: 22.1 days (GCM), 5.2 days (RCP), and 21.5 days (HBV)).

As an example, for the calculated difference of each polygon (Figure 3.6), the derivation for two polygons (marked as A and B) is shown in Appendix 3-1 in the form of a tree diagram. Polygon A shows a large difference between the mean annual inundation days between the two GCMs (mid-century: 30.8 days, end-century: 33.4 days) as well between the different water levels under the HBV, representing the parameter and predictive uncertainties (mid-century: 20.3 days, end-century: 25.7 days), whereas the differences between the RCPs is rather small (mid-century: 1.9 days, end-century: 6.8 days). For polygon B, the difference arising from the RCPs and the water levels from HBV are nearly the same for the mid-century (RCP: 4.7 days, HBV mid-century: 4.3 days), whereas the difference arising from the GCM is about double (9.1 days). For the end-century, the difference between the GCMs and between the parameter and predictive uncertainty of the HBV model are nearly the same (GCM: 5.3, HBV: 5.4 days), and the differences between the RCPs are lower (3.5 days).

Additionally, our findings show that it is necessary to consider as many uncertainties as possible within a modeling procedure, including several models and steps. For example, a difference in the range of mean annual inundation days can be seen when considering the uncertainty introduced by the parameter and predictive uncertainties in the HBV model under the two GCMs. The mean annual inundation days under the HadGEM model are predominantly higher than under the MPI-ESM model (Appendix 3-2, bottom. Reported as HadGEM model, Parameter Uncertainty (HG PaU) vs. MPI-ESM model, Parameter uncertainty (ME PaU) and HadGEM model, predictive uncertainty (HG PrU) vs. MPI-ESM model, predictive uncertainty (ME PrU)).

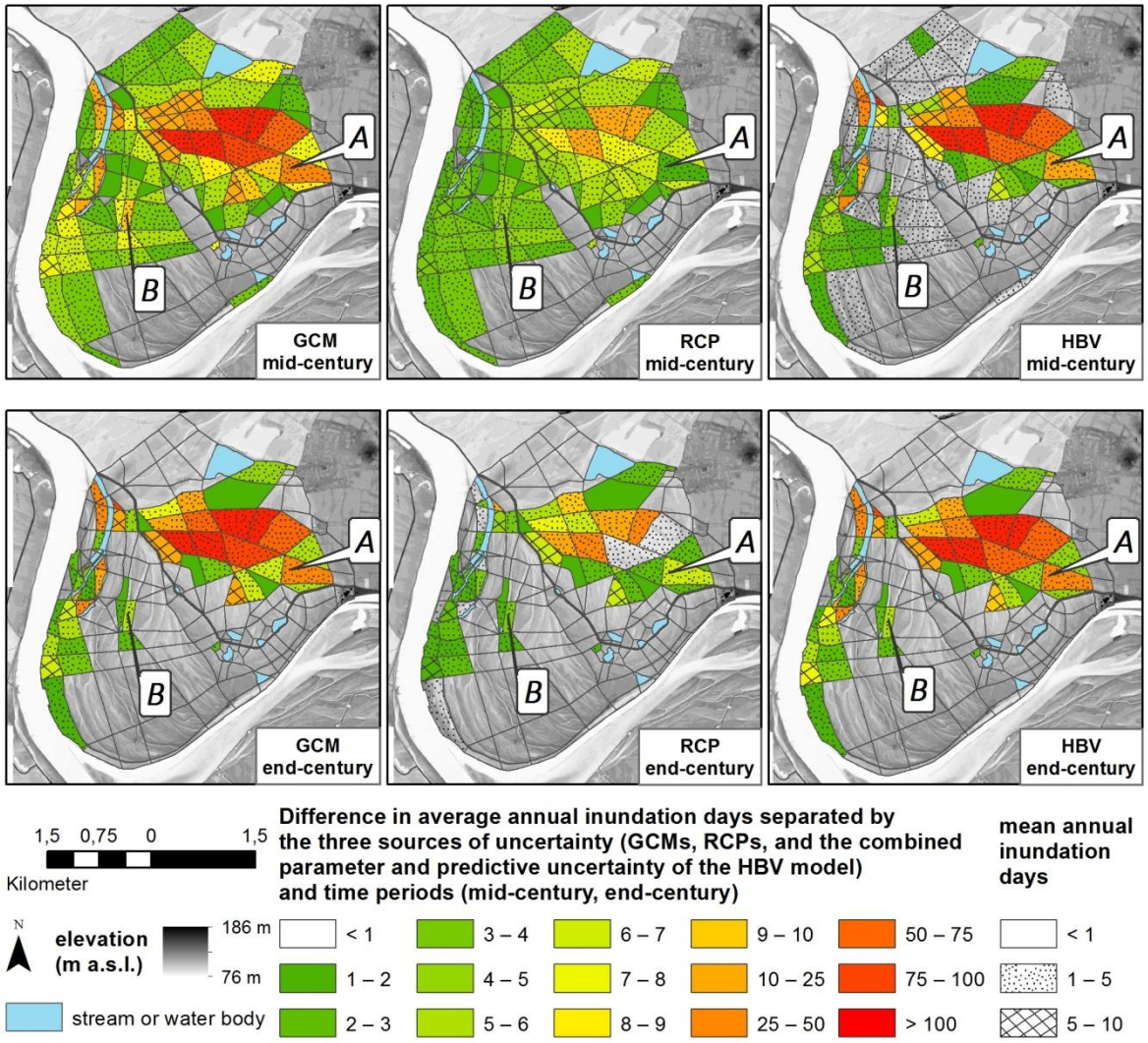

Figure 3.6: Uncertainty of the annual inundation days per time period separated by the three sources of uncertainty: GCMs, RCPs, and the parameter and predictive uncertainty of the HBV model. Each component represents the mean of all possible combinations, whereas each combination indicates the average annual flooding days. The filling patterns depict the mean annual inundation days from all simulations. The top panels show results for the mid-century, bottom panels for the end-century conditions. (A,B) indicate sites that are specifically referred to in the text.

3.4. Discussion

Our HBV model of the Rhine River showed satisfactory results for the calibration and validation periods, and it was able to reproduce peak flow as well as low flow conditions very well (Appendix 3-3). The same results have also been observed in other applications of the HBV model for the Rhine River (e.g., te Linde et al., 2008). We found that the water level of the Rhine River is the primary driving variable for the groundwater–surface water model, as the Rhine River is known to be directly connected with the groundwater of the floodplain and is mainly responsible for the groundwater level changes (Maier et al., 2017).

A similar trend of the water level changes for the best simulation of the HBV model was found for both climate scenarios and the different concentration pathways (differentiated by the month of the year, Figure 3.3). The mean range of the uncertainty band for the different projections (Table 3.1) is smaller for the parameter uncertainty (0.35–0.56 m) than for the predictive uncertainty (1.18–1.35 m). This is an indication for other prominent uncertainty sources for the model (e.g., model context, structure or forcing data), except that of the parameters (Mockler et al., 2016). The differences in the mean range of the water level between the GCMs and RCPs are very small (predictive uncertainty: <0.10 m, parameter uncertainty: <0.17 m). In contrast, the inundation characteristics (annual inundation days and average annual inundation period) show large differences between the climate projections. While HadGEM indicates an increase in annual inundation days over large areas, MPI-ESM actually projects a decrease at some sites (Figure 3.4 and Figure 3.5).

To quantify the magnitude of all three sources (GCMs, RCPs, and the input driving data for CMF from the HBV model), causing differences in the mean annual inundation days, we averaged the annual inundation days of all possible model combinations for each component of each source (Figure 3.6). With this information, we could emphasize that our results are very sensitive to the used GCM. In addition, we showed that the input driving data from the HBV model have an important influence as well on the inundation of the study area. For both components of input driving data (predictive and parameter uncertainty), the annual inundation days are much larger under HadGEM. The mean seasonal amount of precipitation for the two GCMs already indicates different trends (Appendix 3-5). Whereas the HadGEM model shows a larger increase in autumn precipitation (+25.26%) than in spring precipitation (+2.47%), the MPI model shows a larger increase in spring precipitation (+24.47%) than in autumn precipitation (−3.10%). For winter and summer, both models show

the same trend (increasing in winter (HadGEM: +33.85%, MPI-ESM: +47.95%) and decreasing in summer (HadGEM: -13.05%, MPI-ESM: −18.68%)). Following this, under the HadGEM, the mean simulated water level by HBV shows the largest increase (+1.23%) in summer and autumn. Under the MPI-ESM model, the increases in the water levels in summer and autumn are not as high (+0.54%) as under the HadGEM model (Appendix 3-6). This shows that it is necessary to consider the cascading uncertainty, because the final uncertainty is dependent on the uncertainty sources of the driving variables from the previously-applied model, as already depicted by other authors (Refsgaard et al., 2013).

Similar to our study, Her et al. (2016) evaluated the contribution of uncertainties contained in multi-GCM and multi-parameter ensembles. They considered one hydrological model (ABCD) and concluded that the significance of GCM and hydrological parameter selection varies, depending on the hydrological components. For instance, they showed that streamflow is affected by the uncertainty of GCMs and that the uncertainty of parameter ensembles influences groundwater projections. This is partially consistent with our results: the GCMs and the uncertainty of the water level projections of the Rhine River (including parameter uncertainty of HBV) have a large influence on the inundation characteristics. However, our results also indicate that the GCMs are a single, dominating source for different results when neglecting any further possible sources, e.g., the uncertainty of the discharge of the Rhine River (shown in the results of the spatial distribution of inundation days in Figure 3.3). Chen et al. (2011) ranked several uncertainty sources (GCM, emission scenarios, GCM initial conditions, downscaling techniques, hydrological model, and hydrological model parameters) for seven hydrological criteria (annual/seasonal discharge, time to start/peak/end of the flood). GCMs were the largest source of uncertainty for all criteria, which aligns with our results.

Our applied climate change projections show many varying impacts to the floodplain of the Rhine River, from an increasing to decreasing trend of annual inundation days per year, from large to rather small spatial changes in inundation characteristics, and from large to small differences. Only for a small area (3.8 km^2 in the southwest region of the study area, close to the cut-off meander of the Rhine River) no inundation is simulated under any projection.

Choosing a different RCP means choosing a different future, with either higher or lower concentration pathways; hence, the difference of the two is rather representative of the

benefits of mitigation. Strangely enough, our results, especially under the MPI-ESM model, do not really suggest there is much benefit in mitigation. The difference in the rather optimistic RCP 2.6 and the rather pessimistic RCP 8.5 is rather small compared to the differences arising from the selection of the GCM and the underlying uncertainties arising from the hydrological modeling. The future predictions of the Rhine river remains very uncertain compared to other large river basins world-wide (Pechlivanidis et al., 2017).

On the whole, changes in potential habitats on the floodplain are likely, but the extent and the direction of the changes are unclear due to the uncertainties induced by the models and the climate change scenarios. Nevertheless, the estimated changes in inundations would have large effects for species living in these areas, as we identified relevant changes in inundation duration and frequency for as soon as the mid-century period. Not included in our study, but equally important, are land-use modifications, e.g., by humans, political economics or structures. Land use changes, such as forest degradation or fertilization, can lead directly or indirectly through changes of the inundation patterns and water availability to changes in biodiversity and habitat availability. For this reason, such sites should be treated with caution when it comes to the management of natural resources, restoration measures, or implementation of biodiversity protections schemes (Eamus et al., 2006; Opperman et al., 2010).

3.5. Conclusions

The work carried out here presents a methodological approach to evaluating the impact of climate change on the inundation characteristics on a typical floodplain of one of Germany's largest rivers. We considered different climate models, emission scenarios, and Bayesian methods to assess the uncertainty of our model chain. By linking an established rainfall–runoff model with a parsimonious surface water–groundwater model, we are able to project the future habitat conditions of floodplains.

The results presented should be interpreted as trends and not as an accurate quantitative prediction, particularly regarding the uncertainties related to the GCMs. We recommend the consideration of a larger ensemble of GCMs to better constrain the potential effects of climate change in these ecosystems.

The projected shift of inundation patterns and their extent will have consequences for habitat availability and species distribution, which will occur during the course of climate change. Such information is especially valuable for the protection of endangered species and for the long-term planning and success of renaturation projects in biodiversity-rich floodplains. After linking ecological habitat models to our modeling chain, the next step forward will be to project habitat distribution and quality under climate change.

Acknowledgement

Author Contributions: Conceptualization, N.M.; Methodology, N.M., P.K., T.H., A.C.; Software, N.M., P.K., T.H., A.C.; Validation, N.M.; Formal Analysis, N.M.; Investigation, N.M.; Resources, N.M., P.K., T.H., A.C., L.B.; Writing-Original Draft Preparation, N.M.; Writing-Review & Editing, T.H., A.C., L.B., P.K.; Visualization, N.M.; Supervision, T.H., P.K., L.B.; Project Administration, P.K.; Funding Acquisition, P.K., L.B.

Funding: This research was funded by the Deutsche Bundesstiftung Umwelt DBU (project 31612–33/0; www.dbu.de). Tobias Houska and Alejandro Chamorro acknowledge funding through the DFG grants BR2238/13-1 (Uncertainty of predicted hydro-biogeochemical fluxes and trace gas emissions on the landscape scale under climate and land use change) and BR2238/5-2 (Ensemble projections of hydro-biogeochemical fluxes under climate change), respectively.

Acknowledgments: The climate data used are available from Germany's national meteorological service (Deutscher Wetterdienst (DWD), http://www.dwd.de/cdc; ftp://ftp-cdc.dwd.de/pub/CDC). Daily water levels from the Nierstein gauging station are available from the Federal Waterways and Shipping Authority (Wasser und Schifffahrtsverwaltung des Bundes (WSV)) and provided by the Federal Institute of Hydrology (Bundesanstalt für Gewässerkunde (BfG)). Groundwater levels are provided by the Hessian State Office for Conservation, Environment and Geology (Hessisches Landesamt für Naturschutz, Umwelt und Geologie (HLNUG)). Precipitation and temperature data for the GCMs are taken from the IPCC data distribution center (http://cera-www.dkrz.de).

Conflicts of Interest: The authors declare no conflicts of interest. The funders had no role in the design of the study; in the collection, analyses, or interpretation of data; in the writing of the manuscript, and in the decision to publish the results.

Supporting information

Appendix 3-1

Example of the quantification of differences in the mean annual inundation days for the polygons A and B (Figure 3.3) for the mid-century and the end-century, represented in the form of tree diagrams. Each node at the bottom represents the mean annual inundation days of the two polygons (A and B) of a simulation. The nodes one and two levels higher depict the mean of the two lower nodes. Only the node in the top depicts the difference between the two lower nodes (depicted by dashed lines); i.e., the top node indicates the difference between the mean annual inundation days and represents the quantitative uncertainty. Abbreviations used: HG = HadGEM, ME = MPI-ESM, 2.6 = RCP 2.6, 8.5 = RCP 8.5, PrU = predictive uncertainty, PaU = parameter uncertainty.

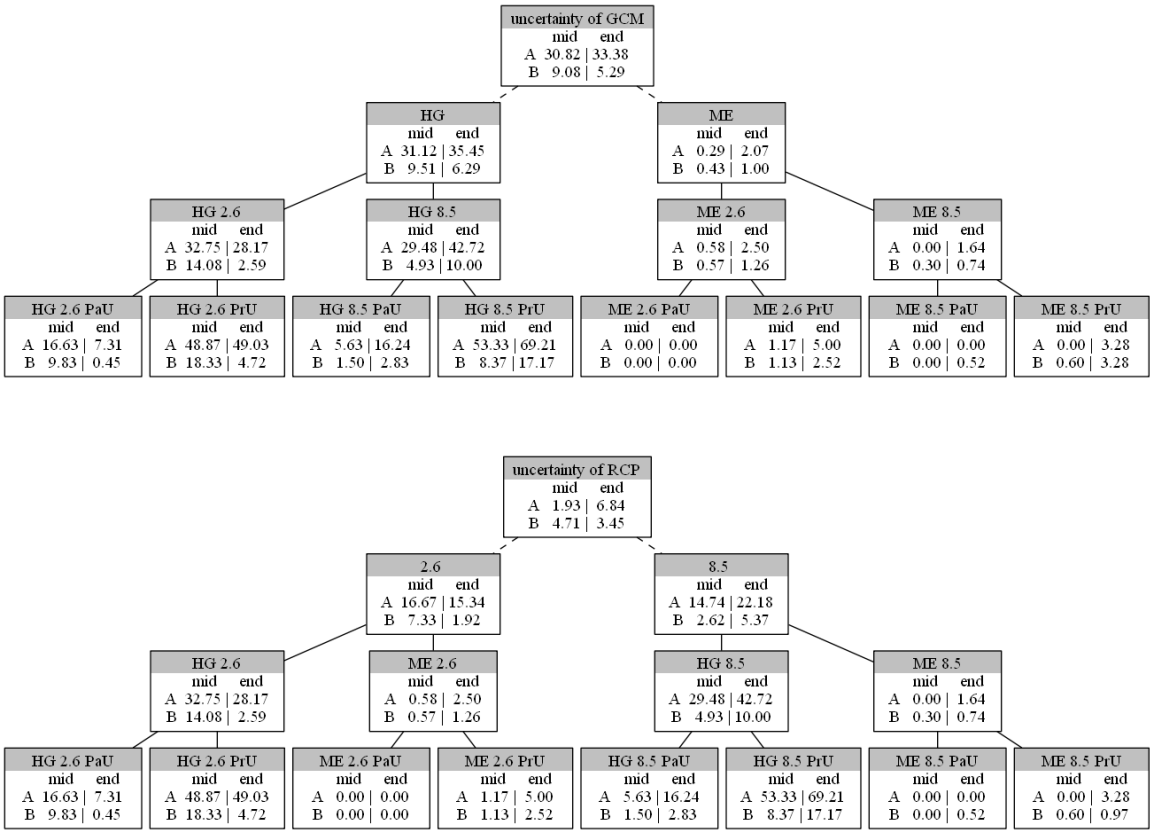

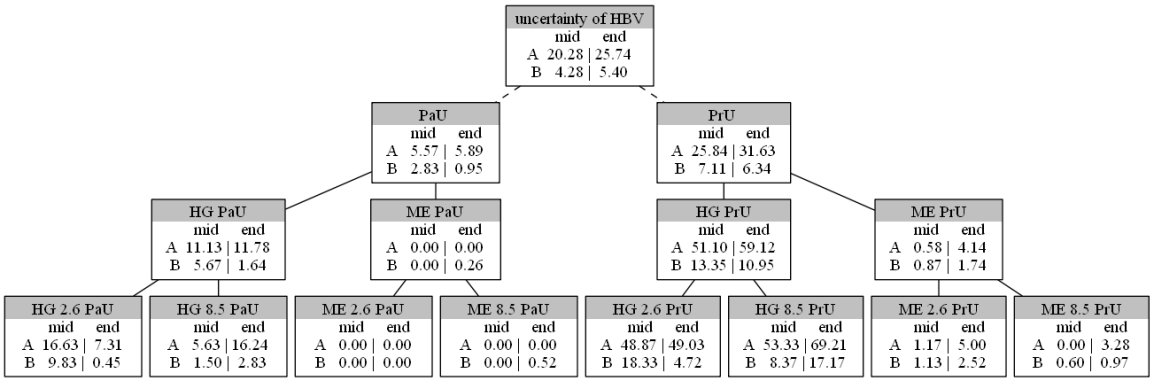

Appendix 3-2

HBV model parameters, their meaning, range for calibration and value for best performing parameter set.

Parameter	Description	Unit	Lower Bound–Upper Bound	Best Parameter Set
CE	Potential evapotranspiration model parameter	-	0.01–0.2	0.09
Theta	Actual evapotranspiration coefficient	-	0.8–1.5	1.00
TT	Threshold melting Temperature	°C	−0.98–2	0.43
Cmelt	Sow melting parameter	-	0.2–2.0	1.10
FC	Field capacity	mm	40–250	207.56
Beta	Model parameter	-	1–5	1.00
PWP	Permanent wilting point	mm	40–250	159.82
L	Depth of upper reservoir	mm	1–100	41.50
K1	Surface flow storage constant	1/d	10–800	25.27
K2	Interflow storage constant	1/d	10–850	35.85
KZ	Percolation storage constant	1/d	10–980	178.53
K3	Baseflow storage constant	1/d	10–1000	353.30

Appendix 3-3

Performance of the HBV model, shown for the best performing parameter set for the years 2001 to 2013 (top) and for the year 2007 with the parameter and the predictive uncertainty band (bottom).

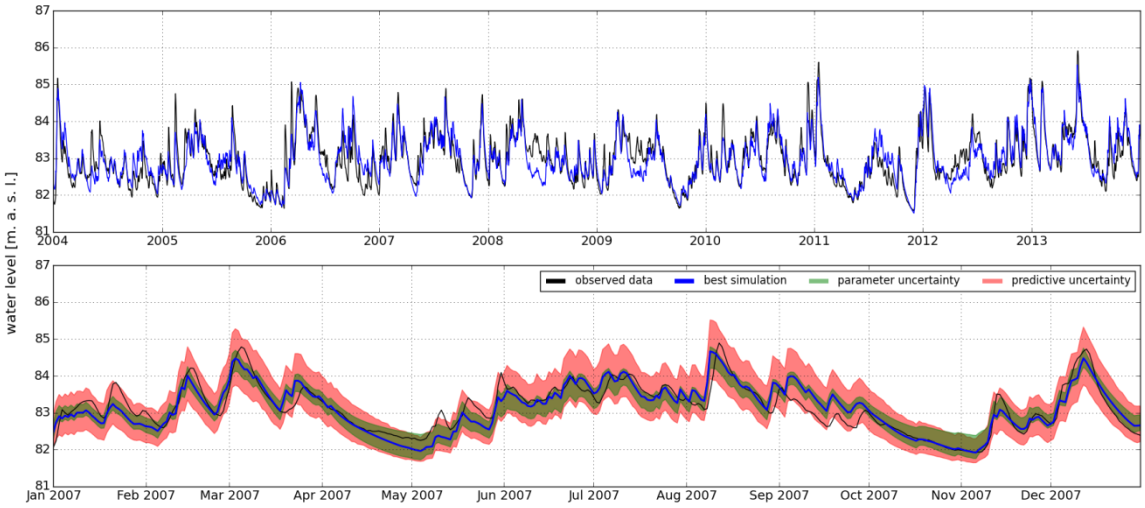

Appendix 3-4

Projected water levels of the Rhine river and the associated uncertainty bands (parameter and predictive uncertainty), exemplarily shown for the years 2040 to 2050 (top) and for the year 2045 (bottom).

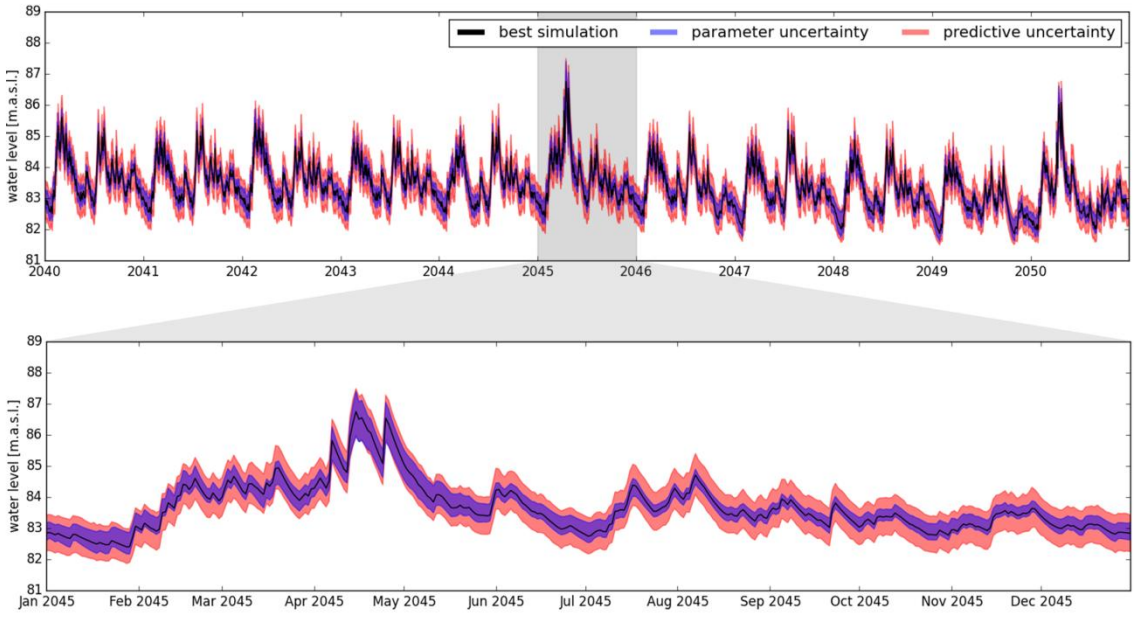

Appendix 3-5

Changes in the amount of precipitation for different seasons for the weather station in Darmstadt. The change is given in percentage compared to the observed period for the historical data (from the GCMs) and compared to the historical period of the GCM for the RCPs. Data are downscaled by using quantile mapping. The arrows indicate the direction and the magnitude of the trend.

	GCM		Winter	Spring	Summer	Autumn
2000–2005		observed	171.50 mm	183.88 mm	197.35 mm	196.72 mm
	HadGEM	historical	−8.53% ↙	−0.17% ↙	−11.75% ↙	−0.27% ↙
	MPI-ESM	historical	−19.80% ↙	−5.06% ↙	−3.95% ↙	0.06% ↗
2021–2050	HadGEM	RCP 2.6	14.73% ↗	−0.05% ↙	−11.42% ↙	17.87% ↗
		RCP 4.5	41.21% ↑	4.62% ↗	−3.77% ↙	24.09% ↑
		RCP 8.5	24.36% ↗	7.29% ↗	−9.52% ↙	30.91% ↑
	MPI	RCP 2.6	49.65% ↑	28.51% ↑	−7.62% ↙	5.53% ↗
		RCP 4.5	48.44% ↑	33.52% ↑	−8.87% ↙	−4.52% ↙
		RCP 8.5	41.14% ↑	19.12% ↗	−15.60% ↙	1.64% ↗
2021–2050	HadGEM	RCP 2.6	34.57% ↑	6.55% ↗	3.68% ↑	15.00% ↗
		RCP 4.5	32.23% ↑	−5.90% ↙	−17.52% ↓	35.25% ↑
		RCP 8.5	55.99% ↑	2.30% ↗	−39.73% ↓	28.44% ↑
	MPI	RCP 2.6	50.70% ↑	17.54% ↗	−12.67% ↙	0.37% ↗
		RCP 4.5	46.24% ↑	23.80% ↗	−23.67% ↓	−13.05% ↙
		RCP 8.5	51.50% ↑	24.30% ↗	−43.64% ↓	−8.56% ↙

Appendix 3-6

Changes in the mean water level at the gauging station Mainz (observed and simulated with HBV) for different seasons. The change is given in percentage compared to the observed period for the historical data from the GCMs) and compared to the historical period of the GCM for the RCP's. The arrows indicate the direction and the magnitude of the trend.

	GCM		Winter	Spring	Summer	Autumn
2000–2005		observed	83.12 m	83.34 m	82.99 m	82.76 m
	HadGEM	historical	−0.31% ↓	0.27% ↗	−0.05% ↙	0.11% ↗
	MPI-ESM	historical	−0.19% ↓	−0.13% ↙	0.04% ↗	0.32% ↗
2021–2050	HadGEM	RCP 2.6	0.68% ↑	0.30% ↗	1.22% ↑	1.21% ↑
		RCP 4.5	0.81% ↑	0.41% ↗	1.33% ↑	1.30% ↑
		RCP 8.5	0.66% ↑	0.29% ↗	1.21% ↑	1.21% ↑
	MPI	RCP 2.6	0.25% ↗	0.39% ↗	0.76% ↑	0.64% ↗
		RCP 4.5	0.18% ↗	0.49% ↗	0.75% ↑	0.59% ↗
		RCP 8.5	0.11% ↗	0.35% ↗	0.74% ↑	0.54% ↗
2021–2050	HadGEM	RCP 2.6	0.64% ↑	0.26% ↗	1.22% ↑	1.18% ↑
		RCP 4.5	0.74% ↑	0.31% ↗	1.24% ↑	1.27% ↑
		RCP 8.5	0.72% ↑	0.25% ↗	1.20% ↑	1.19% ↑
	MPI	RCP 2.6	0.22% ↗	0.39% ↗	0.78% ↑	0.61% ↗
		RCP 4.5	0.07% ↗	0.27% ↗	0.54% ↗	0.35% ↗
		RCP 8.5	0.02% ↗	0.28% ↗	0.17% ↗	0.08% ↗

4. Modeling of rare flood meadow species distribution by a combined habitat-surface water-groundwater model

This chapter has been submitted to the journal *Ecohydrology*.

Johannes P. Gattringer[1]*, Nadine Maier[2]*, Lutz Breuer[2,3], Annette Otte[1,3], Tobias W. Donath[4], Philipp Kraft[2], Sarah Harvolk-Schöning[1]

1 Institute for Landscape Ecology and Resources Management, Division of Landscape Ecology and Landscape Planning, Research Centre for Biosystems, Land Use and Nutrition (iFZ), Justus Liebig University Giessen, Heinrich-Buff-Ring 26–32, 35392 Giessen, Germany
2 Institute for Landscape Ecology and Resources Management, Division of Landscape, Water and Biogeochemical Cycles, Research Centre for Biosystems, Land Use and Nutrition (iFZ), Justus Liebig University Giessen, Heinrich-Buff-Ring 26–32, 35392 Giessen, Germany
3 Centre for International Development and Environmental Research (ZEU), Justus Liebig University Giessen, Senckenbergstraße 3, 35390 Giessen, Germany
4 Department of Landscape Ecology, Institute for Natural Resource Conservation, Kiel University, Olshausenstraße 75, 24118 Kiel, Germany
* These authors contributed equally to the work.

Abstract

Floodplains are highly complex and dynamic systems in terms of their hydrology. Thus, they comprise a wide habitat heterogeneity and therefore harbor highly-specialized species. For future projections of habitat and species diversity, process-based models simulating ecohydrological conditions and resulting habitat and species distributions are needed. We present a new modeling framework that includes a physically-based, surface water-groundwater model coupled with a habitat model. Using the model framework, we simulate the occurrence of 23 flood meadow plant species in a Rhine River floodplain. To benchmark the data, results are compared to a conventional approach with simple spatial hydrological information. Our results show that models with predictors obtained from the surface water-groundwater model are significantly more accurate for rare and endangered species, as well as for typical flood meadow species. Therefore, we recommend including more specific hydrological information in habitat models of species in complex floodplain ecosystems.

4.1. Introduction

River floodplains comprise a large species diversity, and at the same time, they belong to the most endangered ecosystems worldwide (Funk et al., 2013; Tockner and Stanford, 2002; Ward et al., 1999). In regards to their hydrology, they are highly dynamic and complex, because many different components, including surface water, groundwater, and precipitation, are interacting on high temporal and spatial resolution. The driving factor of eco-hydrological functions in floodplains is the connectivity and interaction of shallow groundwater with the surface water due to inundations (Hayashi and Rosenberry, 2002; Krause et al., 2007a).

In river-fed floodplains, the main driving factor of the water table is the river stage (Acreman and Holden, 2013). The response time of the water table to changes in the river stage can be very rapid on a wide spatial extent (Jung et al., 2004). The antecedent soil moisture condition alters the water storage capacity of the soil and thus drives the flood extent, flood duration, and inundation height of water in the floodplain. The actual soil water conditions are not only affected by flood events, but also by previous weather conditions and the ability of the wetland to lose water through soil drainage, evaporation, and transpiration (Acreman and Holden, 2013). This complexity in hydrological fluxes and stages is reflected in floodplain's habitat and species diversity.

Species composition in floodplains is influenced by the tolerance of and assimilation to inter-annual-variation of flooding and droughts, the duration and depth of flooding (David, 1996; Mathar et al., 2015), as well as the groundwater regimes (Newbold, 1997) not only within one year but also during the previous years. Flood meadows are amongst the most threatened plant communities in Central Europe (Finck et al., 2017; Joyce and Wade, 1998). Numerous flood meadow species, also called river corridor plants, grow on such flood meadows. These species have adapted to the specific disturbance regimes of floodplains, but they are often rare and/or endangered (Burkart, 2001).

Flood meadows are often protected, e.g., by the EU Habitats Directive in Europe, not only because of their diversity and threat of extinction, but also the additional ecosystem services they provide, including flood control. Numerous restoration measures have been implemented to help maintain the diversity of species-rich meadows. These measures primarily focus on the reestablishment of rare species (Donath et al., 2007; Engst et al., 2016).

However, the complex hydrological conditions of the target areas (Malanson, 1993) often pose a challenge to such restoration projects. Plant distribution is strongly related to hydrologic conditions that should be considered during restoration, e.g., flood sensitive species occupy elevated microsites, whereas flood tolerant species occur in depressions (Jung et al., 2008; Ludewig et al., 2014; Vervuren et al., 2003). Thus, hydrologic conditions should be incorporated in the planning of flood meadow restoration projects (Gattringer et al., 2017).

Planning, decision-making, and projections for the future require models. Such models need to simulate hydrological processes, and based on this information, define potential habitat characteristics and species abundances. The requirements are high for a hydrological model to simulate the complex hydrodynamic interactions of a floodplain as outlined above. These models need to be capable of simulating water fluxes of and between different landscape components (surface water, groundwater, river water, soil storage, vegetation, and atmosphere) on a high temporal and spatial resolution (Lewin and Hughes, 1980). Recently, Maier et al. (2017) presented a parsimonious floodplain model that includes these mechanisms. They used the Catchment Modeling Framework (Kraft et al., 2011) to set up a tailor-made, fully-distributed surface water-groundwater interaction model for the simulation of the height and duration of inundations as well as the flooding frequency, and they applied it to a nature reserve in the Rhine Valley, Germany.

Habitat models have proven to be an ideal tool for enhancing conservation decisions, especially when modelers and conservationists are working closely together, and thus modeling and decision processes are tightly interwoven (Guisan et al., 2013). However, in the past, it was considered a challenge to model the distribution of rare and endangered species (Elith* et al., 2006; Guisan et al., 2006); rare species datasets are mostly characterized by low occurrences, resulting in potentially over-fitted models when multiple predictors are included (necessary for describing the species' niches) (Lomba et al., 2010). A promising step forward to overcome this obstacle was made by considering model ensembles of small models (ESM) to improve the reliability of habitat models (Breiner et al., 2015, 2018). Few studies have tested this novel approach, but not for rare flood meadow species (Breiner et al., 2018; Di Febbraro et al., 2017).

So far, only a few studies have used hydrological information to simulate the distribution of riparian vegetation or the occurrence of plant species in these regions. Mosner et al. (2011) employed average water level und water level fluctuation to model the distribution of Salix

species on 400 km² along the Elbe River, and Leyer (2005) utilized a similar approach to simulate the abundance of 30 common grassland species in the Elbe River floodplain. Mosner et al. (2015) computed habitat models by relating up to five hydrological variables with occurrence records of several floodplain plants along the Upper Rhine River. However, these studies only included static, interpolated hydrological information, such as average groundwater level or its standard deviation. Nevertheless, this does not reflect the actual dynamic hydrological conditions for the plants with varying length and height of inundation.

This study aims to overcome the static approach implemented in most habitat models. Instead, we propose an integrated model approach with biotic and dynamic abiotic processes. With this method, we are able to project species occurrences and habitat suitability in the light of decision-making, management, or global change studies. This study is based on almost 20 years of practical experience in flood meadow restoration, modeling of species distribution, and process-based hydrological model development. We hypothesize that (1) dynamic hydrological predictors improve the credibility of habitat models for floodplains, and (2) detailed hydrological predictors are necessary to accurately model species occurrence, particularly that of rare and endangered species.

4.2. Material and Methods

4.2.1. Study area and database

The study area (34.5 km²) is located in a Holocene floodplain in the Upper River Rhine approximately 30 km southwest of Frankfurt, Germany (N 49°49', E 8°26'). The nature reserve Kühkopf-Knoblochsaue is the largest of its kind in the federal state of Hesse and is declared as a Special Area of Conservation (Council Directive 92/43/EEC) because of its particular importance for rare and endangered flora and fauna. The meander cutoff of the Rhine forms a loop around the Kühkopf island (19.5 km²), with a length of about 16 km (Figure 4.1). Embankments for river regulation were installed in the 19th and 20th centuries. They divide the area into functional (8.5 km², west of the embankment) and fossil (6.4 km², east of the embankment) floodplain. The two parts vary in their river hydrological connectivity and characteristics, as well as soil types (Böger, 1991).

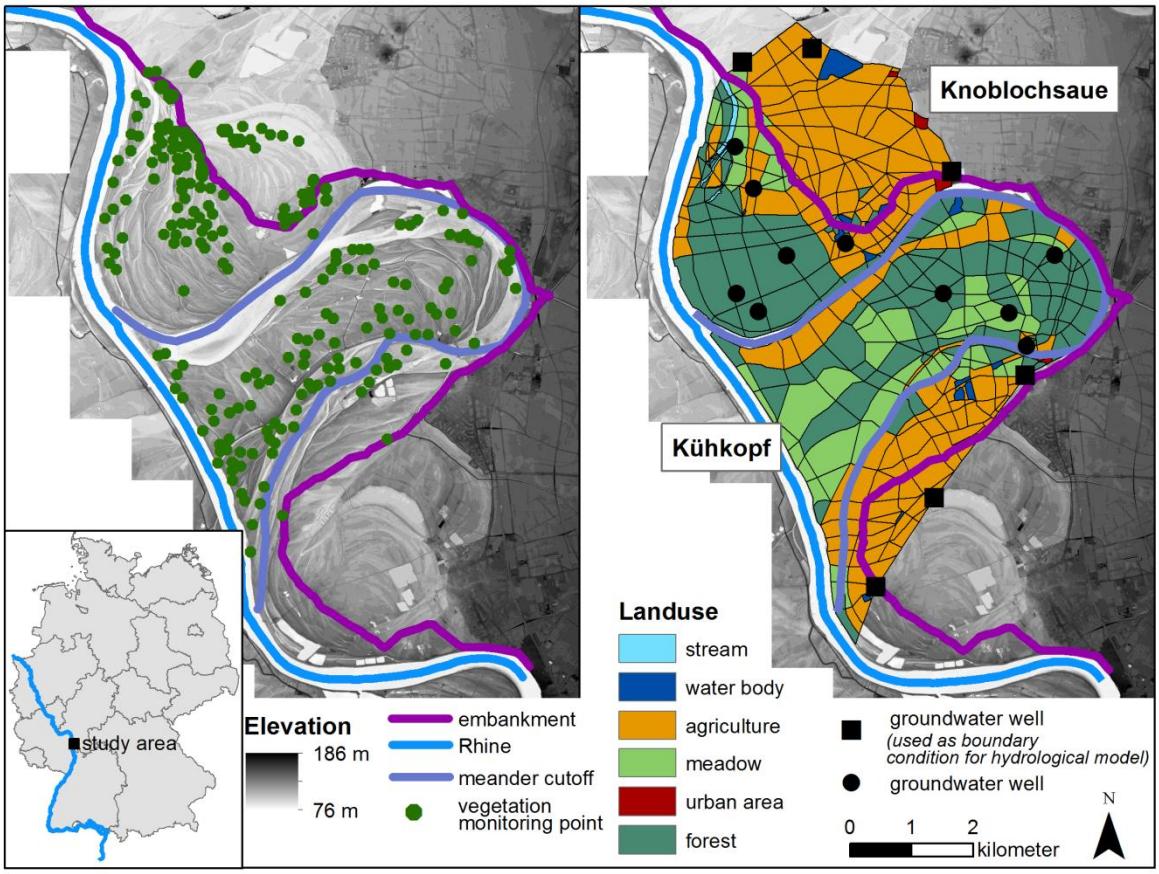

Figure 4.1: Geographic location of the study area in Germany (lower left corner), digital elevation (Hessian Administration for Soil Management and Geographical Information, HVBG, Wiesbaden, Germany) of the study area with the location of vegetation observations (middle) and setup of the surface water-groundwater model (catchment modeling framework, CMF) with its irregular grid and land use, containing the locations of the groundwater wells (right).

The mean daily temperature is about 10 °C, and the mean relative humidity is 78% (2000–2015). The average annual precipitation is 700 mm (2000–2015). 2006 was a wet year with 925 mm, and 2015 a dry year with only 235 mm precipitation.

The study area is dominated by a strong seasonal change between floods and droughts. Flooding occurs mainly from February to June and rarely in summer (Böger, 1991; Hölzel and Otte, 2004). The fine-grained calcareous alluvial soils have high clay contents. Soils desiccate rapidly after the drawdown of floods or high groundwater levels and available soil water content decreases (Burmeier et al., 2010). Flood duration and height vary considerably between the years as well as seasonally. The highest water levels between 2002 and 2013 were reached in April 2003 (87.1 m a.s.l) and March 2003 (86.62 m a.s.l, gauging station

Nierstein-Oppenheim, 3 km downstream). All years during the study period had a flood event in the winter.

Meteorology

The meteorological data are provided by the Deutscher Wetterdienst (DWD) in daily time steps and include minimum and maximum temperature, mean relative humidity, mean wind speed, and precipitation. The meteorological data are used to force the surface water-groundwater model. Five meteorological predictors for the habitat model are directly generated from the daily precipitation records.

Hydrology

Weekly measurements of 15 groundwater wells are available for the study area (Hessian Agency for Nature Conservation, Environment and Geology (HLNUG)). Six groundwater wells are installed in the fossil floodplain and there are nine wells in the functional floodplain **(**Figure 4.1**).** The groundwater level time series of the groundwater wells in the floodplain correlate, with a short time lag, with the water level time series of the Rhine. The flood signal smoothes out with increasing distance from the river. In case daily water levels are needed, linear interpolation is used.

The water level of the Rhine River is obtained from the FLYS software (Flusshydrologischer Webdienst, German Federal Institute of Hydrology, BfG, Koblenz, Germany) for every 100 m along the Rhine River (values for river-kilometers 468 to 480 were considered).

Plant species

The 23 plant species used for modeling in this study (Appendix 4-1 in Supporting Information) were target species in numerous restoration projects focusing on the reestablishment of species-rich flood meadows along the northern Upper Rhine (Donath et al., 2007). In total, 226 vegetation plots with information on presence and absence of target species served as basis for the habitat modeling (for further information on vegetation data, see Appendix 4-1).

4.2.2. Integrated model setup

In the following section, the different steps implemented in this study are explained in detail. Figure 4.2 represents the main steps in the modeling process. The surface water groundwater model depicts the main component for the hydrological representation of the floodplain and the basis for the hydrological predictors of the habitat model. The model is fed by data from the meteorological database and the digital elevation model, as well as other hydrological data (groundwater levels and river water stages). Alongside the hydrological predictors, meteorological and morphological predictors were also derived. After the identification of the best and most powerful predictors, the best 100 predictor sets were used for the calculation of ensembles of small models (ESM strategy).

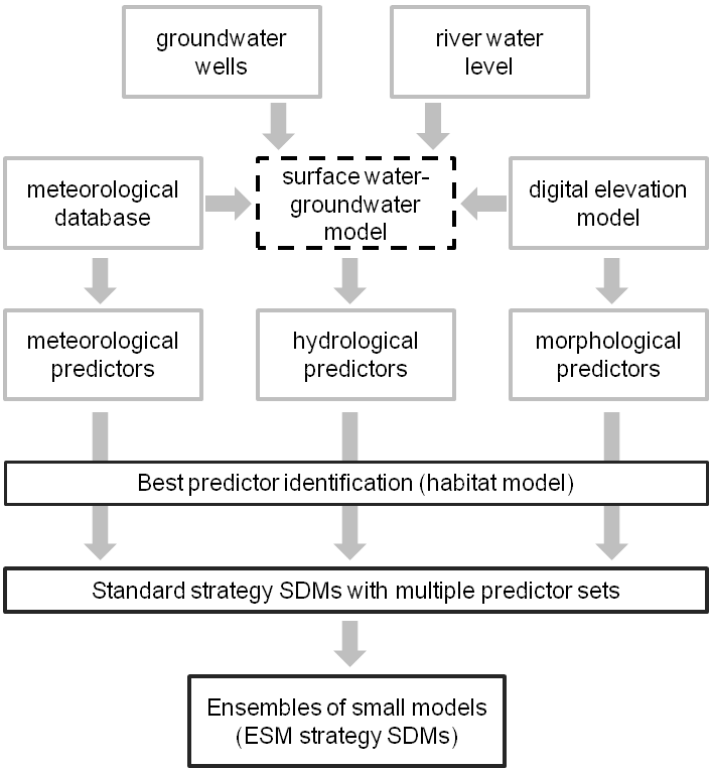

Figure 4.2: Representation of the main steps of the integrated model setup. ESM=Ensembles of Small Models, SDM=Species Distribution Model. The grey boxes depict input data for the following steps. The black boxes indicate modeling steps. The surface water-groundwater model is described in the Methodology section (dashed black box). The solid black boxes depict the main results and are described in the results section.

4.2.2.1. Surface water-groundwater model

In order to simulate the high-resolution input data (temporal and spatial) of groundwater levels and inundation events required for the habitat model, we developed a spatially explicit, fully-distributed dynamic surface water-groundwater model. Full details about the hydrological model setup are described in Maier et al. (2017). In short, the model is built with the Catchment Modeling Framework (CMF) (Kraft et al., 2011) and includes the interaction of surface water and groundwater flow. As input data, the model requires daily stream water levels (in our case study, data from the Rhine River) and weekly groundwater levels at the upslope, daily minimum and maximum temperature and relative humidity for the estimation of potential evapotranspiration, and daily precipitation. The floodplain is split into the two regions Kühkopf and Knoblochsaue (Figure 4.1). These are further subdivided into polygons ($N = 657$) of different sizes (114 – 480,000 m^2), based on similar elevation and land use. For simplicity, the polygons are not further discretized vertically. For each region, the water level of the Rhine and groundwater levels of three monitoring wells are used as input data (Dirichlet boundary conditions). Initial conditions, i.e., the water level of each polygon at the first day of simulation, are calculated using external drift kriging (Goovaerts, 1997). To evaluate the surface water-groundwater model, we use observation data from four to six groundwater monitoring wells in each region. We ran 5,000 simulations following a Latin Hypercube sampling procedure to derive behavioral model runs. We receive a mean root-mean-square error of 0.25 m (Knoblochsaue) and 0.39 m (Kühkopf) for the different groundwater wells for the calibration period of 2.5 years (7.1.2002–30.6.2004), and 0.23 m (Knoblochsaue) and 0.36 m (Kühkopf) for the validation period of 9.5 years (1.7.2004–31.12.2013). As model output, we obtain the water level for the center of each polygon. We use the mean of all behavioral model runs to further estimate the hydrological predictors for the habitat model. The daily water level of each vegetation plot is estimated by inverse distance weighting. Hydrological predictors for the habitat model were calculated from the obtained daily time series of each vegetation plot.

4.2.2.2. Habitat model

Due to the large number of potential hydrological predictors, we follow a three-tiered approach in our modeling cascade to reduce the high computational effort of the final habitat model. As the first step, we identify predictor variables with high explanatory power. Second, we identify the best predictor sets using standard strategy SDMs (species distribution models). Third, we compute ensembles of small bivariate SDMs using the best predictor sets from the second step to overcome possible limitations of standard strategy SDMs due to low presence levels of the modeled species.

Best predictor identification

To identify relevant predictors for species distribution, we established single predictor SDMs for seven target species (i.e., *Arabis nemorensis, Centaurea jacea, Inula silicina, Leucanthemum vulgare, Ranunculus acris, Sanguisorba officinalis,* and *Veronica maritima*) with acceptable occurrence levels within the study area. These seven target species are representative for the total list of the 23 target species (Appendix 4-1). We selected species with low (< 26) or high (> 50) occurrences in the database in combination with species of high relatedness to flood meadows (Burkart=1) or ubiquitous distribution ranges (Burkart=0). We computed generalized linear models (GLMs using the BIOMOD framework (Thuiller et al., 2009) by relating predictors separately with presence-absence of the seven target species. To evaluate the models, we calculated Nagelkerke's R^2 value (Nagelkerke, 1991) for the single predictor SDMs to identify predictors with a large explanatory power. Based on these results, we rejected predictors with little to no explanatory power (i.e., not among the best 50% for most species) or predictors with almost identical information.

The environmental variables used for the species distribution modeling are time invariant (Mieszkowska et al., 2013), whereas the water table and the meteorological conditions vary over time. The meteorological conditions are assumed to be the same over the entire study area. In contrast, the groundwater water table is not static over time or space. To overcome this issue, we transformed the time series into hydrological predictors.

For each vegetation plot, we generated 81 hydrological predictors (Appendix 4-2). These predictors are based on various experimental studies (Gattringer et al., 2017, 2018; e.g., Van Eck et al., 2004) or observational studies (e.g., Leyer, 2005; Mosner et al., 2015). We derived the hydrological predictors either for the entire year or only for the vegetation period, and we considered up to six years before the monitoring year, thus resulting in n=14 different

variations. Beyond that, we identified five meteorological and nine morphological predictors. We used all predictors and time periods to perform single predictor SDMs. Consequently, we computed 1,213 single predictor SDMs per species ((81 hydrological predictors + 5 meteorological predictors) x 14 time periods + 9 morphological predictors).

Standard strategy SDMs with multiple predictor sets

In the next step, we computed standard strategy SDMs with multiple predictor sets from the selected best predictor variables from the single predictor SDMs. Therefore, we calculated GLMs using the BIOMOD framework (Thuiller et al., 2009) for all 23 species. We used all possible combinations of predictors (i.e., predictor sets) that were not correlated according to the rule of thumb as set by Dormann et al. (2013), i.e., correlation coefficients of predictors from a set of 10,000 random points should not exceed 0.7. We calculated Nagelkerke's R2 value (Nagelkerke, 1991) based on a repeated (3 times) split-sampling approach, in which models were calibrated with 80% of the data and evaluated over the remaining 20%. We chose the best 100 predictor sets of each species for the subsequent modeling based on the mean R^2 over the three data splits.

Ensembles of small models (ESM strategy SDMs)

When computing models for rare and endangered species, which are fitted with a high number of predictors, model overfitting may occur. This overfitting can result in decreased generalizability of the models (Vaughan and Ormerod, 2005). To overcome these limitations of standard strategy SDMs of rare species, we computed ensembles of small bivariate SDMs (ESM strategy SDMs) as described by Breiner et al. (2015), which means ESM strategy SDMs are based on a two-step approach. First, bivariate models of all possible twofold combinations of predictors are calibrated and evaluated separately (i.e., by means of the area under the receiver operating characteristic curve; AUC (Hanley and McNeil, 1982)). Second, ensemble models are computed and evaluated (by means of AUC and true skills statistic (TSS)) as a weighted average by means of Somers' D with a threshold of 0, where Somers' D = 2 x AUC - 1 of the bivariate models. This approach avoids overfitting without reducing the number of predictor variables and thus without loss of explanatory power (Breiner et al., 2015). We used predictor sets with up to ten predictors and computed ESM strategy SDMs for the target species. We utilized the R-package ecospat (Broennimann et al., 2016) and a 80:20 cross validation procedure (ten data splits) to calculate the AUC and the TSS (Allouche et al., 2006).

4.2.3. Model evaluation

As we hypothesized that the integrated surface water-groundwater-species distribution model would be superior in simulating species distribution of flood meadows, we rigorously tested our approach. Therefore, we compared model results calculated with hydrological predictors from the surface water-groundwater model with results of a habitat model using similar hydrological predictors, which have been derived from other data sources (i.e., different predictor calculation databases). In one case, we derived the hydrological predictors from daily water levels of the Rhine River and extrapolated to the floodplain (riv, Table 4.1). In the second case, we used the weekly measured groundwater data, and interpolated to daily time steps and extrapolated to the floodplain (gww, Table 4.1). This benchmark approach followed the same procedure as for the surface water-groundwater model. The meteorological and morphological predictors remained the same for both applications. Additionally, to account for the explanatory power of the hydrological variables alone, we also ran the habitat model without any hydrological predictors (nhy, Table 4.1).

Table 4.1: Definition of the four predictor calculation databases used for the evaluation of the habitat model. The superscript indicates for which predictor the input data are relevant.

	Hydrological predictor derived from …	Included predictors	Used input data
sgm	**s**urface water-**g**roundwater **m**odel	[1] hydrological [2] meteorological [3] morphological	water levels of the Rhine River [1], groundwater levels [1], DEM [1,3], meteorological data [2]
gww	**g**round**w**ater **w**ells (observation data, n=16, Figure 4.1)	[1] hydrological [2] meteorological [3] morphological	groundwater levels [1], DEM [1,3], meteorological data [2]
riv	simulated water levels of the Rhine **Riv**er (FLYS)	[1] hydrological, [2] meteorological [3] morphological	water levels of Rhine River [1], DEM [1,3], meteorological data [2]
nhy	(**n**o **hy**drological data)	[2] meteorological [3] morphological	meteorological data[2], DEM [3]

To test for differences in modeling results between the predictor calculation databases, we calculated linear mixed-effects models according to Zuur et al. (2009) (function *lme* in the R-package *nlme*) (Pinheiro et al., 2017). Here, we chose a subset of the seven best predictor sets for every species and every predictor calculation database, because we wanted to identify the best predictor sets – and in the next step, the best explaining predictors. We used – as proxies for quality of habitat models – Fisher-Z-transformed AUC and Fisher-Z-transformed TSS as response variables, the hydrological calculation method as fixed effect, and the factor species as a random effect in the mixed models. We subsequently computed post hoc Tukey contrasts for pairwise comparisons (function *glht* in the R-package *multcomp*) (Hothorn et al., 2008). To compare the influence of the predictor calculation database on model success for individual species, we then calculated ANOVAs for every species separately and subsequently computed post hoc Tukey HSD tests for pairwise comparisons.

Additionally, we accounted for possible impacts of rarity and Red List status of plants on model quality. To do this, we tested whether or not including the factors (i) Red List status in Hesse (Hemm et al., 2008), and (ii) the classification as a flood meadow species according to Burkart (2001) (Appendix 4-1) considered as fixed factors in linear mixed-effects models lead to differences in AUC or TSS values.

Finally, yet importantly, we evaluated the relative frequency of hydrological predictors in the best seven predictor sets per species to account for their relevance. The habitat modeling, analysis, and data visualization were carried out in R 3.4.2 (R Core Team, 2017) and ggplot2 2.2.1 (Wickham, 2009).

4.3. Results

4.3.1. Best predictor identification

Based on the modeling results with the 95 a priori defined predictors (81 hydrological, 5 meteorological, and 9 morphological predictors, Appendix 4-2), we selected 19 significant and differentiating predictors for multi-predictor SDMs. The hydrological predictors can be grouped by their indication of drought, wetness, or inundation. A detailed description of the selected predictors is given in Table 4.2. The largest explanatory value for the individual predictors was obtained if the vegetation period of the previous six years (before the vegetation survey date) was considered. As a result, we used only this period for the 16 time-dependent predictors (PH01–PH15 and PM16).

From the 19 predictors (Table 4.2), we defined predictor combinations following the rule of thumb as defined by Dormann et al. (2013). As predictor correlations are likely different for each of the three predictor calculation databases (Table 4.1), we defined individual predictor sets for each predictor calculation database. The maximum number of predictors for a set was 10, 9, and 8 predictors for the sgm, gww, and riv predictor calculation databases, respectively. In total, 25,252 (sgm), 9,052 (gww), and 7,540 (riv) predictor sets were possible.

Table 4.2: Selected predictors used as input data for the multi-predictor species distribution models. PH = hydrological predictors, PM = meteorological predictors, PN = morphological predictors, * = time independent predictors (i.e., same value for all years and periods)

Predictor	Description	Indication
PH01	Standard deviation of the groundwater level (m)	
PH02	Absolute range of the groundwater level (m)	
PH03, PH04, PH05	Longest period during which the groundwater level was less than 1 m / 1.5 m / 2.5 m below ground (days)	Drought
PH06, PH07	Longest period during which the groundwater level was more than 2.5 m / 0.5 m below ground (days)	Wetness
PH08, PH09	Sum of days on which the groundwater level was more than 2.5 m / 0.7 m below ground (days)	Drought (Wetness)
PH10	Sum of days on which the inundation height was a minimum 50 cm (days)	Inundation
PH11	Longest period during which the inundation height was a minimum 50 cm (days)	Inundation
PH12, PH13, PH14	Sum of days on which the groundwater level was less than 50 cm below ground and the daily precipitation was less than 1 mm during the first 60 / 80 / 100 days of the vegetation period (days)	Drought
PH15	Sum of days on which the groundwater level was less than 50 cm below ground and the daily precipitation was above 1 mm during the first 100 days of the vegetation period (days)	Wetness
PM16	Longest period of wet days (daily precipitation > 1 mm) (days)	
PN17*	Height above sea level, derived from the digital elevation model (m)	
PN18*	Distance to the Rhine or the meander cutoff (m)	
PN19*	Distance to any water surface (distance to Rhine, the meander cutoff or lake) (m)	

4.3.2. Evaluation of habitat model

Overall, the mean AUC was highest for the sgm predictor calculation database (0.83 ± SE 0.006), followed by gww (0.82 ± SE 0.006), riv (0.81 ± SE 0.006), and nhy (0.72 ± SE 0.008) (Figure 4.3 A). Evaluations of habitat models based on AUC were highly correlated with evaluations based on TSS (Pearson correlation coefficient = 0.94; $p < 0.001$); therefore, we present only AUC results. Linear mixed-effects models showed that models with hydrological predictors result in better evaluation scores than models without hydrological predictors (nhy, $p < 0.001$, Figure 4.3 A). Furthermore, AUC was higher for the sgm predictor calculation database in comparison to the riv and gww predictor calculation databases ($p < 0.05$). Habitat model performance also differed significantly for endangered and vulnerable Red List species (Figure 4.3 B), as well as when only flood meadow species according to Burkart were assessed (Figure 4.3 C).

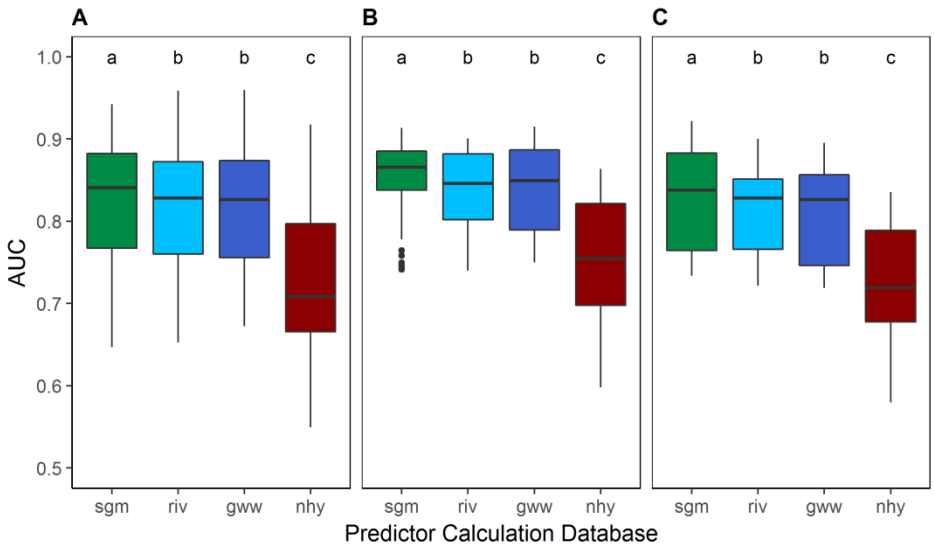

Figure 4.3: Simulated area under the receiver operating characteristic curve (AUC) for flood meadow species without using hydrological predictors (nhy), using hydrological predictors derived from the surface-groundwater-model (sgm), measured groundwater data (gww), and simulated water level of the Rhine River (riv). (A) Results for all 23 species. (B) Results for endangered and vulnerable species listed on the Red List in Hesse (Hemm et al., 2008). (C) Results for flood meadow species according to Burkart (2001). Letters denote significant differences across predictor calculation databases ($p < 0.05$).

For single species, habitat models with predictors from the sgm database outperform other predictor calculation databases in almost half of the modeled species (10 of 23), followed by models with predictors from the gww (9 of 23) and riv databases (4 of 23) (Appendix 4-3). ANOVA revealed that 2 out of the 10 species showed significantly better habitat model quality for the sgm input data. In general, models with hydrological predictors (sgm, riv, gww) significantly outperformed the models without hydrological predictors (nhy). Including hydrological predictors, and in particular, those resulting from the surface water groundwater model, lead to better habitat model results. Therefore, from here on, we present only results of the habitat model based on the hydrological predictors obtained from the surface water-groundwater model.

4.3.3. Significance of individual predictor variables

A set of 19 predictors for the simulation of species habitats may seem large; however, given that we simulate vulnerable, endangered, and flood meadow species, specific predictors might be needed to project the occurrence for specific individual species. We therefore analyzed the occurrence of predictors for each of the 23 species. For both species groups (flood meadow species, and vulnerable and endangered Red List species), five predictors are used in over 50% of the model runs (Figure 4.4), of which four are the same (PN19, PN18, PH16, PH01). For the flood meadow species, the predictor PH08 was used, and for the vulnerable and endangered Red List species, the predictor PH09 is used more frequently. Both predictors are based on the same measurement, i.e., the sum of days on which the groundwater level exceeds a certain level (PH08: 2.5 m below ground; PH08: 0.7 m below ground). The least common predictors for both species groups are predictors PH12, PH13, and PH15 (< 25%; Figure 4.4). Nevertheless, predictors PH12 and PH13 are relevant in models of 5 Red List and 7 flood meadow species, and even the least common predictor PH15 contributes to about 10% of the habitat models (in 1 flood meadow and 3 Red List species).

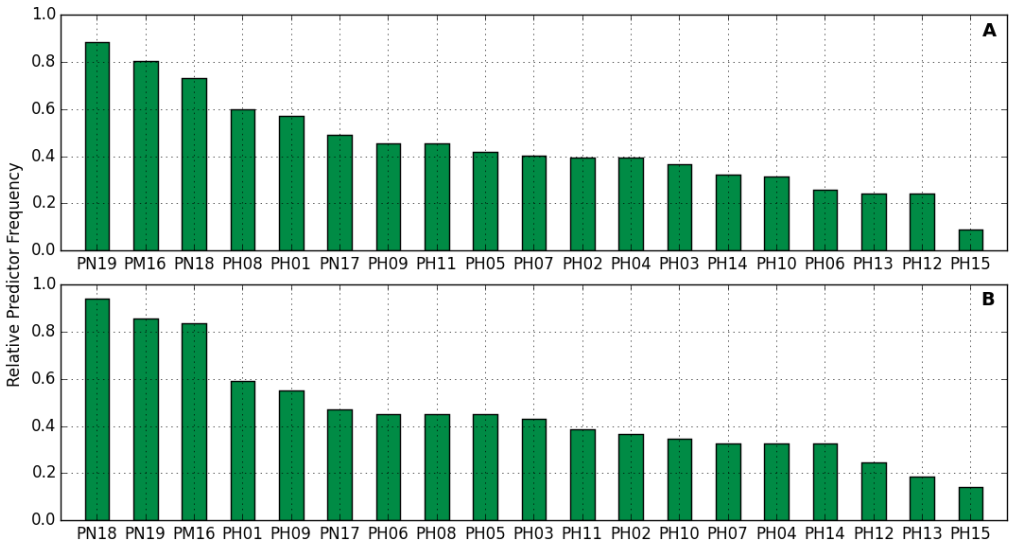

Figure 4.4: Relative predictor frequency for all model runs separated for the (A) flood meadow species according to Burkart (2001) and (B) species on the Red List (vulnerable and endangered).

4.4. Discussion

Relevance of hydrological predictors for flood meadow habitat simulations

The aim of our study was to assess possible options to include hydrological information in habitat modeling of flood meadow species. The significance of water level fluctuations and water level variability for ecological modeling of wetlands has been emphasized by several studies (Kopeć et al., 2013; e.g., Leyer, 2005). We included hydrological predictors from a dynamic surface water-groundwater model in a habitat model, and found a significant improvement of the model quality compared to habitat models derived only from morphological data (Figure 4.3).

Only few studies have linked detailed hydrological variables to habitat models (e.g., Mosner et al., 2011, 2015). Mosner et al. (2011) derived their hydrological predictors from a combination of river water level and groundwater data from the adjacent river (similar to our gww database), while variables in Mosner et al. (2015) were derived from a model of the adjacent river (similar to our riv dataset). Our results showed a significant model improvement when utilizing hydrological predictors from the surface water-groundwater model (sgm database) over the two other possibilities. We conclude that for

rare species the complexity of habitat requirements can be better described with predictors from a detailed and spatially explicit hydrological model than with interpolated, measured hydrological variables.

Specialized species need specific predictors

As for most modeling approaches, it seems desirable to reduce the complexity of model input data to help simplify models. Mosner et al. (2011) and (2015) modeled species occurrence with only two predictors, i.e., water level and water level fluctuations of the adjacent river. Our results suggest that more (i.e., from 6 to 10) specific predictors are needed to simulate habitats and occurrences for the rare and endangered species. In comparison to the study by Mosner et al. (2011), we included more specified predictors (e.g., longest period of days with a specific water level or specific inundation height), and we showed that those predictors are used relatively often. For flood meadow species and vulnerable and endangered Red List species, two morphological, one meteorological, and two hydrological predictors (standard deviation and sum of days with low ground water level) are used in over 50% of all final habitat model runs (Figure 4.4). Only three of the 19 predictors we identified are used less frequently than in one-fourth of all model runs. Nevertheless, they are relevant to predict the occurrence of all flood meadow and Red List species. Those three predictors refer to periods with dry soil in the first days of the growing period. Reversely, this means wet soil conditions are relevant for flood meadow species and especially for vulnerable and endangered Red List species. This is in line with Boswell et al. (2007), who designated the duration of saturation at the surface and at the saturation in the root zone, as well as the distribution of open water, as essential hydrological variables for modeling groundwater-dominated wetland habitats.

Our most frequently used hydrological predictors included values indicating dry conditions, wet conditions, or inundation length. This provides evidence that the habitat requirements of flood meadow species are complex. They are not only able to cope with flooding, but also with drought periods (Burkart, 2001), and thus one requires multiple variables in order to properly represent this complex environment. Other than the hydrological predictors, two morphological predictors (i.e., distance to the river or water surfaces) are frequently considered in our habitat models. In literature, these predictors are seen as proxies for several factors (e.g., soil texture) (He and Walling, 1998; Leyer, 2005), which affect species distribution and are linked to the distance to the river. Thus, those morphological predictors are generally useful for floodplain species' modeling in case there

is an absence of other data (Mosner et al., 2015). Furthermore, in our study, the distance to water seems to reflect the land-use legacies: The target species mostly occur on "original" sites (i.e., in close proximity to the river) where the ancient habitat conditions were sufficient for the plants to colonize, and they could persevere on these sites to the present, despite the strong impacts of land use in the past centuries (Böger, 1991).

This study revealed that more specified hydrological predictors should be considered when modeling species' distribution, and that it is important from which data sources these hydrological predictors are generated. Chui et al. (2011) stated the importance of models for generating hydrological predictors, considering surface hydrology and surface water-groundwater interactions. Boswell et al. (2007) also believed in the great implication of hydrological modeling for planning and prioritization of wetland restoration. However, despite their suggestions, we are not aware of any integrated model approach that has been developed and successfully applied to simulate not only flood meadow species in general, but also the occurrence of rare and endangered species.

Conclusion and further applications

We conclude that habitat models achieve better results when hydrological predictors of a detailed surface water-groundwater model are included. Averaged over all species, the results are marginally, yet still significantly, better when compared to habitat models based on readily available observation data alone (groundwater level, river water level). However, a clear advantage of utilizing complex hydrological models for predictor generation is obvious for rare specialist species with complex habitat requirements. Particularly for such species, habitat models should include detailed hydrological predictors with high temporal and spatial resolution. We recognize two prominent fields, in which spatially explicit habitat models, like those developed in this study, are needed: (1) conservation planning and (2) global change studies.

In today's conservation planning, the decisions about whether a specific site is suitable and promising for restoration are often based on soft data and subjective appreciation. This method often neglects elevation or small-scale spatial variation in soil conditions. We question whether the current method of spending large amounts of money for such restoration without considering site-specific characteristics is the way forward. Applications of complex habitat models possess the power to improve conservation outcomes (Guisan et al., 2013), by identifying suitable habitats prior to management activities.

To evaluate the global change impact, such as land management and/or climate change, process-based hydrological models are a good choice. Our habitat model is capable of simulating changes in vegetation cover (selection of species, changes in land management), morphological characteristics (floodplain reconstruction, construction of embankments, river regulation) and climate (precipitation amounts and seasonal patterns, temperature affecting evapotranspiration). For example, it is possible to run the model with different land-use change scenarios (Maier et al., 2018). The resulting water levels can be integrated in the habitat models, and predictions can be made for species occurrence and recommendations for wetland restoration under the hypothetical and predicted land use changes. Furthermore, the hydrological model can be forced by climate change projections. Thus, hydrological predictors over several years in the near and distant future can be derived. The species distribution model can then be used to make predictions for future species occurrence (Elith and Leathwick, 2009) and particularly for rare and endangered species.

Acknowledgements

This research was funded by the Deutsche Bundesstiftung Umwelt (DBU; Project-No. 31612/01; www.dbu.de). The funder had no role in the study design, data collection and analysis, decision to publish, or preparation of the manuscript. We thank all contributors of vegetation data for their willingness to share datasets, i.e., the KLIWAS project group and the City of Riedstadt. The climate data are available from the Germany's national meteorological service (Deutscher Wetterdienst (DWD), http://www.dwd.de/cdc; ftp://ftp-cdc.dwd.de/pub/CDC). Daily water levels from the gauging station Nierstein are available from the Federal Waterways and Shipping Authority (Wasser und Schifffahrtsverwaltung des Bundes (WSV)) and provided by the Federal Institute of Hydrology (Bundesanstalt für Gewässerkunde (BfG)). Groundwater levels are provided by the Hessian Agency for Nature Conservation, Environment and Geology (Hessisches Landesamt für Naturschutz, Umwelt und Geologie (HLNUG)). The digital elevation model (DEM) was provided by the Hessian State Office of Land Management and Geological Information (Hessisches Landesamt für Bodenmanagement und Geoinformation (HLBG)).

Supporting information

Appendix 4-1

The 23 target species and indices used for the SDM. Burkart: classification as river corridor plant or floodplain meadow species (Burkart, 2001); RLS Hesse: Red List status in Hesse (Hemm et al. 2008), Endangered = EN, Vulnerable = VU, Near Threatened = NT, Least Concern = LC; DB presence: species' presence in database (number of occurrences); ELL F: Ellenberg indicator value (EIV) for moisture (Ellenberg et al., 1991); ELL WF: EIV for alternating moisture conditions (Ellenberg et al., 1991). Species nomenclature followed Jäger (2017). In total, 226 vegetation plots served as a basis for habitat modeling; 78 vegetation plots (sampled 2011–2012) were taken from the KLIWAS project (Horchler et al., 2012) and 31 plots (sampled 2014) were derived from a resampling of restoration sites of the City of Riedstadt. To gain a spatially equaled number of plots over the whole study area we sampled 117 plots in 2015 and 2016. To avoid a modeling bias through spatial autocorrelation, we assured that the minimum distance between plots was higher than 50 m (Dormann et al., 2007).

Species	Burkart	RLS Hesse	DB presence	ELL F	ELL WF
Achillea millefolium L.	0	LC	95	4	0
Agrimonia eupatoria L.	0	LC	49	4	0
Arabis nemorensis (Hoffm.) W. D. J. Koch	1	EN	20	7	0
Bromus racemosus L.	0	VU	25	8	1
Centaurea jacea L.	0	LC	25	indifferent	0
Galium boreale L.	1	VU	14	6	1
Inula salicina L.	0	NT	23	6	1
Iris pseudacorus L.	0	LC	15	9	0
Iris spuria L.	0	VU	15	7	0
Leucanthemum vulgare (Vaill.) Lam.	0	LC	51	4	0
Linum catharticum L.	0	LC	10	indifferent	0
Lotus corniculatus L.	0	LC	49	4	0
Lysimachia vulgaris L.	0	LC	21	8	1
Peucedanum officinale L.	1	VU	19	4	1
Prunella vulgaris L.	0	LC	43	5	0
Ranunculus acris L.	0	LC	64	6	0
Rhinanthus alectorolophus Pollich	0	NT	11	4	0
Sanguisorba officinalis L.	1	LC	57	6	1
Serratula tinctoria L.	0	EN	13	indifferent	0
Silaum silaus (L.) Schinz & Thell.	1	LC	30	indifferent	1
Thalictrum flavum L.	1	LC	16	8	1
Veronica maritima L.	1	VU	20	8	1
Vincetoxicum hirundinaria Medik.	0	LC	12	3	0

Appendix 4-2

All a priori hydrological, meteorological and morphological predictors

Nr.	Description of hydrological predictor
01	Mean of groundwater level (m)
02	Maximum of groundwater level (m)
03	Minimum of groundwater level (m)
04	Standard deviation of groundwater level (m)
05	Range of groundwater level (m)
06	Sum of days with inundation
07	Longest inundation period (days)
08	Maximum height of inundation (m)
09	Day after start of growing season, on which longest inundation period starts
10	Day of year, on which longest inundation period starts
11–13	Sum of inundation days in the first 60, 80, 100 days after start of growing season
14–16	Longest inundation period in the first 60, 80, 100 days after start of growing season (days)
17–23	Sum of days with groundwater level below 30, 50, 70, 100, 150, 200, 250 cm below ground
24–30	Sum of days with groundwater level above 30, 50, 70, 100, 150, 200, 250 cm below ground
31–37	Longest period with groundwater level below 30, 50, 70, 100, 150, 200, 250 cm below ground (days)
38–44	Longest period with groundwater level above 30, 50, 70, 100, 150, 200, 250 cm below ground (days)
45–52	Sum of days with inundation height more than 5, 10, 15, 20, 30, 50, 100, 150 cm
53–60	Longest period with inundation height more than 5, 10, 15, 20, 30, 50, 100, 150 cm (days)
61–63	Sum of days with groundwater level below 50 cm below ground in the first 60, 80, 100 days after start of growing season
64–66	Longest period with groundwater level below 50 cm below ground in the first 60, 80, 100 days after start of growing season (days)
67–69	Days with groundwater level below 50 cm below ground and precipitation < 1 mm in the first 60, 80, 100 days after start of growing season
70–72	Days with groundwater level below 50 cm below ground and precipitation ≥ 1 mm in the first 60, 80, 100 days after start of growing season
73–75	Longest period with groundwater level below 50 cm below ground and precipitation < 1 mm in the first 60, 80, 100 days after start of growing season (days)
76–78	Longest period with groundwater level below 50 cm below ground and precipitation ≥ 1 mm in the first 60, 80, 100 days after start of growing season (days)
79–81	Number of periods with inundation periods longer than 5, 7, 10 days

Nr.	Description of meteorological predictor
01	Sum of precipitation (mm)
02	Sum of wet days (Precipitation ≥ 1 mm)
03	Sum of dry days (Precipitation < 1 mm)
04	Longest period of wet days (Precipitation ≥ 1 mm) (days)
05	Longest period of dry days (Precipitation < 1 mm) (days)

Nr.	Description of morphological predictor
01	Height above NN (derived from the digital elevation model) (m)
02–03	Northness and Eastness
04–05	Northing and Easting
06	Distance to the Rhine River (m)
07	Distance to the Rhine or the meander cutoff (m)
08	Distance to any water surface (distance to Rhine or the meander cutoff or lake) (m)
09	Topographic wetness index

Appendix 4-3

Comparison of model quality (area under the receiver operating characteristic curve, AUC) of 4 different predictor calculation databases for species distribution models for 23 target species of floodplain restoration projects. Predictor calculation databases: surface-groundwater model, sgm; interpolated water level Rhine River data, riv; interpolated groundwater level data, gww; non hydrological, nhy. Letters denote significant differences of hydrological calculation method ($p < 0.05$) according to ANOVA post hoc Tukey tests for each species.

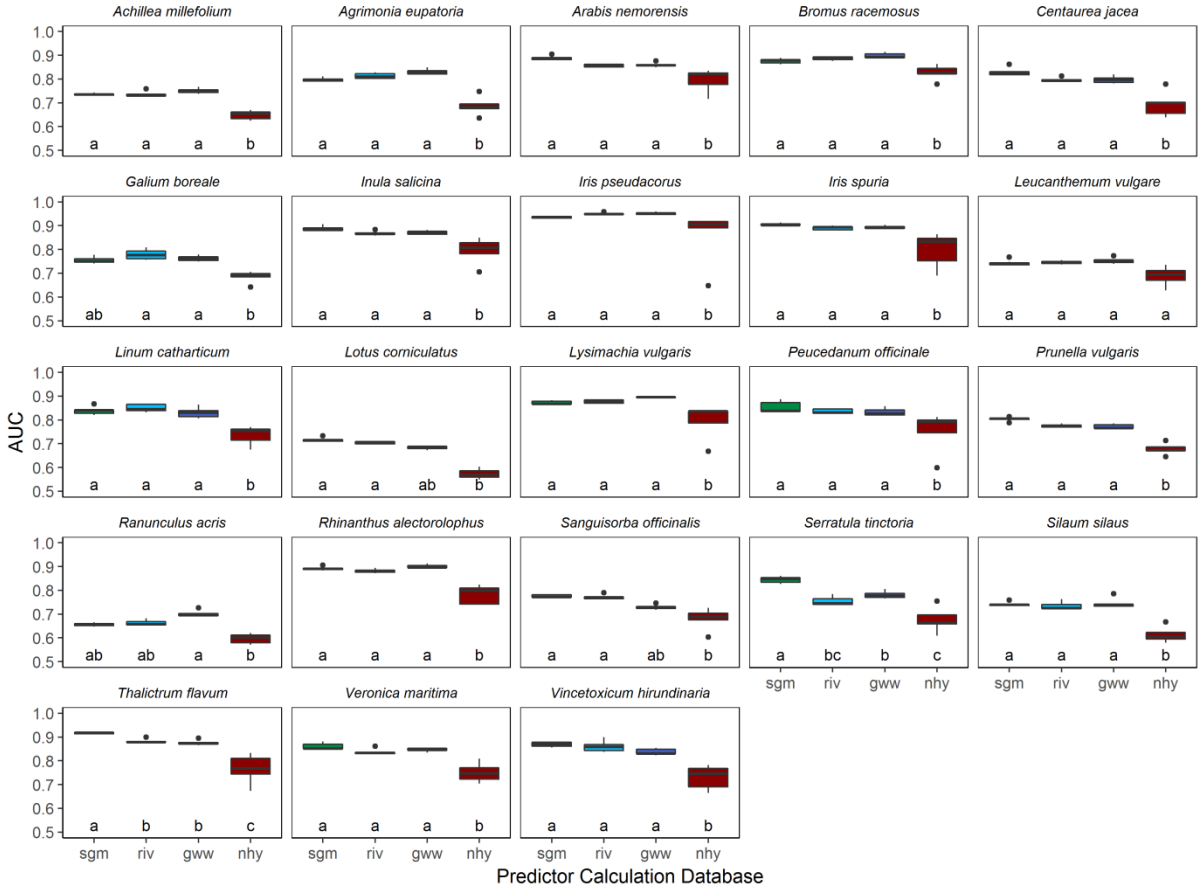

References

Acreman, M. and Holden, J. (2013): How Wetlands Affect Floods, *Wetlands*, 33(5), 773–786, doi: 10.1007/s13157-013-0473-2.

Acreman, M. C., Blake, J. R., Booker, D. J., Harding, R. J., Reynard, N., Mountford, J. O. and Stratford, C. J. (2009): A simple framework for evaluating regional wetland ecohydrological response to climate change with case studies from Great Britain, *Ecohydrology*, 2(1), 1–17, doi: 10.1002/eco.37.

Acremann, M. C. and Miller, F. (2007): Hydrological impact assessment of wetlands, in S. Ragone, A. de la Hera, N. Hernandez-Mora (eds.) *The Global Importance of Groundwater in the 21st Century*, pp. 89–92, NGWA Press.

Ajami, H., McCabe, M. F. and Evans, J. P. (2015): Impacts of model initialization on an integrated surface water-groundwater model, *Hydrological Processes*, 29(17), 3790–3801, doi: 10.1002/hyp.10478.

Alaghmand, S., Beecham, S., Woods, J. A., Holland, K. L., Jolly, I. D., Hassanli, A. and Nouri, H. (2016): Quantifying the impacts of artificial flooding as a salt interception measure on a river-floodplain interaction in a semi-arid saline floodplain, *Environmental Modelling & Software*, 79, 167–183, doi: 10.1016/j.envsoft.2016.02.006.

Allen, R. G., Pereira, L. S., Raes, D. and Smith, M. (1998): *Crop evapotranspiration*, FAO irrigation and drainage paper, Rome.

Allouche, O., Tsoar, A. and Kadmon, R. (2006): Assessing the accuracy of species distribution models: prevalence, kappa and the true skill statistic (TSS), *Journal of Applied Ecology*, 43(6), 1223–1232, doi: 10.1111/j.1365-2664.2006.01214.x.

Ameli, A. A. and Creed, I. F. (2017): Quantifying hydrologic connectivity of wetlands to surface water systems, *Hydrology and Earth System Sciences*, 21(3), 1791–1808, doi: 10.5194/hess-21-1791-2017.

Arnold, J. G., Allen, P. M. and Bernhardt, G. (1993): A comprehensive surface-groundwater flow model, *Journal of Hydrology*, 142(1–4), 47–69, doi: 10.1016/0022-1694(93)90004-S.

Bakker, J. and Berendse, F. (1999): Constraints in the restoration of ecological diversity in grassland and heathland communities, *Trends in Ecology & Evolution*, 14(2), 63–68, doi: 10.1016/S0169-5347(98)01544-4.

Bárdossy, A. and Singh, S. K. (2008): Robust estimation of hydrological model parameters, *Hydrology and Earth System Sciences*, 12(6), 1273–1283, doi: 10.5194/hess-12-1273-2008.

Barron, O., Silberstein, R., Ali, R., Donohue, R., McFarlane, D. J., Davies, P., Hodgson, G., Smart, N. and Donn, M. (2012): Climate change effects on water-dependent ecosystems in south-western Australia, *Journal of Hydrology*, 434–435, 95–109, doi: 10.1016/j.jhydrol.2012.02.028.

Barthel, R. and Banzhaf, S. (2016): Groundwater and Surface Water Interaction at the Regional-scale – A Review with Focus on Regional Integrated Models, *Water Resources Management*, 30(1), 1–32, doi: 10.1007/s11269-015-1163-z.

Baumgärtel, R. (2004): Zur aktuellen Situation der Hartholzauenwälder im Naturschutzgebiet „Kühkopf-Knoblochsaue“ (The current situation of the hardwood forests in the "Kühkopf-Knoblochsaue" nature reserve), *Botanik und Naturschutz in Hessen*, 17, 53–61.

Bergström, S. (1995): The HBV model, in V. P. Singh (eds.) *Computer models of watershed hydrology*, pp. 443–476, Water Resources Publications, Highlands Ranch, Colorado, USA.

Bernard-Jannin, L., Brito, D., Sun, X., Jauch, E., Neves, R., Sauvage, S. and Sánchez-Pérez, J.-M. (2016): Spatially distributed modelling of surface water-groundwater exchanges during overbank flood events – a case study at the Garonne River, *Advances in Water Resources*, 94, 146–159, doi: 10.1016/j.advwatres.2016.05.008.

Betts, A. R. (2005): Integrated approaches to climate-crop modelling: needs and challenges, *Philosophical Transactions of the Royal Society B: Biological Sciences*, 360(1463), 2049–2065, doi: 10.1098/rstb.2005.1739.

Beven, K. (1993): Prophecy, reality and uncertainty in distributed hydrological modelling, *Advances in Water Resources*, 16(1), 41–51, doi: 10.1016/0309-1708(93)90028-E.

Beven, K. (2001): How far can we go in distributed hydrological modelling?, *Hydrology and Earth System Sciences*, 5(1), 1–12, doi: 10.5194/hess-5-1-2001.

Beven, K. and Binley, A. (1992): The future of distributed models: Model calibration and uncertainty prediction, *Hydrological Processes*, 6, 279–298.

Böger, K. (1991): *Grünlandvegetation im Hessischen Ried - pflanzensoziologische Verhältnisse und Naturschutzkonzeption (Grassland vegetation in the Hessian reed - plant-sociological conditions and nature conservation concept),* Botanik und Naturschutz in Hessen, Beiheft 3, Frankfurt/Main.

Bonan, G. B. (2008): Forests and Climate Change: Forcings, Feedbacks, and the Climate Benefits of Forests, *Science*, 320(5882), 1444–1449, doi: 10.1126/science.1155121.

Boswell, J. S. and Olyphant, G. A. (2007): Modeling the hydrologic response of groundwater dominated wetlands to transient boundary conditions, *Journal of Hydrology*, 332(3–4), 467–476, doi: 10.1016/j.jhydrol.2006.08.004.

Box, G. E. P. and Cox, D. R. (1982): An Analysis of Transformations - Revisited, *Journal of the American Statistical Association*, 77, 177–182, doi: 10.2307/2287831.

Brands, S., Herrera, S., Fernández, J. and Gutiérrez, J. M. (2013): How well do CMIP5 Earth System Models simulate present climate conditions in Europe and Africa?, *Climate Dynamics*, 41(3–4), 803–817, doi: 10.1007/s00382-013-1742-8.

Branfireun, B. A. and Roulet, N. T. (1998): The baseflow and storm flow hydrology of a precambrian shield headwater peatland, *Hydrological Processes*, 12(1), 57–72, doi: 10.1002/(SICI)1099-1085(199801)12:1<57::AID-HYP560>3.0.CO;2-U.

Bredehoeft, J. (2005): The conceptualization model problem?, *Hydrogeology Journal*, 13(1), 37–46, doi: 10.1007/s10040-004-0430-5.

Breiner, F. T., Guisan, A., Bergamini, A. and Nobis, M. P. (2015): Overcoming limitations of modelling rare species by using ensembles of small models, *Methods in Ecology and Evolution*, 6(10), 1210–1218, doi: 10.1111/2041-210X.12403.

Breiner, F. T., Nobis, M. P., Bergamini, A. and Guisan, A. (2018): Optimizing ensembles of small models for predicting the distribution of species with few occurrences, *Methods in Ecology and Evolution*, 9(4), 802–808, doi: 10.1111/2041-210X.12957.

Breuer, L., Huisman, J. A., Willems, P., Bormann, H., Bronstert, A., Croke, B. F. W., Frede, H.-G., Gräff, T., Hubrechts, L., Jakeman, A. J., Kite, G., Lanini, J., Leavesley, G., Lettenmaier, D. P., Lindström, G., Seibert, J., Sivapalan, M. and Viney, N. R. (2009): Assessing the impact of land use change on hydrology by ensemble modeling (LUCHEM). I: Model intercomparison with current land use, *Advances in Water Resources*, 32(2), 129–146, doi: 10.1016/j.advwatres.2008.10.003.

Broennimann, O., Di Cola, V. and Guisan, A. (2016): *ecospat: Spatial Ecology Miscellaneous Methods*. R package version 2.1.1. URL: https://CRAN.R-project.org/package=ecospat.

Brunotte, E., Dister, E., Günther-Diringer, D., Koenzen, U. and Mehl, D. (2009): *Flussauen in Deutschland. Erfassung und Bewertung des Auenzustandes (Floodplains in Germany. Recording and evaluation of floodplain conditions)*. Naturschutz und biologische Vielfalt 87, Bundesamt für Naturschutz, Bonn - Bad Godesberg.

Burkart, M. (2001): River corridor plants (Stromtalpflanzen) in Central European lowland: a review of a poorly understood plant distribution pattern, *Global Ecology and Biogeography*, 10(5), 449–468, doi: 10.1046/j.1466-822x.2001.00270.x.

Burmeier, S., Eckstein, R. L., Otte, A. and Donath, T. W. (2010): Desiccation cracks act as natural seed traps in flood-meadow systems, *Plant and Soil*, 333(1–2), 351–364, doi: 10.1007/s11104-010-0350-1.

Burt, T. ., Bates, P. ., Stewart, M. ., Claxton, A. ., Anderson, M. . and Price, D. . (2002): Water table fluctuations within the floodplain of the River Severn, England, *Journal of Hydrology*, 262(1–4), 1–20, doi: 10.1016/S0022-1694(01)00567-4.

Butturini, A., Bernal, S., Sabater, S. and Sabater, F. (2002): The influence of riparian-hyporheic zone on the hydrological responses in an intermittent stream, *Hydrology and Earth System Sciences*, 6(3), 515–526, doi: 10.5194/hess-6-515-2002.

Camporese, M., Paniconi, C., Putti, M. and Orlandini, S. (2010): Surface-subsurface flow modeling with path-based runoff routing, boundary condition-based coupling, and assimilation of multisource observation data, *Water Resources Research*, 46(2), doi: 10.1029/2008WR007536.

Capon, S. J., Chambers, L. E., Nally, R. M., Naiman, R. J., Davies, P., Marshall, N., Pittock, J., Reid, M., Capon, T., Douglas, M., Catford, J., Baldwin, D. S., Stewardson, M., Roberts, J., Parsons, M. and Williams, S. E. (2013): Riparian Ecosystems in the 21st Century: Hotspots for Climate Change Adaptation?, *Ecosystems*, 16(3), 359–381, doi: 10.1007/s10021-013-9656-1.

Chen, J., Brissette, F. P., Poulin, A. and Leconte, R. (2011): Overall uncertainty study of the hydrological impacts of climate change for a Canadian watershed, *Water Resources Research*, 47(12), 176, doi: 10.1029/2011WR010602.

Chen, J., Brissette, F. P., Chaumont, D. and Braun, M. (2013): Finding appropriate bias correction methods in downscaling precipitation for hydrologic impact studies over North America, *Water Resources Research*, 49(7), 4187–4205, doi: 10.1002/wrcr.20331.

Chui, T. F. M., Low, S. Y. and Liong, S.-Y. (2011): An ecohydrological model for studying groundwater–vegetation interactions in wetlands, *Journal of Hydrology*, 409(1–2), 291–304, doi: 10.1016/j.jhydrol.2011.08.039.

Cirpka, O. A. and Valocchi, A. J. (2016): Debates-Stochastic subsurface hydrology from theory to practice, *Water Resources Research*, 52(12), 9218–9227, doi: 10.1002/2016WR019087.

Clark, M. P., Fan, Y., Lawrence, D. M., Adam, J. C., Bolster, D., Gochis, D. J., Hooper, R. P., Kumar, M., Leung, L. R., Mackay, D. S., Maxwell, R. M., Shen, C., Swenson, S. C. and Zeng, X. (2015): Improving the representation of hydrologic processes in Earth System Models: Representing Hydrologic Processes in Earth System Models, *Water Resources Research*, 51(8), 5929–5956, doi: 10.1002/2015WR017096.

Condon, L. E. and Maxwell, R. M. (2013): Implementation of a linear optimization water allocation algorithm into a fully integrated physical hydrology model, *Advances in Water Resources*, 60, 135–147, doi: 10.1016/j.advwatres.2013.07.012.

Cramer, W., Bondeau, A., Woodward, F. I., Prentice, I. C., Betts, R. A., Brovkin, V., Cox, P. M., Fisher, V., Foley, J. A., Friend, A. D., Kucharik, C., Lomas, M. R., Ramankutty, N., Sitch, S., Smith, B., White, A. and Young-Molling, C. (2001): Global response of terrestrial ecosystem structure and function to CO_2 and climate change: results from six dynamic global vegetation models, *Global Change Biology*, 7(4), 357–373, doi: 10.1046/j.1365-2486.2001.00383.x.

Dataflow Systems Limited (2018): Odyssey Capacitance Water Level Logger - product view, retrieved: 05/0382018 from URL: http://odysseydatarecording.com/index.php?route=product/product&path=59&product_id=50.

David, P. G. (1996): Changes in plant communities relative to hydrologic conditions in the Florida Everglades, *Wetlands*, 16(1), 15–23, doi: 10.1007/BF03160642.

Demirel, M. C., Booij, M. J. and Hoekstra, A. Y. (2013): Impacts of climate change on the seasonality of low flows in 134 catchments in the River Rhine basin using an ensemble of bias-corrected regional climate simulations, *Hydrology and Earth System Sciences*, 17(10), 4241–4257, doi: 10.5194/hess-17-4241-2013.

Di Febbraro, M., Carotenuto, F., Castiglione, S., Russo, D., Loy, A., Maiorano, L. and Raia, P. (2017): Does the jack of all trades fare best? Survival and niche width in Late Pleistocene megafauna, *Journal of Biogeography*, 44(12), 2828–2838, doi: 10.1111/jbi.13078.

Dister, E., Schneider, E., Fritz, H.-G., Winkel, S. and Flößer, E. (1992): Wissenschaftliche Erfahrungen aus Renaturierungsprojekten. Großflächige Renaturierung des 'Kühkopfes' in der hessischen Rheinaue – Ablauf, Ergebnisse und Folgerungen der Sukzessionsforschung (Scientific experience from renaturation projects. Large-scale renaturation of the 'Kühkopf' in the Hessian Rhine floodplain - process, results and conclusions of succession research), *Beiträge der Akademie Natur- und Umweltschutz Baden-Württemeberg*, 13 b, 20–36.

Dobler, C., Hagemann, S., Wilby, R. L. and Stötter, J. (2012): Quantifying different sources of uncertainty in hydrological projections in an Alpine watershed, *Hydrology and Earth System Sciences*, 16(11), 4343–4360, doi: 10.5194/hess-16-4343-2012

Dokulil, M. (2014): Impact of climate warming on European inland waters, *Inland Waters*, 4(1), 27–40, doi: 10.5268/IW-4.1.705.

Donath, T. W., Bissels, S., Hölzel, N. and Otte, A. (2007): Large scale application of diaspore transfer with plant material in restoration practice – Impact of seed and microsite limitation, *Biological Conservation*, 138(1–2), 224–234, doi: 10.1016/j.biocon.2007.04.020.

Donath, T. W., Schmiede, R., Harnisch, M., Burmeier, S. and Otte, A. (2009): Renaturierung von Auenwiesen - Perspektiven für die langfristige Entwicklung (Restoration of alluvial meadows - perspectives for the long-term development), *ANL Laufener Spezialbeiträge*, 2/09, 122–132.

Dormann, C. F., McPherson, J. M., Araújo, M. B., Bivand, R., Bolliger, J., Carl, G., Davies, R. G., Hirzel, A., Jetz, W., Daniel Kissling, W., Kühn, I., Ohlemüller, R., Peres-Neto, P. R., Reineking, B., Schröder, B., Schurr, F. M. and Wilson, R. (2007): Methods to account for spatial autocorrelation in the analysis of species distributional data: a review, *Ecography*, 30(5), 609–628, doi: 10.1111/j.2007.0906-7590.05171.x.

Dormann, C. F., Elith, J., Bacher, S., Buchmann, C., Carl, G., Carré, G., Marquéz, J. R. G., Gruber, B., Lafourcade, B., Leitão, P. J., Münkemüller, T., McClean, C., Osborne, P. E., Reineking, B., Schröder, B., Skidmore, A. K., Zurell, D. and Lautenbach, S. (2013): Collinearity: a review of methods to deal with it and a simulation study evaluating their performance, *Ecography*, 36(1), 27–46, doi: 10.1111/j.1600-0587.2012.07348.x.

Drost, B. W. and Lum, W. E. (1999): *Conceptual Model and Numerical Simulation of the Groundwater Flow System in the Unconsolidated Sediments of Thurston County,* U.S. Geological Survey Water-Resources Investigations Report 99-4165, Washington, USA.

Eamus, D., Froend, R., Loomes, R., Hose, G. and Murray, B. (2006): A functional methodology for determining the groundwater regime needed to maintain the health of groundwater-dependent vegetation, *Australian Journal of Botany*, 54(2), 97–114, doi: 10.1071/BT05031.

Ebel, B. A., Loague, K., Vanderkwaak, J. E., Dietrich, W. E., Montgomery, D. R., Torres, R. and Anderson, S. P. (2007): Near-surface hydrologic response for a steep, unchanneled catchment near Coos Bay, Oregon: 2. Physics-based simulations, *American Journal of Science*, 307(4), 709–748, doi: 10.2475/04.2007.03.

Ebel, B. A., Loague, K., Montgomery, D. R. and Dietrich, W. E. (2008): Physics-based continuous simulation of long-term near-surface hydrologic response for the Coos Bay experimental catchment, *Water Resources Research*, 44(7), doi: 10.1029/2007WR006442.

van Eck, W. H. J. M., van de Steeg, H. M., Blom, C. W. P. M. and Kroon, H. (2004): Is tolerance to summer flooding correlated with distribution patterns in river floodplains?, *Oikos*, 107(2), 393–405, doi: 10.1111/j.0030-1299.2004.13083.x.

Elith, J. and Leathwick, J. R. (2009): Species Distribution Models: Ecological Explanation and Prediction Across Space and Time, *Annual Review of Ecology, Evolution, and Systematics*, 40(1), 677–697, doi: 10.1146/annurev.ecolsys.110308.120159.

Elith*, J., Graham*, C. H., Anderson, R. P., Dudík, M., Ferrier, S., Guisan, A., Hijmans, R. J., Huettmann, F., Leathwick, J. R., Lehmann, A., Li, J., G. Lohmann, L., A. Loiselle, B., Manion, G., Moritz, C., Nakamura, M., Nakazawa, Y., McC. M. Overton, J., Townsend Peterson, A., J. Phillips, S., Richardson, K., Scachetti-Pereira, R., E. Schapire, R., Soberón, J., Williams, S., S. Wisz, M. and E. Zimmermann, N. (2006): Novel methods improve prediction of species' distributions from occurrence data, *Ecography*, 29(2), 129–151, doi: 10.1111/j.2006.0906-7590.04596.x.

Ellenberg, H., Weber, H. E., Düll, R., Wirth, V., Werner, W. and Paulissen, D. (1991): *Zeigerwerte von Pflanzen in Mitteleuropa (Indicator values of plants in Central Europe),* Scripta Geobotanica, 3rd ed., Goltze, Göttingen.

Ely, D. M. and Kahle, S. C. (2004): *Conceptual Model and Numerical Simulation of the Groundwater Flow System in the Unconsolidated Deposits of the Colville River Watershed*, Stevens County, Washington, U. S. Geological Survey Investigations Report 2004-5237.

Engst, K., Baasch, A., Erfmeier, A., Jandt, U., May, K., Schmiede, R. and Bruelheide, H. (2016): Functional community ecology meets restoration ecology: Assessing the restoration success of alluvial floodplain meadows with functional traits, *Journal of Applied Ecology*, 53(3), 751–764, doi: 10.1111/1365-2664.12623.

Esri (2018): Esri, DigitalGlobe, GeoEye, i-cubed, USDA FSA, USGS, AEX, Getmapping, Aerogrid, IGN, IGP, swisstopo, and the GIS User Community.

Finck, P., Heinze, S., Raths, U., Riecken, U. and Ssymank, A. (2017): Rote Liste der gefährdeten Biotoptypen Deutschlands. Dritte fortgeschriebene Fassung. (Red list of threatened habitat types in Germany. Third updated version), *Naturschutz und Biologische Vielfalt*, 156, 1–460.

Follner, K., Ehlert, T. and Neukirchen, B. (2010): *The status report on German floodplains*, 38th IAD Conference, June 2010, Dresden, Germany.

Funk, A., Gschöpf, C., Blaschke, A. P., Weigelhofer, G. and Reckendorfer, W. (2013): Ecological niche models for the evaluation of management options in an urban floodplain—conservation vs. restoration purposes, *Environmental Science & Policy*, 34, 79–91, doi: 10.1016/j.envsci.2012.08.011.

Furman, A. (2008): Modeling Coupled Surface–Subsurface Flow Processes, *Vadose Zone Journal*, 7(2), 741, doi: 10.2136/vzj2007.0065.

Gattringer, J. P., Donath, T. W., Eckstein, R. L., Ludewig, K., Otte, A. and Harvolk-Schöning, S. (2017): Flooding tolerance of four floodplain meadow species depends on age, *PLoS ONE*, 12(5), doi: 10.1371/journal.pone.0176869.

Gattringer, J. P., Ludewig, K., Harvolk-Schöning, S., Donath, T. W. and Otte, A. (2018): Interaction between depth and duration matters: flooding tolerance of 12 floodplain meadow species, *Plant Ecology*, 219(8), 973–984, doi: 10.1007/s11258-018-0850-2.

Gauthier, M. J., Camporese, M., Rivard, C., Paniconi, C. and Larocque, M. (2009): A modeling study of heterogeneity and surface water-groundwater interactions in the Thomas Brook catchment, Annapolis Valley (Nova Scotia, Canada), *Hydrology and Earth System Sciences*, 13(9), 1583–1596, doi: 10.5194/hess-13-1583-2009.

Golden, H. E., Lane, C. R., Amatya, D. M., Bandilla, K. W., Raanan Kiperwas, H., Knightes, C. D. and Ssegane, H. (2014): Hydrologic connectivity between geographically isolated wetlands and surface water systems: A review of select modeling methods, *Environmental Modelling & Software*, 53, 190–206, doi: 10.1016/j.envsoft.2013.12.004.

Gonnermann, H. (2002): *Die Wälder des Naturschutzgebietes – von der Pappelwirtschaft zum Prozeßschutz (The forests of the nature reserve - from poplar farming to process protection)*, 50 Jahre Naturschutzgebiet Kühkopf-Knoblochsaue, pp. 28–42, RP Darmstadt.

Goovaerts, P. (1997): *Geostatistics for natural resources evaluation*, Oxford Univ. Press, New York.

Gregory, S. V., Swanson, F. J., McKee, W. A. and Cummins, K. W. (1991): An ecosystem perspective of riparian zones. Focus on links between land and water, *BioScience*, 41, 540–551.

Gudmundsson, L., Bremnes, J. B., Haugen, J. E. and Engen-Skaugen, T. (2012): Downscaling RCM precipitation to the station scale using statistical transformations – a comparison of methods, *Hydrology and Earth System Sciences*, 16(9), 3383–3390, doi: 10.5194/hess-16-3383-2012.

Guisan, A. and Thuiller, W. (2005): Predicting species distribution: offering more than simple habitat models, *Ecology Letters*, 8(9), 993–1009, doi: 10.1111/j.1461-0248.2005.00792.x.

Guisan, A., Broennimann, O., Engler, R., Vust, M., Yoccoz, N. G., Lehmann, A. and Zimmermann, N. E. (2006): Using Niche-Based Models to Improve the Sampling of Rare Species, *Conservation Biology*, 20(2), 501–511, doi: 10.1111/j.1523-1739.2006.00354.x.

Guisan, A., Tingley, R., Baumgartner, J. B., Naujokaitis-Lewis, I., Sutcliffe, P. R., Tulloch, A. I. T., Regan, T. J., Brotons, L., McDonald-Madden, E., Mantyka-Pringle, C., Martin, T. G., Rhodes, J. R., Maggini, R., Setterfield, S. A., Elith, J., Schwartz, M. W., Wintle, B. A., Broennimann, O., Austin, M., Ferrier, S., Kearney, M. R., Possingham, H. P. and Buckley, Y. M. (2013): Predicting species distributions for conservation decisions, *Ecology Letters*, 16(12), 1424–1435, doi: 10.1111/ele.12189.

Gupta, V. K. and Sorooshian, S. (1985): The relationship between data and the precision of parameter estimates of hydrologic models, *Journal of Hydrology*, 81(1–2), 57–77, doi: 10.1016/0022-1694(85)90167-2.

Hancock, P. J., Boulton, A. J. and Humphreys, W. F. (2005): Aquifers and hyporheic zones, *Hydrogeology Journal*, 13(1), 98–111, doi: 10.1007/s10040-004-0421-6.

Hanley, J. A. and McNeil, B. J. (1982): The meaning and use of the area under a receiver operating characteristic (ROC) curve, *Radiology*, 143(1), 29–36, doi: 10.1148/radiology.143.1.7063747.

Hardy, R. J., Bates, P. D. and Anderson, M. G. (1999): The importance of spatial resolution in hydraulic models for floodplain environments, *Journal of Hydrology*, 216(1–2), 124–136, doi: 10.1016/S0022-1694(99)00002-5.

Harnisch, M., Otte, A., Schmiede, R. and Donath, T. W. (2014): Verwendung von Mahdgut zur Renaturierung von Auengrünland (Use of mowed material for the renaturation of floodplain grassland), Naturschutz und Landschaftsplanung , Ulm, Stuttgart.

Hattermann, F., Krysanova, V., Wechsung, F. and Wattenbach, M. (2004): Integrating groundwater dynamics in regional hydrological modelling, *Environmental Modelling & Software*, 19(11), 1039–1051, doi: 10.1016/j.envsoft.2003.11.007.

Hayashi, M. and Rosenberry, D. O. (2002): Effects of Ground Water Exchange on the Hydrology and Ecology of Surface Water, *Ground Water*, 40(3), 309–316, doi: 10.1111/j.1745-6584.2002.tb02659.x.

He, Q. and Walling, D. E. (1998): An investigation of the spatial variability of the grain size composition of floodplain sediments, *Hydrological Processes*, 12(7), 1079–1094, doi: 10.1002/(SICI)1099-1085(19980615)12:7<1079::AID-HYP642>3.0.CO;2-E.

Hemm, K., Frede, A., Kubosch, R., Mahn, D., Nawrath, S., Uebeler, M., Barth, U., Gregor, T., Buttler, K. P., Hand, R., Cezanne, R., Hodvina, S. and Huck, S. (2008): *Rote Liste der Farn- und Samenpflanzen Hessens (Red list of fern and seed plants in Hesse),* 4th ed., Hessisches Ministerium für Umwelt, ländlichen Raum und Verbraucherschutz (HMULV), Wiesbaden.

Heppner, C. S., Loague, K. and VanderKwaak, J. E. (2007): Long-term InHM simulations of hydrologic response and sediment transport for the R-5 catchment, *Earth Surface Processes and Landforms*, 32(9), 1273–1292, doi: 10.1002/esp.1474.

Her, Y., Yoo, S.-H., Seong, C., Jeong, J., Cho, J. and Hwang, S. (2016): Comparison of uncertainty in multi-parameter and multi-model ensemble hydrologic analysis of climate change, *Hydrology and Earth System Sciences Discussions*, 1–44, doi: 10.5194/hess-2016-160

Herron, N., Davis, R. and Jones, R. (2002): The effects of large-scale afforestation and climate change on water allocation in the Macquarie River catchment, NSW, Australia, *Journal of Environmental Management*, 65(4), 369–381, doi: 10.1006/jema.2002.0562.

Hester, E. T., Guth, C. R., Scott, D. T. and Jones, C. N. (2016): Vertical surface water-groundwater exchange processes within a headwater floodplain induced by experimental floods, *Hydrological Processes*, doi: 10.1002/hyp.10884.

Hindmarsh, A. C. and Sandu, R. (2016): *User Documentation for CVODE v2.9.0*, LLNL Software Manual, UCRL-SM-208108.

Hindmarsh, A. C., Brown, P. N., Grant, K. E., Lee, S. L., Serban, R., Shumaker, D. E. and Woodward, C. S. (2005): SUNDIALS: Suite of nonlinear and differential/algebraic equation solvers, *ACM Transactions on Mathematical Software*, 31(3), 363–396, doi: 10.1145/1089014.1089020.

Hölzel, N., Ed. (2006): *Renaturierung von Stromtalwiesen am hessischen Oberrhein: Ergebnisse einse E+E-Vorhabens des Bundesamts für Naturschutz (Restoration of flood meadows in the Hessian Upper Rhine: Results of an E+E project of the Federal Agency for Nature Conservation),* Bundesamt für Naturschutz, Bonn-Bad Godesberg.

Hölzel, N. and Otte, A. (2003): Restoration of a species-rich flood meadow by topsoil removal and diaspore transfer with plant material, *Applied Vegetation Science*, 6(2), 131–140, doi: 10.1111/j.1654-109X.2003.tb00573.x.

Hölzel, N. and Otte, A. (2004): Inter-annual variation in the soil seed bank of flood-meadows over two years with different flooding patterns, *Plant Ecology*, 174(2), 279–291, doi: 10.1023/B:VEGE.0000049108.04955.e2.

Hölzel, N. and Otte, A. (2009): The impact of flooding regime on the soil seed bank of flood-meadows, *Journal of Vegetation Science*, 12(2), 209–218, doi: 10.2307/3236605.

Hölzel, N., Donath, T. W., Bissels, S. and Otte, A. (2002): Auengrünlandrenaturierung am hessischen Oberrhein - Defizite und Erfolge nach 15 Jahren Laufzeit (Restoration of floodplain grassland in the Hessian Upper Rhine - deficits and successes after 15 years of operation), *Schriftenreihe für Vegetationskunde*, 36, 131–137.

Horchler, P., Mosner, E. and Peper, J. (2012): AuVeg – a database of German floodplain vegetation, *Biodiversity & Ecology*, 4, 367–367, doi: 10.7809/b-e.00158.

Hothorn, T., Bretz, F. and Westfall, P. (2008): Simultaneous Inference in General Parametric Models, *Biometrical Journal*, 50(3), 346–363, doi: 10.1002/bimj.200810425.

House, A. R., Thompson, J. R. and Acreman, M. C. (2016): Projecting impacts of climate change on hydrological conditions and biotic responses in a chalk valley riparian wetland, *Journal of Hydrology*, 534, 178–192, doi: 10.1016/j.jhydrol.2016.01.004.

Houska, T., Kraft, P., Chamorro-Chavez, A. and Breuer, L. (2015): SPOTting Model Parameters Using a Ready-Made Python Package, *PloS one*, 10(12), e0145180, doi: 10.1371/journal.pone.0145180.

Huang, S., Kumar, R., Flörke, M., Yang, T., Hundecha, Y., Kraft, P., Gao, C., Gelfan, A., Liersch, S., Lobanova, A., Strauch, M., van Ogtrop, F., Reinhardt, J., Haberlandt, U. and Krysanova, V. (2017): Evaluation of an ensemble of regional hydrological models in 12 large-scale river basins worldwide, *Climatic Change*, 141(3), 381–397, doi: 10.1007/s10584-016-1841-8.

Jäger, E. J., Ed. (2017): *Rothmaler - Exkursionsflora von Deutschland. Gefäßpflanzen: Grundband (Fieldflora of Germany, vascular plants, basic volume)*, 21st ed., Springer Spektrum, Berlin.

James, L. S. and Burges, S. J. (1982): Selection, Calibration, and Testing of Hydrologic Models in C. T. Haan, H. P. Johnson and D. L. Brakensiek (eds) *Hydrologic Modeling of Small Watersheds*, pp. 437–472, American Society of Agricultural Engineers, Hydrologic Modeling Monograph.

Jones, J. P., Sudicky, E. A. and McLaren, R. G. (2008): Application of a fully-integrated surface-subsurface flow model at the watershed-scale, *Water Resources Research*, 44(3), doi: 10.1029/2006WR005603.

Joyce, C. B. and Wade, P. M. (1998): Wet Grasslands: A European Perspective in C.B. Joyce, P. M. Wade (eds.) *European Wet Grasslands: Biodiversity, Management and Restoration*, pp. 1–12, Wiley, Chichester, UK.

Jung, M., Burt, T. P. and Bates, P. D. (2004): Toward a conceptual model of floodplain water table response, *Water Resources Research*, 40(12), 565, doi: 10.1029/2003WR002619.

Jung, V., Hoffmann, L. and Muller, S. (2008): Ecophysiological responses of nine floodplain meadow species to changing hydrological conditions, *Plant Ecology*, 201(2), 589–598, doi: 10.1007/s11258-008-9508-9.

Karim, F., Petheram, C., Marvanek, S., Ticehurst, C., Wallace, J. and Hasan, M. (2016): Impact of climate change on floodplain inundation and hydrological connectivity between wetlands and rivers in a tropical river catchment, *Hydrological Processes*, 30(10), 1574–1593, doi: 10.1002/hyp.10714.

Kay, A. L., Davies, H. N., Bell, V. A. and Jones, R. G. (2009): Comparison of uncertainty sources for climate change impacts, *Climatic Change*, 92(1–2), 41–63, doi: 10.1007/s10584-008-9471-4.

Keuler, K., Radtke, K., Kotlarski, S. and Lüthi, D. (2016): Regional climate change over Europe in COSMO-CLM, *Meteorologische Zeitschrift*, 25(2), 121–136, doi: 10.1127/metz/2016/0662.

Kiedrzyńska, E., Kiedrzyński, M. and Zalewski, M. (2015): Sustainable floodplain management for flood prevention and water quality improvement, *Natural Hazards*, 76(2), 955–977, doi: 10.1007/s11069-014-1529-1.

Kopeć, D., Michalska-Hejduk, D. and Krogulec, E. (2013): The relationship between vegetation and groundwater levels as an indicator of spontaneous wetland restoration, *Ecological Engineering*, 57, 242–251, doi: 10.1016/j.ecoleng.2013.04.028.

Kraft, P. (2011): cmf - catchment modelling framework; URL: https://philippkraft.github.io/cmf.

Kraft, P. (2012): *A hydrological programming language extension for integrated catchment models*, Dissertation, Justus Liebig University, Gießen.

Kraft, P., Vaché, K. B., Frede, H.-G. and Breuer, L. (2011): A hydrological programming language extension for integrated catchment models, *Environmental Modelling & Software*, 26(6), 828–830, doi: 10.1016/j.envsoft.2010.12.009.

Krause, S. and Bronstert, A. (2005): An advanced approach for catchment delineation and water balance modelling within wetlands and floodplains, *Advances in Geosciences*, 5, 1–5, doi: 10.5194/adgeo-5-1-2005.

Krause, S. and Bronstert, A. (2007): The impact of groundwater–surface water interactions on the water balance of a mesoscale lowland river catchment in northeastern Germany, *Hydrological Processes*, 21(2), 169–184, doi: 10.1002/hyp.6182.

Krause, S., Bronstert, A. and Zehe, E. (2007a): Groundwater–surface water interactions in a North German lowland floodplain – Implications for the river discharge dynamics and riparian water balance, *Journal of Hydrology*, 347(3–4), 404–417, doi: 10.1016/j.jhydrol.2007.09.028.

Krause, S., Jacobs, J. and Bronstert, A. (2007b): Modelling the impacts of land-use and drainage density on the water balance of a lowland–floodplain landscape in northeast Germany, *Ecological Modelling*, 200(3–4), 475–492, doi: 10.1016/j.ecolmodel.2006.08.015.

Krysanova, V., Müller-Wohlfeil, D.-I. and Becker, A. (1998): Development and test of a spatially distributed hydrological/water quality model for mesoscale watersheds, *Ecological Modelling*, 106(2–3), 261–289, doi: 10.1016/S0304-3800(97)00204-4.

Lafon, T., Dadson, S., Buys, G. and Prudhomme, C. (2013): Bias correction of daily precipitation simulated by a regional climate model: a comparison of methods, *International Journal of Climatology*, 33(6), 1367–1381, doi: 10.1002/joc.3518.

Lewin, J. and Hughes, D. (1980): Welsh floodplain studies, *Journal of Hydrology*, 46(1–2), 35–49, doi: 10.1016/0022-1694(80)90034-7.

Leyer, I. (2005): Predicting plant species' responses to river regulation, *Journal of Applied Ecology*, 42(2), 239–250, doi: 10.1111/j.1365-2664.2005.01009.x.

Li, S.-G., McLaughlin, D. and Liao, H.-S. (2003): A computationally practical method for stochastic groundwater modeling, *Advances in Water Resources*, 26(11), 1137–1148, doi: 10.1016/j.advwatres.2003.08.003.

te Linde, A. H., Aerts, J. C. J. H., Hurkmans, R. T. W. L. and Eberle, M. (2008): Comparing model performance of two rainfall-runoff models in the Rhine basin using different atmospheric forcing data sets, *Hydrology and Earth System Sciences*, 12(3), 943–957, doi: 10.5194/hess-12-943-2008.

Lindström, G., Johansson, B., Persson, M., Gardelin, M. and Bergström, S. (1997): Development and test of the distributed HBV-96 hydrological model, *Journal of Hydrology*, 201(1–4), 272–288, doi: 10.1016/S0022-1694(97)00041-3.

Lippert, K., Braun, C. and Klute, M. (2012): *Erstellung eines Grundwassermodells am nördlichen Oberrehin – Modellaufbau und Kalibrierung – (Creation of a groundwater model at the northern Upper Rhine – model construction and calibration –).* Björnsen Beratende Ingenieure GmbH, Koblenz.

Loague, K., Heppner, C. S., Abrams, R. H., Carr, A. E., VanderKwaak, J. E. and Ebel, B. A. (2005): Further testing of the Integrated Hydrology Model (InHM): event-based simulations for a small rangeland catchment located near Chickasha, Oklahoma, *Hydrological Processes*, 19(7), 1373–1398, doi: 10.1002/hyp.5566.

Lomba, A., Pellissier, L., Randin, C., Vicente, J., Moreira, F., Honrado, J. and Guisan, A. (2010): Overcoming the rare species modelling paradox: A novel hierarchical framework applied to an Iberian endemic plant, *Biological Conservation*, 143(11), 2647–2657, doi: 10.1016/j.biocon.2010.07.007.

Ludewig, K., Korell, L., Löffler, F., Scholz, M., Mosner, E. and Jensen, K. (2014): Vegetation patterns of floodplain meadows along the climatic gradient at the Middle Elbe River, *Flora - Morphology, Distribution, Functional Ecology of Plants*, 209(8), 446–455, doi: 10.1016/j.flora.2014.04.006.

Maier, N., Breuer, L. and Kraft, P. (2017): Prediction and uncertainty analysis of a parsimonious floodplain surface water - groundwater interaction model, *Water Resources Research*, doi: 10.1002/2017WR020749.

Maier, N., Breuer, L., Chamorro, A., Kraft, P. and Houska, T. (2018): Multi-Source Uncertainty Analysis in Simulating Floodplain Inundation under Climate Change, *Water*, 10(6), 809, doi: 10.3390/w10060809.

Malanson, G. P. (1993): *Riparian Landscapes*, Cambridge University Press, Cambridge, UK.

Maltby, E. and Barker, T., Eds. (2009): *The Wetlands Handbook*, Wiley-Blackwell, Oxford, UK.

Maraun, D., Wetterhall, F., Ireson, A. M., Chandler, R. E., Kendon, E. J., Widmann, M., Brienen, S., Rust, H. W., Sauter, T., Themeßl, M., Venema, V. K. C., Chun, K. P., Goodess, C. M., Jones, R. G., Onof, C., Vrac, M. and Thiele-Eich, I. (2010): Precipitation downscaling under climate change, *Reviews of Geophysics*, 48(3), 219, doi: 10.1029/2009RG000314.

Mathar, W., Kleinebecker, T., Hölzel, N. and Collins, B. (2015): Environmental variation as a key process of co-existence in flood-meadows, *Journal of Vegetation Science*, 26(3), 480–491, doi: 10.1111/jvs.12254.

Maxwell, R. M., Putti, M., Meyerhoff, S., Delfs, J.-O., Ferguson, I. M., Ivanov, V., Kim, J., Kolditz, O., Kollet, S. J., Kumar, M., Lopez, S., Niu, J., Paniconi, C., Park, Y.-J., Phanikumar, M. S., Shen, C., Sudicky, E. A. and Sulis, M. (2014): Surface-subsurface model intercomparison, *Water Resources Research*, 50(2), 1531–1549, doi: 10.1002/2013WR013725.

McInerney, D., Thyer, M., Kavetski, D., Lerat, J. and Kuczera, G. (2017): Improving probabilistic prediction of daily streamflow by identifying Pareto optimal approaches for modeling heteroscedastic residual errors, *Water Resources Research*, 53(3), 2199–2239, doi: 10.1002/2016WR019168.

McKay, M. D., Beckman, R. J. and Conover, W. J. (1979): A Comparison of Three Methods for Selecting Values of Input Variables in the Analysis of Output from a Computer Code, *Technometrics*, 21(2), 239–245, doi: 10.1080/00401706.1979.10489755.

McMillan, H. K. and Brasington, J. (2008): End-to-end flood risk assessment, *Water Resources Research*, 44(3), 295, doi: 10.1029/2007WR005995.

McSweeney, C. F., Jones, R. G., Lee, R. W. and Rowell, D. P. (2015): Selecting CMIP5 GCMs for downscaling over multiple regions, *Climate Dynamics*, 44(11–12), 3237–3260, doi: 10.1007/s00382-014-2418-8.

Middelkoop, H., Daamen, K., Gellens, D., Grabs, W., Kwadijk, J. C., Lang, H., Parmet, B. W., Schädler, B., Schulla, J. and Wilke, K. (2001): Impact of climate change on hydrological regimes and water resources management in the Rhine basin, *Climatic change*, 49(1–2), 105–128, doi: 10.1023/A:1010784727448.

Mieszkowska, N., Milligan, G., Burrows, M. T., Freckleton, R. and Spencer, M. (2013): Dynamic species distribution models from categorical survey data, *The Journal of animal ecology*, 82(6), 1215–1226, doi: 10.1111/1365-2656.12100.

Mockler, E. M., Chun, K. P., Sapriza-Azuri, G., Bruen, M. and Wheater, H. S. (2016): Assessing the relative importance of parameter and forcing uncertainty and their interactions in conceptual hydrological model simulations, *Advances in Water Resources*, 97, 299–313, doi: 10.1016/j.advwatres.2016.10.008.

Mortsch, L. D. (1998): Assessing the impact of climate change on the Great Lakes shoreline wetlands, *Climatic Change*, 40(2), 391–416, doi: 10.1023/A:1005445709728.

Mosner, E., Schneider, S., Lehmann, B. and Leyer, I. (2011): Hydrological prerequisites for optimum habitats of riparian Salix communities - identifying suitable reforestation sites, *Applied Vegetation Science*, 14(3), 367–377, doi: 10.1111/j.1654-109X.2011.01121.x.

Mosner, E., Weber, A., Carambia, M., Nilson, E., Schmitz, U., Zelle, B., Donath, T. and Horchler, P. (2015): Climate change and floodplain vegetation—future prospects for riparian habitat availability along the Rhine River, *Ecological Engineering*, 82, 493–511, doi: 10.1016/j.ecoleng.2015.05.013.

Moss, T. and Monstadt, J., Eds. (2008): *Restoring floodplains in Europe: policy contexts and project experiences*, IWA Pub, London.

Nagelkerke, N. J. D. (1991): A note on a general definition of the coefficient of determination, *Biometrika*, 78(3), 691–692, doi: 10.1093/biomet/78.3.691.

Nash, J. E. and Sutcliffe, J. V. (1970): River flow forecasting through conceptual models part I — A discussion of principles, *Journal of Hydrology*, 10(3), 282–290, doi: 10.1016/0022-1694(70)90255-6.

Newbold, C. (1997): *Water level requirements of wetland plants and animals*, English Nature, Peterborough.

Oliver, T. H. and Morecroft, M. D. (2014): Interactions between climate change and land use change on biodiversity: attribution problems, risks, and opportunities: Interactions between climate change and land use change, *Wiley Interdisciplinary Reviews: Climate Change*, 5(3), 317–335, doi: 10.1002/wcc.271.

Opperman, J. J., Galloway, G. E., Fargione, J., Mount, J. F., Richter, B. D. and Secchi, S. (2009): Sustainable floodplains through large-scale reconnection to rivers, *Science*, 1487–1488, doi: 10.1126/science.1178256.

Opperman, J. J., Luster, R., McKenney, B. A., Roberts, M. and Meadows, A. W. (2010): Ecologically Functional Floodplains: Connectivity, Flow Regime, and Scale, *JAWRA Journal of the American Water Resources Association*, 46(2), 211–226, doi: 10.1111/j.1752-1688.2010.00426.x.

Pappenberger, F. and Beven, K. J. (2006): Ignorance is bliss, *Water Resources Research*, 42(5), doi: 10.1029/2005WR004820.

Pappenberger, F., Beven, K. J., Hunter, N. M., Bates, P. D., Gouweleeuw, B. T., Thielen, J. and Roo, A. P. J. (2005): Cascading model uncertainty from medium range weather forecasts (10 days) through a rainfall-runoff model to flood inundation predictions within the European Flood Forecasting System (EFFS), *Hydrology and Earth System Sciences*, 9(4), 381–393, doi: 10.5194/hess-9-381-2005.

Pearson, R. G., Thuiller, W., Araújo, M. B., Martinez-Meyer, E., Brotons, L., McClean, C., Miles, L., Segurado, P., Dawson, T. P. and Lees, D. C. (2006): Model-based uncertainty in species range prediction, *Journal of Biogeography*, 33(10), 1704–1711, doi: 10.1111/j.1365-2699.2006.01460.x.

Pechlivanidis, I. G., Arheimer, B., Donnelly, C., Hundecha, Y., Huang, S., Aich, V., Samaniego, L., Eisner, S. and Shi, P. (2017): Analysis of hydrological extremes at different hydro-climatic regimes under present and future conditions, *Climatic Change*, 141(3), 467–481, doi: 10.1007/s10584-016-1723-0.

Peterson, A. T., Soberón, J., Pearson, R. G., Anderson, R., Martinez-Meyer, E., Nakamura, M. and Araújo, M. B. (2011): *Ecological Niches and Geographic Distributions*, Princeton University Press.

Pinheiro, J., Bates, D., DeBroy, S., Sarkar, D. and R Core Team (2017): *nlme: Linear and Nonlinear Mixed Effects Models*. R package version 3.1-131. URL: https://CRAN.R-project.org/package=nlme.

Pirastru, M. and Niedda, M. (2013): Evaluation of the soil water balance in an alluvial flood plain with a shallow groundwater table, *Hydrological Sciences Journal*, 58(4), 898–911, doi: 10.1080/02626667.2013.783216.

Price, J. S. and Waddington, J. M. (2000): Advances in Canadian wetland hydrology an biogeochemistry, *Hydrological Processes*, 14(9), 1579–1589, doi: 10.1002/1099-1085(20000630)14:9<1579::AID-HYP76>3.0.CO;2-#.

Prudhomme, C. and Davies, H. (2009): Assessing uncertainties in climate change impact analyses on the river flow regimes in the UK. Part 2, *Climatic Change*, 93(1–2), 197–222, doi: 10.1007/s10584-008-9461-6.

Qu, Y. and Duffy, C. J. (2007): A semidiscrete finite volume formulation for multiprocess watershed simulation, *Water Resources Research*, 43(8), doi: 10.1029/2006WR005752.

Quintana Seguí, P., Ribes, A., Martin, E., Habets, F. and Boé, J. (2010): Comparison of three downscaling methods in simulating the impact of climate change on the hydrology of Mediterranean basins, *Journal of Hydrology*, 383(1–2), 111–124, doi: 10.1016/j.jhydrol.2009.09.050.

R Core Team (2017): *R: A Language and Environment for Statistical Computing*, R Foundation for Statistical Computing, Vienna, Austria.

Refsgaard, J. C., Sørensen, H. R., Mucha, I., Rodak, D., Hlavaty, Z., Bansky, L., Klucovska, J., Topolska, J., Takac, J., Kosc, V., Enggrob, H. G., Engesgaard, P., Jensen, J. K., Fiselier, J., Griffioen, J. and Hansen, S. (1998): An Integrated Model for the Danubian Lowland – Methodology and Applications, *Water Resources Management*, 12(6), 433–465, doi: 10.1023/A:1008088901770.

Refsgaard, J. C., van der Sluijs, J. P., Brown, J. and van der Keur, P. (2006): A framework for dealing with uncertainty due to model structure error, *Advances in Water Resources*, 29(11), 1586–1597, doi: 10.1016/j.advwatres.2005.11.013.

Refsgaard, J. C., Arnbjerg-Nielsen, K., Drews, M., Halsnæs, K., Jeppesen, E., Madsen, H., Markandya, A., Olesen, J. E., Porter, J. R. and Christensen, J. H. (2013): The role of uncertainty in climate change adaptation strategies—A Danish water management example, *Mitigation and Adaptation Strategies for Global Change*, 18(3), 337–359, doi: 10.1007/s11027-012-9366-6.

Reif, A., Baumgärtel, R., Dister, E. and Schneider, E. (2016): Waldökologie, Landschaftsforschung und Naturschutz (Forest Ecology, Landscape Research and Nature Conservation), *Waldökologie, Landschaftsforschung und Naturschutz*, 15, 69–92.

Rojas, R., Kahunde, S., Peeters, L., Batelaan, O., Feyen, L. and Dassargues, A. (2010): Application of a multimodel approach to account for conceptual model and scenario uncertainties in groundwater modelling, *Journal of Hydrology*, 394(3–4), 416–435, doi: 10.1016/j.jhydrol.2010.09.016.

van Roosmalen, L., Christensen, B. S. B. and Sonnenborg, T. O. (2007): Regional Differences in Climate Change Impacts on Groundwater and Stream Discharge in Denmark, *Vadose Zone Journal*, 6(3), 554–571, doi: 10.2136/vzj2006.0093.

Rosenberger, W. (2007): *Bodenkarte von Hessen, L6116 Darmstadt West (Soil map of Hessian)*, RP Darmstadt, Darmstadt.

Russo, T. A., Fisher, A. T. and Roche, J. W. (2012): Improving riparian wetland conditions based on infiltration and drainage behavior during and after controlled flooding, *Journal of Hydrology*, 432–433, 98–111, doi: 10.1016/j.jhydrol.2012.02.022.

Rutter, A. J. and Morton, A. J. (1977): A Predictive Model of Rainfall Interception in Forests. III. Sensitivity of The Model to Stand Parameters and Meteorological Variables, *The Journal of Applied Ecology*, 14(2), 567, doi: 10.2307/2402568.

Saha, G., Li, J. and Thring, R. (2017): Understanding the Effects of Parameter Uncertainty on Temporal Dynamics of Groundwater-Surface Water Interaction, *Hydrology*, 4(2), 28, doi: 10.3390/hydrology4020028.

Sanchez-Vila, X. and Fernàndez-Garcia, D. (2016): Debates-Stochastic subsurface hydrology from theory to practice, *Water Resources Research*, 52(12), 9246–9258, doi: 10.1002/2016WR019302.

Schneider, E. (2010): Floodplain Restoration of Large European Rivers, with Examples from the Rhine and the Danube, in M. Eiseltová (eds.) *Restoration of Lakes, Streams, Floodplains, and Bogs in Europe*, pp. 185–223, Springer Netherlands, Dordrecht.

Sebben, M. L., Werner, A. D., Liggett, J. E., Partington, D. and Simmons, C. T. (2013): On the testing of fully integrated surface-subsurface hydrological models, *Hydrological Processes*, 27(8), 1276–1285, doi: 10.1002/hyp.9630.

Singh, A., Mishra, S. and Ruskauff, G. (2010): Model averaging techniques for quantifying conceptual model uncertainty, *Ground Water*, 48(5), 701–715, doi: 10.1111/j.1745-6584.2009.00642.x.

Singh, V. P. (1996): *Kinematic wave modeling in water resources*, Wiley, New York.

Sophocleous, M. (2002): Interactions between groundwater and surface water: the state of the science, *Hydrogeology Journal*, 10(1), 52–67, doi: 10.1007/s10040-001-0170-8.

Sorenson, L. G., Goldberg, R., Root, T. L. and Anderson, M. G. (1998): Potential Effects of Global Warming on Waterfowl Populations Breeding in the Northern Great Plains, *Climatic Change*, 40(2), 343–369, doi: 10.1023/A:1005441608819.

Sorribas, M. V., Paiva, R. C. D., Melack, J. M., Bravo, J. M., Jones, C., Carvalho, L., Beighley, E., Forsberg, B. and Costa, M. H. (2016): Projections of climate change effects on discharge and inundation in the Amazon basin, *Climatic Change*, 136(3–4), 555–570, doi: 10.1007/s10584-016-1640-2.

Taylor, K. E., Stouffer, R. J. and Meehl, G. A. (2012a): An Overview of CMIP5 and the Experiment Design, *Bulletin of the American Meteorological Society*, 93(4), 485–498, doi: 10.1175/BAMS-D-11-00094.1.

Taylor, R. G., Scanlon, B., Döll, P., Rodell, M., van Beek, R., Wada, Y., Longuevergne, L., Leblanc, M., Famiglietti, J. S., Edmunds, M., Konikow, L., Green, T. R., Chen, J., Taniguchi, M., Bierkens, M. F. P., MacDonald, A., Fan, Y., Maxwell, R. M., Yechieli, Y., Gurdak, J. J., Allen, D. M., Shamsudduha, M., Hiscock, K., Yeh, P. J.-F., Holman, I. and Treidel, H. (2012b): Ground water and climate change, *Nature Climate Change*, 3(4), 322–329, doi: 10.1038/NCLIMATE1744.

Teng, J., Vaze, J., Chiew, F. H. S., Wang, B. and Perraud, J.-M. (2012): Estimating the Relative Uncertainties Sourced from GCMs and Hydrological Models in Modeling Climate Change Impact on Runoff, *Journal of Hydrometeorology*, 13(1), 122–139, doi: 10.1175/JHM-D-11-058.1.

Teng, J., Potter, N. J., Chiew, F. H. S., Zhang, L., Wang, B., Vaze, J. and Evans, J. P. (2015): How does bias correction of regional climate model precipitation affect modelled runoff?, *Hydrology and Earth System Sciences*, 19(2), 711–728, doi: 10.5194/hess-19-711-2015.

Teutschbein, C. and Seibert, J. (2012): Bias correction of regional climate model simulations for hydrological climate-change impact studies, *Journal of Hydrology*, 456–457, 12–29, doi: 10.1016/j.jhydrol.2012.05.052.

Themeßl, M. J., Gobiet, A. and Leuprecht, A. (2011): Empirical-statistical downscaling and error correction of daily precipitation from regional climate models, *International Journal of Climatology*, 31(10), 1530–1544, doi: 10.1002/joc.2168.

Thompson, J. R., Gavin, H., Refsgaard, A., Refstrup Sørenson, H. and Gowing, D. J. (2009): Modelling the hydrological impacts of climate change on UK lowland wet grassland, *Wetlands Ecology and Management*, 17(5), 503–523, doi: 10.1007/s11273-008-9127-1.

Thuiller, W., Lafourcade, B., Engler, R. and Araújo, M. B. (2009): BIOMOD – a platform for ensemble forecasting of species distributions, *Ecography*, 32(3), 369–373, doi: 10.1111/j.1600-0587.2008.05742.x.

Tockner, K. and Stanford, J. A. (2002): Riverine flood plains: present state and future trends, *Environmental Conservation*, 29(03), 308–330, doi: 10.1017/S037689290200022X.

Tockner, K., Pennetzdorfer, D., Reiner, N., Schiemer, F. and Ward, J. V. (1999): Hydrological connectivity, and the exchange of organic matter and nutrients in a dynamic river-floodplain system (Danube, Austria), *Freshwater Biology*, 41(3), 521–535, doi: 10.1046/j.1365-2427.1999.00399.x.

Van Eck, W. H. J. M., Van De Steeg, H. M., Blom, C. W. P. M. and De Kroon, H. (2004): Is tolerance to summer flooding correlated with distribution patterns in river floodplains? A comparative study of 20 terrestrial grassland species, *Oikos*, 107(2), 393–405, doi: 10.1111/j.0030-1299.2004.13083.x.

Vasiliev, O. F. (1987): System modelling of the interaction between surface and ground waters in problems of hydrology, *Hydrological Sciences Journal*, 32(3), 297–311, doi: 10.1080/02626668709491190.

Vaughan, I. P. and Ormerod, S. J. (2005): The continuing challenges of testing species distribution models, *Journal of Applied Ecology*, 42(4), 720–730, doi: 10.1111/j.1365-2664.2005.01052.x.

Vervuren, P. J. A., Blom, C. W. P. M. and De Kroon, H. (2003): Extreme flooding events on the Rhine and the survival and distribution of riparian plant species, *Journal of Ecology*, 91(1), 135–146, doi: 10.1046/j.1365-2745.2003.00749.x.

Vetter, T., Huang, S., Aich, V., Yang, T., Wang, X., Krysanova, V. and Hattermann, F. (2015): Multi-model climate impact assessment and intercomparison for three large-scale river basins on three continents, *Earth System Dynamics*, 6(1), 17–43, doi: 10.5194/esd-6-17-2015.

Ward, J. V., Tockner, K. and Schiemer, F. (1999): Biodiversity of floodplain river ecosystems, *Regulated Rivers: Research & Management*, 15(1–3), 125–139, doi: 10.1002/(SICI)1099-1646(199901/06)15:1/3<125::AID-RRR523>3.0.CO;2-E.

Wesche, K., Krause, B., Culmsee, H. and Leuschner, C. (2012): Fifty years of change in Central European grassland vegetation, *Biological Conservation*, 150(1), 76–85, doi: 10.1016/j.biocon.2012.02.015.

Wickham, H. (2009): *ggplot2: Elegant Graphics for Data Analysis*, Springer, New York. URL: http://ggplot2.org.

Wiedner, E. (1990): Bodenkarte der nördlichen Oberrheinebene 1 : 50000. (Soil map of the northern Upper Rhine Plain), Hessisches Landesamt für Umwelt und Geologie, Wiesbaden.

Wilby, R. L. (2005): Uncertainty in water resource model parameters used for climate change impact assessment, *Hydrological Processes*, 19(16), 3201–3219, doi: 10.1002/hyp.5819.

Wilby, R. L., Whitehead, P. G., Wade, A. J., Butterfield, D., Davis, R. J. and Watts, G. (2006): Integrated modelling of climate change impacts on water resources and quality in a lowland catchment, *Journal of Hydrology*, 330(1–2), 204–220, doi: 10.1016/j.jhydrol.2006.04.033.

Woessner, W. W. (2000): Stream and Fluvial Plain Ground Water Interactions, *Ground Water*, 38(3), 423–429, doi: 10.1111/j.1745-6584.2000.tb00228.x.

Woodcock, B. A., Mann, D. J., Mirieless, C., McGavin, G. C. and McDonald, A. W. (2005): Re-creation of a lowland flood-plain meadow, *Journal of Insect Conservation*, 9(3), 207–218, doi: 10.1007/s10841-005-6608-x.

Wu, J. and Zeng, X. (2013): Review of the uncertainty analysis of groundwater numerical simulation, *Chinese Science Bulletin*, 58(25), 3044–3052, doi: 10.1007/s11434-013-5950-8.

Xu, F., Otte, A., Ludewig, K., Donath, T. and Harvolk-Schöning, S. (2017): Land Cover Changes (1963–2010) and Their Environmental Factors in the Upper Danube Floodplain, *Sustainability*, 9(6), 943, doi: 10.3390/su9060943.

Yu, D. and Lane, S. N. (2006): Urban fluvial flood modelling using a two-dimensional diffusion-wave treatment, part 1, *Hydrological Processes*, 20(7), 1541–1565, doi: 10.1002/hyp.5935.

Zorn, M. I., Van Gestel, C. A. M. and Eijsackers, H. (2005): Species-specific earthworm population responses in relation to flooding dynamics in a Dutch floodplain soil, *Pedobiologia*, 49(3), 189–198, doi: 10.1016/j.pedobi.2004.08.004.

Zubler, E. M., Fischer, A. M., Fröb, F. and Liniger, M. A. (2016): Climate change signals of CMIP5 general circulation models over the Alps - impact of model selection, *International Journal of Climatology*, 36(8), 3088–3104, doi: 10.1002/joc.4538.

Zuur, A. F., Ieno, E. N., Walker, N., Saveliev, A. A. and Smith, G. M. (2009): *Mixed effects models and extensions in ecology with R*, Springer, New York.

Acknowledgements

This dissertation was part of a joint research project by the Division of Landscape, Water and Biogeochemical Cycle and the Division of Landscape Ecology and Landscape Planning of the Institute for Landscape Ecology and Resources Management at the Justus Liebig University Giessen. Special thanks to the funder: The Deutsche Bundesstiftung Umwelt (DBU). Thank you to the project initiator and coordinators: Prof. Dr. Dr. habil. Dr. h. c. Annette Otte, Prof. Dr. Lutz Breuer, Dr. Philipp Kraft and Dr. Sarah Harvolk-Schöning. Additionally, this work would not have been possible without the uncomplicated support of: Ralph Baumgärtel, Matthias Harnisch, Peter Horchler, and the staff members from the regional council and the HLNUG.

My sincere thanks go to my supervisors Prof. Dr. Lutz Breuer and Dr. Philipp Kraft. I appreciate the freedom they gave me for my work while simultaneously supporting me with valuable advice, patience, motivation, and immense knowledge. Particularly, I would like to mention here the persevering attempts from both of them to teach me enthusiasm on modeling results and their endurance to give me motivation in times of stress and scientific crises. I am especially grateful for Philipp tirelessly teaching me programming in general and CMF specifically. I would also like to thank Prof. Dr. Dr. habil. Dr. h. c. Annette Otte for her willingness to act as second examiner.

Following, I would like to thank all members of the Institute of Landscape Ecology and Resources Management creating a friendly and productive work environment, and the amusing and educational breaks. To all my co-authors of the last published papers: Thank you for the joyful and productive work together. Special thanks also go to my colleagues from the Chair of Landscape Ecology for the last years, for the discussions, patience and endurance during the introduction into the world of plants, and the delicious cakes. A great thank to Johannes for his support, the joyful and scientific coffee breaks and discussions, and his everlasting hospitality. But also to all the others, who always welcomed me with joy.

Last, but certainly not least, my deepest thanks go to all the people who have supported me outside of work. I would like to thank my parents for their support and the freedom they gave me to find and go my way. Special thanks to my brother and his family in supporting me via cheerful free time activities and holidays. Nicolas, thank you for your love, perseverance, patience and all kinds of support.

Declaration

I declare that I have completed this dissertation single-handedly without the unauthorized help of a second party and only with the assistance acknowledged therein. I have appropriately acknowledged and cited all text passages that are derived verbatim from or are based on the content of published work of others, and all information relating to verbal communications. I consent to the use of an anti-plagiarism software to check my thesis. I have abided by the principles of good scientific conduct laid down in the charter of the Justus Liebig University Giessen „Satzung der Justus-Liebig-Universität Gießen zur Sicherung guter wissenschaftlicher Praxis“ in carrying out the investigations described in the dissertation.

Gießen, 17th July 2018 Nadine Maier, M. Sc.